Proceedings of the seminar Cement and concrete, June 1-2, 1988 at ENIT, Tunis

Boström, Lars

1988

Link to publication

Citation for published version (APA):
Boström, L. (Ed.) (1988). *Proceedings of the seminar Cement and concrete, June 1-2, 1988 at ENIT, Tunis*. (Report TVBM 3037). Division of Building Materials, LTH, Lund University.

Total number of authors:
1

General rights
Unless other specific re-use rights are stated the following general rights apply:
Copyright and moral rights for the publications made accessible in the public portal are retained by the authors and/or other copyright owners and it is a condition of accessing publications that users recognise and abide by the legal requirements associated with these rights.

- Users may download and print one copy of any publication from the public portal for the purpose of private study or research.
- You may not further distribute the material or use it for any profit-making activity or commercial gain
- You may freely distribute the URL identifying the publication in the public portal

Read more about Creative commons licenses: https://creativecommons.org/licenses/

Take down policy
If you believe that this document breaches copyright please contact us providing details, and we will remove access to the work immediately and investigate your claim.

LUND UNIVERSITY

PO Box 117
221 00 Lund
+46 46-222 00 00

Download date: 17. May. 2025

DIVISION OF BUILDING MATERIALS
LUND INSTITUTE OF TECHNOLOGY

Proceedings of the seminar

CEMENT AND CONCRETE

June 1-2,1988 at ENIT, Tunis

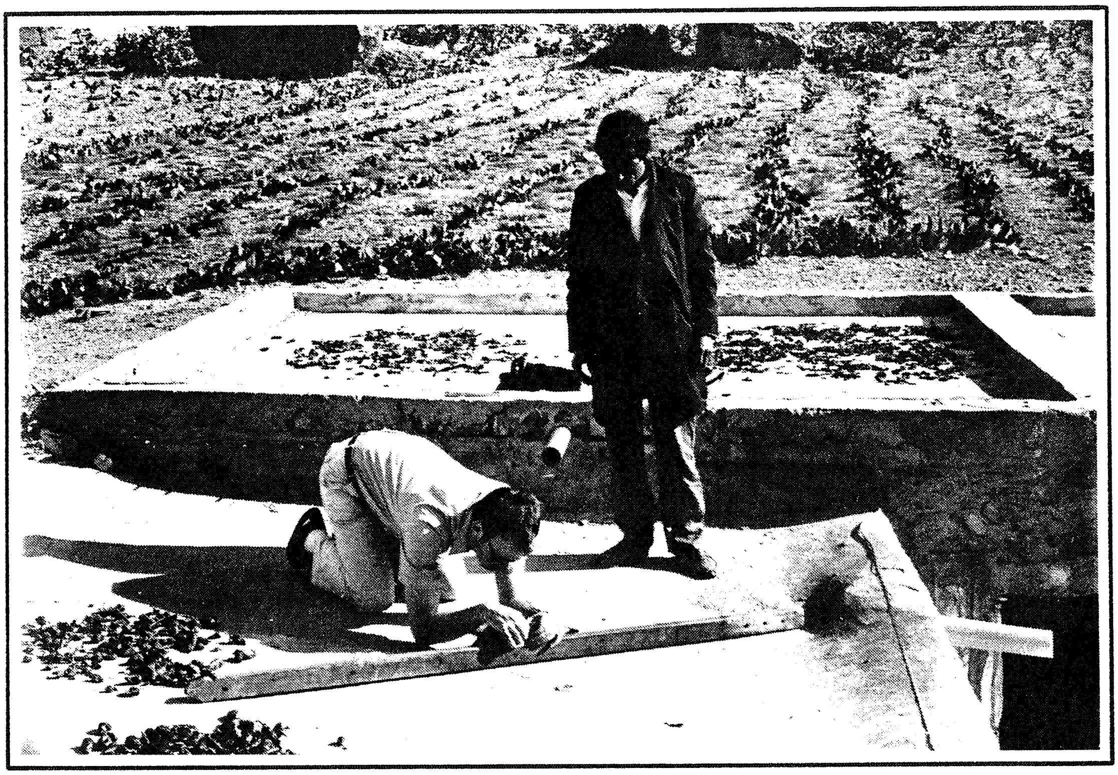

المدرسة القومية للمهندسين - تونس
école nationale d'ingénieurs de tunis

LUND INSTITUTE
OF TECHNOLOGY

REPORT TVBM-3037
LUND SWEDEN 1988

CODEN: LUTVDG/(TVBM-3037)/1-136/(1988)

Proceedings of the seminar

CEMENT AND CONCRETE

June 1-2,1988 at ENIT, Tunis

ISSN 0348-7911

CONTENTS

Preface 7

Introduction speach 9
by A.Friaa

Recherche pratique sur le béton à l'Université de Lund 11
by L.Boström and B.Johansson

Méthodes d'étude de la dégradation des bétons en milieux agressifs 25
by L.Hachani, E.Triki and M.T.Chaieb

Problems in service life prediction of buildings and construction materials 27
by G.Fagerlund

Etude de la dégradation des bétons tunisiens: méthodes expérimentales 53
by M.Ben Cheika, E.Triki and M.T.Chaieb

Transfert d'humidité dans le béton 59
by R.Mensi

Béton à base de sable du désert 61
by A.Aouididi and M.T.Chaieb

The advanced strip method - a simple design tool 71
by A.Hillerborg

Application of fracture mechanics to concrete 79
by A.Hillerborg

On a model on thermodynamic concepts for reinforced concrete behaviour at degradation state 107
by A.Friaa and K.Ben Amara

Development 1944-1988 within the Swedish cement industry 119
by O.Peterson

PREFACE

In 1982, a collaboration started between Ecole Nationale d'Ingénieurs de Tunis, ENIT, and the division of Building Materials at Lund University in Sweden. The first project in this collaboration, was an examination of a soil called Torba, and the possibility to stabilaze this soil with cement for production of bricks to be used on the countryside in building constructions.

Since the project worked out well, the collaboration has continued. In 1987 a new project started. The objective of the project, called the roof project, was to investigate the problem with water leaking through flat roofs and to find a possible solution on the water leakage problem. The swedish part of the contribution, is financially supported by the swedish agency for international technical and economic cooperation (BITS). This seminar is a part of the roof project.

To the seminar, specialists in the area of cement and concrete have been invited from ENIT in Tunisia and from different organisations in Sweden. Because of the limited time, only a few persons was invited to give a presentation due to the fact that the objective was to give the speachers all the time needed for their presentation.

The invited speachers are all specialists in different areas of cement and concrete research. In this way, both Tunisia and Sweden gets an idea of the research which is going on in the two countries, and it is possible to find areas in which there is a possibility for a collaboration.

As a final, I wish to thank all personal at ENIT who have been involved in the preparations of this seminar and specially Mr Chaieb, Mr Aouididi, Mr Ben Hassin and Miss Rafika. I also thank Britt Andersson for her invaluable help to get all these papers together to a publication.

Lars Boström, November 1988

Chers invités, chers collègues, Mesdames et Messieurs

Des obligations non prévues m'empêchent d'être parmi vous pour prendre part aux travaux de votre séminaire - Je le regrette et vous prie de m'en excuser.

Le thème choisi d'un commun accord revêt un caractère particulièrement important. D'abord parce que le béton constitue de nos jours le matériau de construction le plus communément utilisé et parce que d'autre part, il est encore, malgré sa relative ancienneté, l'objet de nombreuses études dont l'objectif est une meilleure connaissance de son comportement complexe et une optimisation de son utilisation.

En effet, plusieurs questions de première importance n'ont toujours pas recu de réponses satisfaisantes. Il convient de citer particulièrement les deux suivantes:

1) Quelles sont les lois qui regissent le comportement d'une structure en béton qui est le siège de phénomènes assurément couplés de transfert d'hygrométrie et de chaleur et d'endommagement sachant qu'il s'agit d'un matériau vieillissant, évoluant dans le temps?

2) Comment évolue une structure en béton plongée dans un milieu agressif et comment assurer correctement sa protection?

Ce sont précisément ces deux questions centrales qui occupent le plus de place dans le programme de ce séminaire.

Une coincidence heureuse a voulu qu'elles interessent des équipes de chercheurs à l'ENIT et à l'Université de Lund. Et, il est réconfortant de constater que des résultats forts utiles ont été obtienus de part et d'autres.

C'est précisément pour confronter ces résultats respectives et s'enrichir de ses expériences que ce séminaire a été organisé. Il constitut également un jalon supplémentaire sur le chemin d'une coopération entre l'ENIT et l'Université de Lund démarrée voici peu qui est déjà riche en réalisation concrètes.

C'est ainsi qu'un premier travail en commun a pu se faire dès 1985 sur les briques de terre stabilisées. Il a été suivi en 1987 d'un projet sur l'étancheité des toitures en cours d'élaboration. parrallélement, un échange de chercheurs a pu se réaliser.

Nous pensons en effet que la meilleure facon de réussir une coopération est l'entente entre les hommes sencés la concrétiser. Une rencontre telle que la vôtre contribuera sans doute à nous rapporcher de cet objectif.

Je tiens à remercier chaleureusement les éminents scientifiques venus pour nous faire part de leur résultats les plus actuels et réhausser par leur présence cette importante manifestation.

Je remercie également les collègues tunisiens qui ont eu la lourde tâche d'assurer la préparation matérielle de cette rencontre et je cite en particulier, mon collègue et ami Mohamed Tahar CHAIEB qui, fidèle à son habitude, a beaucoup donné de lui même, pour que ce séminaire se déroule dans de bonnes conditions.

Je vous souhaite à tous beaucoup de succès dans vos travaux et je souhaite à nos amis de l'Université de Lund un agréable séjour en Tunisie.

-A.FRIAA-

Recherche pratique sur le béton à l'Universite de Lund

Lars Boström, Bo Johansson
Division of Building Materials
Lund Institute of Technology

Abstract

At the departemnt of Building Materials in Lund has the behaviour of concrete been studied since a long time. The international collaboration has been an important part of the work and quiet a few thesesis has been published at the department. This means, there exists a long experiance of concrete research at Building Materials in Lund.

Two big areas of research is fracture mechanics and humidity research and here are some of the more practical research described. The present paper is not an intention to be a research report, but more of a presentation of the activities during the last decade at Building Materials in Lund. But some of the results presented are from recently made experiments.

Fracture Mechanics, Mode I

In the conventional fracture mechanics, Linear Elastic Fracture Mechanics, is the material supposed to behave linear elastic. This method can be applied under certain circumstances. It is possible to investigate the stability and propagation of an existing crack.

In 1976, Hillerborg et al. proposed a fracture mechanics approach, which made it possible to investigate not only the stability and propagation of an existing crack, but also the formation of a crack. This model, called the Fictitious Crack Model, is a strain softening model and the whole stress-deformation relation in tension is used. The model is described in detail in this proceeding, [1].

When working with the Fictitious Crack Model, do we need to know a bit more about the material then the modulus of elasticity and tensile strength. We have to find the complete stress-deformation relation in tension. Usually when looking in literature, the stress-deformation behaviour in tension is described as a line up to the tensile strength, whereafter a brittle fracture occures. This is not true, there exists a strain-softening behaviour after the tensile strength is reached. A typical behaviour for concrete in tension is shown in Figure 1. This curve can be split into two curves, where one curve describes the stress-strain relation for the material outside the fracture zone (damage zone), and one curve describing the stress-deformation realtion in the fracture zone [1].

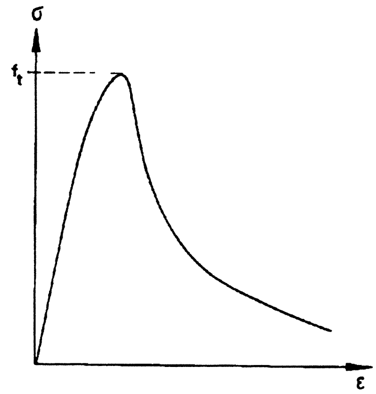

Figure 1. Complete σ-ε curve for concrete [2].

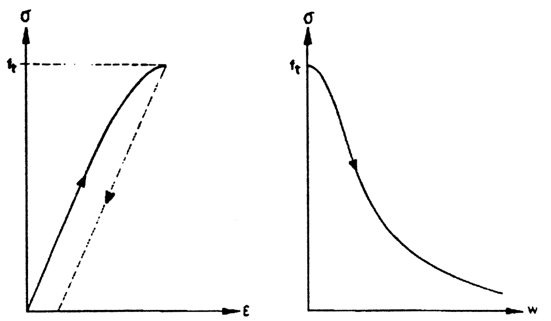

Figure 2. σ-ε curve and σ-w curve for concrete [2].

But, there are difficulties involved in the testing procedure. The test have to be stable, and therefore a very stiff testing machine is necessary, or a testing system with closed loop. The early tests was made without closed loop and a theoretical discussion was made to find a testing system which gives a testing arrangement suitable for this kind of tests.

A testing arrangement can schematically be illustrated by springs, Figure 3 and 4, with different stiffness.

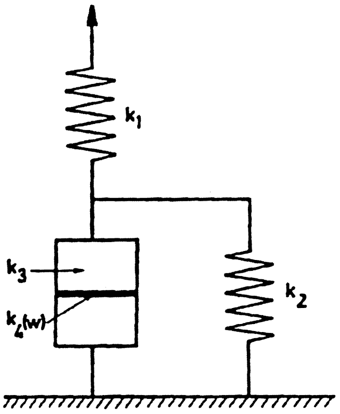

Figure 3. A schematic illustration of a direct tensile test (2).

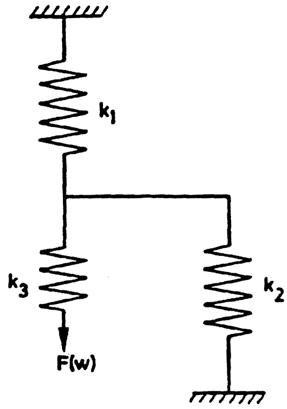

Figure 4. The system of springs used for the calculation of the stiffness k_s [2].

k_1 = the stiffness of the testing machine

k_2 = the stiffness of, for example, steel rods, which can be coupled parallel with the specimen in order to make the testing arrangement stiffer.

k_3 = the stiffness of the specimen outside the fracture zone.

$k_4(w)$ = the stiffness of the fracture zone when the widening of the zone is w. This stiffness depends on the widening of the fracture zone according to the σ-w curve for the material.

If we regard the amount of energy in the two different parts of the testing arrangement, i.e. the amount of energy necessary to widen the fracture zone from 0 to w, (Q_F), and the amount of energy stored in the system of springs outside the fracture zone when the widening of the fracture zone equals w, (Q_S). These energies can be expressed as

$$Q_F = A\int_0^w \sigma(w)\,dw \qquad \text{Eq (1)}$$

$$Q_S = \frac{(F(w))^2}{2k_S} = \frac{A^2(\sigma(w))^2}{2k_S} \qquad \text{Eq (2)}$$

A = cross sectional area of the specimen where the fracture zone is located.

k_s = the stiffness of the system of springs shown in Figure 3.

The stiffness k_s can be expressed as

$$k_s = k_3(k_1 + k_2)/(k_1 + k_2 + k_3) \qquad \text{Eq. (3)}$$

If the width of the fracture zone increases from w to w + dw, the fracture will be stable if energy is consumed. And from this do we get the conditions which gives a stable tensile test.

$$\frac{\partial}{\partial w}(Q_F + Q_S) = A\sigma(w) + \frac{A^2\sigma(w)}{k_S}\,\frac{\partial\sigma(w)}{\partial w} > 0 \qquad \text{Eq (4)}$$

If we assume the unloading curve for the material outside the fracture zone to be parallel to the initial slope, the modulus of elasticity, then can the stiffness of the specimen, k_3, be expressed as

$$k_3 = AE/l \qquad \text{Eq. (5)}$$

A = cross sectional area of specimen

l = length of specimen

We can now express a stability criterion as a function of geometrical data and stiffness of the specimen, slope of the σ-w curve and stiffness of the testing machine.

$$l < -\frac{E}{\left(\frac{\partial\sigma}{\partial w}\right)_{max}} - \frac{AE}{k_1 + k_2} \qquad \text{Eq (6)}$$

where $\left(\frac{\partial\sigma}{\partial w}\right)_{max}$ = steepest slope of the σ-w curve

From this discussion it was found that the ordinary testing machines was to weak for this kind of tests. A new type of testing machine had to be made.

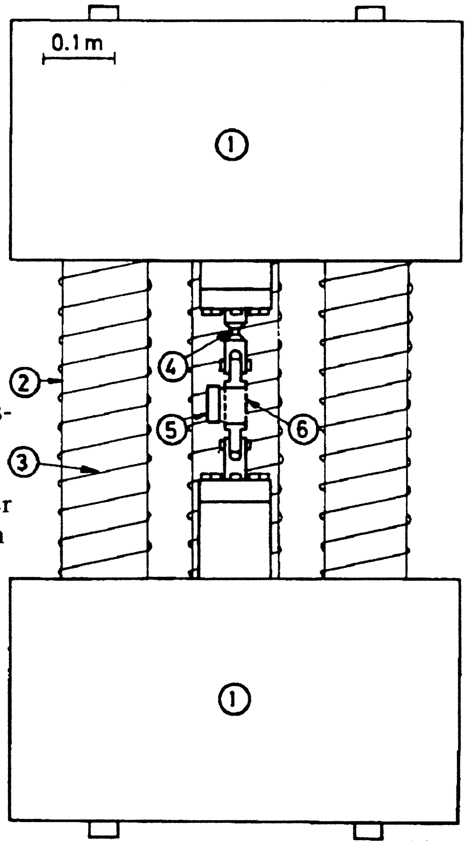

1. Concrete block
2. Aluminum column
3. Heating element
4. Strain gauge for load registration
5. Deformation transducer for deformation registration
6. Specimen

Figure 5. Drawing of a stiff testing arrangement to carry out stable tensile tests on concrete

Figure 5 shows a drawing of the new testing machine in which it is possible to carry out stable tensile tests for concrete. The machine is made from three aluminum columns which are fixed between two concrete blocks. On the columns are heating elements attatched. These heating elements are used to heat the columns and by that, elongate the columns. The specimen is fixed (glued) between the concrete blocks in special holders. When the columns are heated and they elongate, the specimen is subjected to a load which is measured by strain gauges attached to one of the holders. The elongations of the specimen are measured by inductive deformation transducers, which are fixed directly on the specimen. It is important to keep the temperature around the specimen constant, so the aluminum columns are insolated by mineral wool during the test.

To make it possible for the columns to keep a constant temperature, coils of tubes was mounted around the columns. In these coils can kerosene tempered by a thermostat be circulated. This is specially important during the hardening period of the glue when the specimen is fixed between the holders.

Experimental results, Mode I

By use of the stiff testing machine presented, stable tensile tests was carried out on a number of different concrete qualities. In Table 1 are the different mix proportions for the concrete described and the results from the tests are shown in Figure 5.

		Mix 1	Mix 2	Mix 3	Mix 4
Cement (ordinary Portland)	kg/m^3	370	296	296	370
Water	kg/m^3	185	207	207	185
Aggregate	kg/m^3	1755	1755	1755	1755
Max aggr particel size	mm	8	8	2	8
Age at the testing	days	28	28	28	7
Water-cement-ratio		0.5	0.7	0.7	0.5

Table 1. The concrete qualities used in the tests [2].

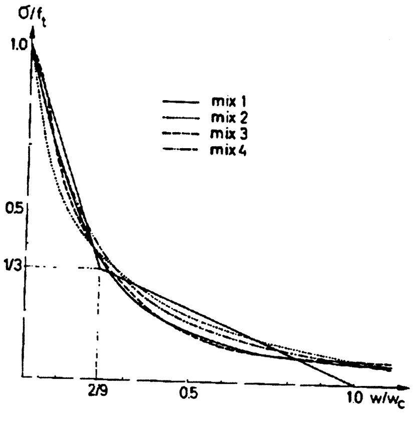

Figure 6. σ/f_t as function of w/w_c for the four concrete qualities presented in Table 1. The two straight lines correspondes to an approximeted relation between relative stress and relative deformation in the fracture zone [2].

Fracture Mechanics, Mixed Mode I and II

The definition of mixed mode is different for different models. The definition used here states that a damage zone always develops in a pure tension mode and that there is no shear stress involved in this state. Following this state, shear stresses will occur, if the principal stress direction changes.

In plain concrete, a damage zone starts developing when the first principal stress reaches the tensile strength of the material. The stress magnetude and mode within the damage zone depend on the deformation size and the variation of stress direction within the zone. If the stress direction remains unchanged while deformation increases (mode I), the damage zone behaviour can be described by a simple stress-deformation curve, σ-w.

In some cases, the stress direction changes after the first formation of the damage zone and it varies with increasing deformation. In such a case, shear stress and shear deformation occur within the damage zone. The damage zone behaviour can be described by a normal stress - normal deformation curve σ-w_n, and a shear stress - shear deformation curve τ-w_s. These properties are path dependent, i.e. σ and τ are functions of both w_n and w_s.

The tests are intended to be performed in such a way that a tensile deformation is first applied so that a damage zone is formed. After the tensile stress has fallen to a predetermined value due to the tensile deformation and the corresponding damage, shear deformations are also imposed. Thus, for example, the tensile deformation may be kept constant while the shear deformation is increased and the corresponding normal and shear forces are measured. Alternatively, the tensile and shear deformations may be increased simultaneosly.

The test arrangement thus has to permit a controlled stable deformation in the two directions. At the same time it has to prevent other deformations, and particulary deformations of an unstable and uncontrollable nature.

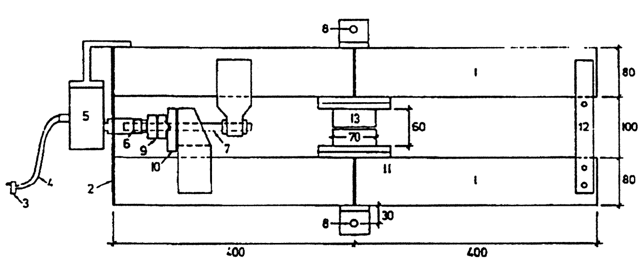

1 - Box Beams (hight=80mm. width=40mm. thickness=3mm)
2 - Steel sheet (hight=260mm. width=100mm. thickness=1mm)
3 - Crank
4 - Flexible axle
5 - Gear box
6 - Nut
7 - Steel bar with strain gauges
8 - Connection point to testing machine
9 - Roller support
10 - Slip support
11 - Steel plates
12 - Lock (it is removed during the test)
13 - Specimen

Figure 7. Test equipment for mixed mode I and II.

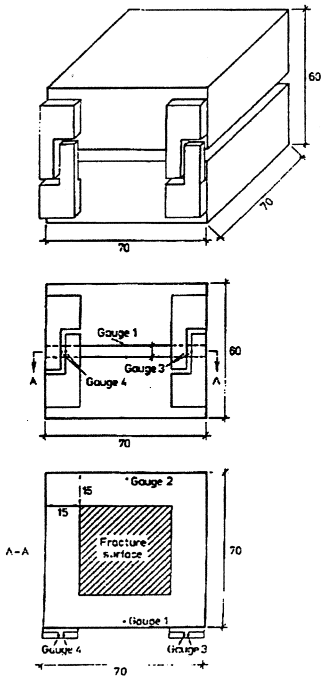

Figure 8. Measuring points in mm.

A real material is never completly homogenous. Even if the force is exactly centered in the specimen during the test, the stress will not be exactly even. As long as the stresses are increasing the test is stable, but as soon as the mean stress starts decreasing the test tends to become unstable.

It can be demonstrated that a test with force centration is always unstable after a damage zone has formed, even if the material is ideally homogenous. Therefore, force application through hinges cannot be expected to give uniform stresses in a damage zone during a tensile test, and the measured decending part of the load-deformation curve for the specimen cannot be used for the evalution of the stress-deformation curve for the material.

What happens in a test with force centration is that the two parts of the specimen on both sides of the damage zone rotate with respect to each other, resulting in an uneaven distribution of the deformations across the damage zone.

In order to make a stable test possible it is necessary to design the test in a way that the force is not centered, but the rotation of the two parts of the specimen with respect to each other is counteracted. Ideally, the deformation should consist of a pure translation.

In practice it is hardly possible to reach this ideal test condition of a pure translation, as the tendency for instability of the specimen will cause bending moments, which in their turn will cause rotational deformations, as no stiffness is infinite. In order to limit the rotation as far as possible the stiffness of that part of the testing arrangement which counteracts the rotation must be high.

The test equipment we are looking for should give the possibility to perform translation deformations in two perpendicular directions at the same time as it contains a stiff arrangement that prevents rotations. We have not been able to design a test equipment which fulfills all these requierments. We have therefore chosen a compromise, which is shown in Figure 6. The specimen is inserted (glued) between two steel beams with high flexural and torsonal stiffness. These beams are connected at one end by means of a thin steel sheet, which keeps the beam ends at a constant distance and prevents their torsonal rotation. The deformations are imposed to the beams. This design permits the fulfilment of the requirment of a high rotational stiffness in spite of deformations in two directions. On the other hand, it does not give a pure translation, but a small rotation, which is however known and not accidental.

It is possible to perform theoretical analyses of this test design in order to check the influence of the rotation, the stiffness, and possible exentricities. Such analyses have been made by means of the fictitious crack model [3], and it shows that the rotation caused by this design causes small errors in the results compared to the errors which may be caused by an insufficient stiffness. The choice of the details of the test equipment has been made on this theoretical analysis.

Test results, Mixed Mode I and II

The tests which will be presented were performed in such a way that a normal deformation is first applied so that a damage zone is formed. After the normal stress has reached the tensile strength of the material due to the normal deformation, shear deformations are also imposed. After this point the tests have been continued in such a way that the imposed shear deformations and normal deformations have fulfilled a predetermined function, by means of continuous adjustment of the shear deformation with respect to normal deformation.

The function used was a parabel function with the relation between normal deformation and shear deformation as follows:

$$w_n = \beta \sqrt{w_s} \qquad \text{Eq. (7)}$$

where $\beta = 0.40, 0.50, 0.60, 0.70, 0.80, 0.90 \text{ mm}^{0.5}$

The normal load is measured by means of a load cell on the testing machine. The shear load is measured by means of strain gauges glued on the steel bar, see Figure 7.

Deformations are measured by means of clip gauges. The position of the measuring points are shown in Figure 8. The normal deformation is the mean value of gauge 1 and 2 and shear deformation is the mean value of gauge 3 and 4.

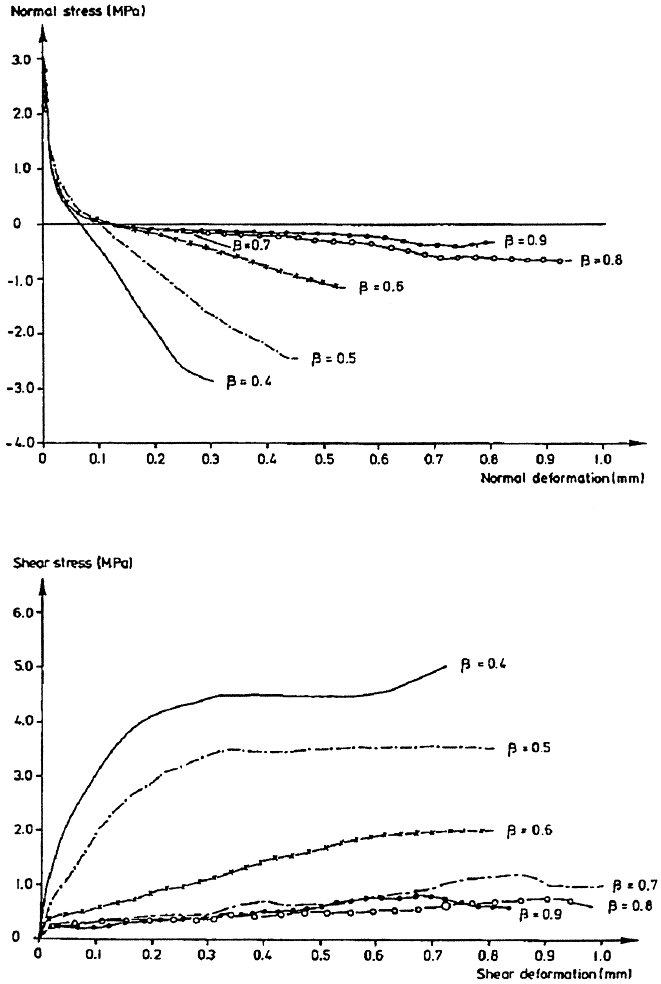

Figure 9. Test results for parable paths in mixed mode I and II.

The results from the tests are shown in Figure 9. They show that the initial part of the normal stress - normal deformation curve is almost unaffected by the deformation path. If there are any path dependencies they are not significant due to scatter in this type of test.

In the lower parts of the normal stress - normal deformation curves a linear relation between stress and deformation can be recognized. The slope of this part decreases when β increases and it approaches the slope of curves from mode I.

The initial part of the shear stress - shear deformation curves has a relatively steep slope, which decreases with increasing stress and β. The results show that there is no significant difference between the curves when β is greater than 0.7 [4].

Humidity Researche

In the area of humidity research and especially the research of water vapour permeability in concrete has been studied at the department of Building Materials in Lund for many years. Here is a new method described from which it is possible to calculate the moisture permeability and to determine its dependence on the relative humidity. The main work has been carried out by Göran Hedenblad at the division of Building Materials in Lund.

Experimental arrangement

The principle of the experimental arrangement is shown in Figure 10. The water vapour flow is unidimensional going from bottom to top of the specimen.

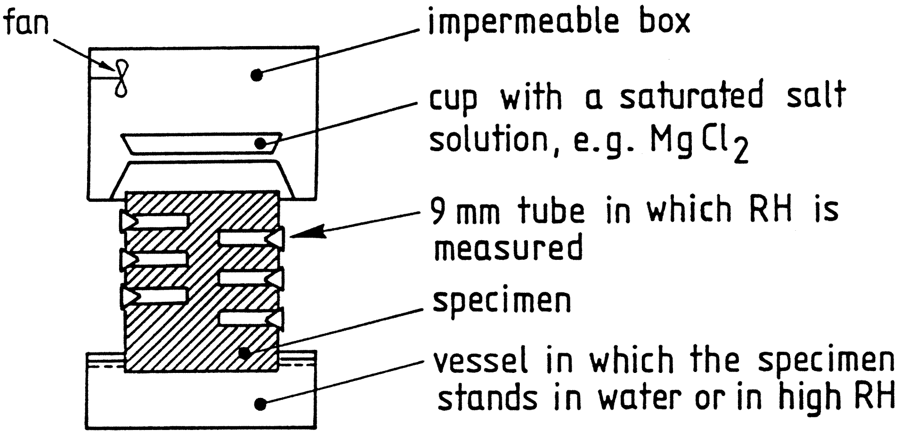
fan
impermeable box
cup with a saturated salt solution, e.g. $MgCl_2$
9 mm tube in which RH is measured
specimen
vessel in which the specimen stands in water or in high RH

Figure 10. Principle of the experiment [5].

The upper part consists of a impermeable box, in which the relative humidity (ϕ) is held constant by means of a saturated salt solution in a cup. In our case, magnesium chloride for which ϕ is 33% was used. The cup is weighed every week, so that the flow from the specimen is obtained. The air inside the box is circulated by a small fan. The upper surface of the specimen is exposed to the air inside the box.

Surfaces of the specimen exposed to the surrounding air in the room are sealed with 2 mm nearly impermeable epoxy resin. The bottom surface of the specimen stands in water or in air with high relative humidity.

Tubes about 9 mm in diameter, are embedded in the sides of the specimen. Internal end surfaces of the tubes are open to the concrete so that ϕ in the tubes is in equilibrium with ϕ in the concrete. Starting with the uppermost tube, ϕ is measured gradually downwards with a small capacitive ϕ-sensor.

The bottom surface of the specimen is 0.2 x 0.2 m^2. The heights of the specimen are 0.063, 0.100 and 0.150 m. The results, presented in this paper, derive from specimens with a height of 0.100 m.

In order to determine moisture permeability (δ_v) of concrete not dried to a large extent, specimens are seal cured for at least one month preceeding the test.

Tested materials

The following test program concerning different compositions of concrete is carried out:

- concrete with different water-cement ratio, see Table 2.
- concrete with $W_0/C = 0.7$ with different amounts of aggregate.
- concrete with $W_0/C = 0.7$ with different amounts of air.

The crushed stone, 8-18 mm, consists of quartzite.

W_o/C	Cement, C kg/m^3	Water, W_o kg/m^3	Sand/Gravel kg/m^3	Crushed stone 8-18 mm kg/m^3
0.5	368	184.0	990	810
0.6	328	196.8	990	810
0.7	296	207.2	990	810
0.8	270	216.0	990	810

Table 2. Composition of concrete with different W_0/C.

Evalution of moisture permeability

According to Fick's first law we can write

$$g = -\delta_v \cdot \text{grad } v \quad \text{Eq. (8)}$$

where

g = density of moisture flow rate (kg/m^2s)

v = humidity by volume in the pores of the specimen (kg/m^3)

Under isothermal conditions, Fick's first law can be written

$$\delta_v = -g/v_s / \text{grad } \phi \quad \text{Eq. (9)}$$

where

v_s = v at saturation

Under stationary conditions g and grad ϕ can be measured and δ_v can be calculated as a function of ϕ.

The moisture flow rate from the top surface of the specimen advances according to Figure 11. The moisture flow rate in Figure 11 is not corrected for influence of tubes in the specimen, tightening between specimen and upper box, and flow through the epoxy resin.

The principle ϕ-distribution in a specimen is shown in Figure 12. Grad ϕ is graphically derived from the slope of the ϕ-distribution curve.

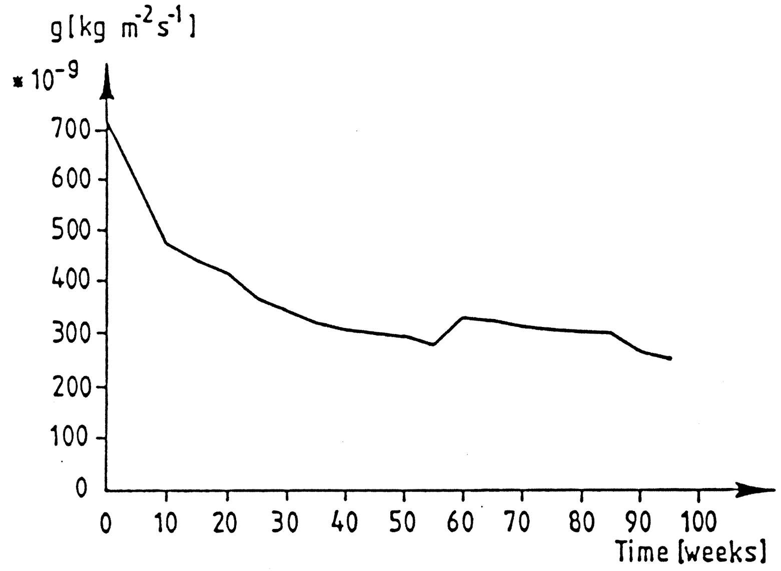

Figure 11. Moisture flow rate from a specimen.

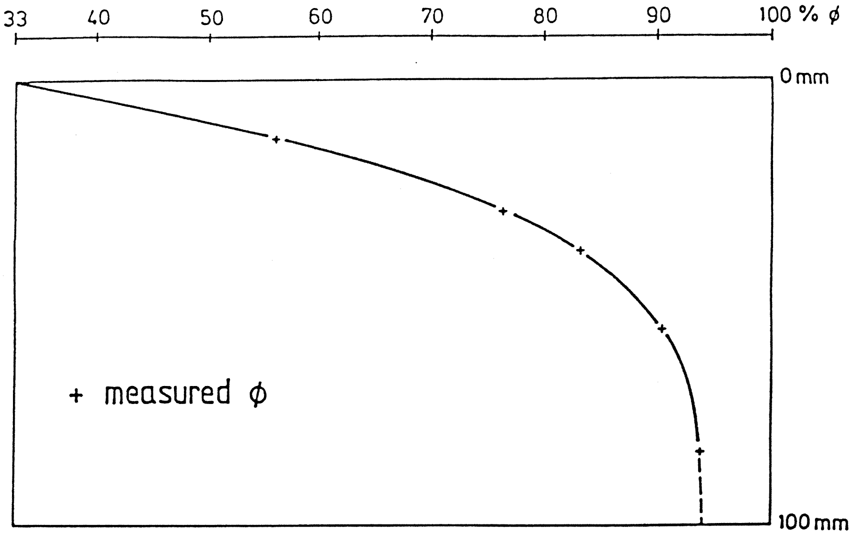

Figure 12. Principle ϕ-distribution in a specimen with a height of 0.100 m.

Some results

Flows and distributions

Some ϕ-distributions from the specimens with different W_0/C are shown in Figure 13, next page.

For most of the specimens, measured and calculated ϕ-distributions are nearly the same. In the calculated ϕ-distributions the flows are assumed to be correctly measured. For the calculated ϕ-distributions, see mean for δ_v value in Table 4.

As shown in Figure 13, relative humidities in the bottom of specimens standing in water are probably lower than 100%. This can be explained by the fact that cement containing alkali metal compounds has a lower maximun ϕ than 100%, [6].

In Table 3 the measured flows are shown as a function of W_0/C and the circumstances at the bottom of the specimens.

Comparing flows in specimens standing in water with flows in specimens in moist air, it can be seen that the difference is very small at $W_0/C = 0.5$, and at $W_0/C = 0.8$ flows differ only by a factor of about 4. Flows for specimens standing in moist air are nearly the same for different values of W_0/C. This means W_0/C has very little influence on the moisture flow if ϕ on the moisty side is below about 95%.

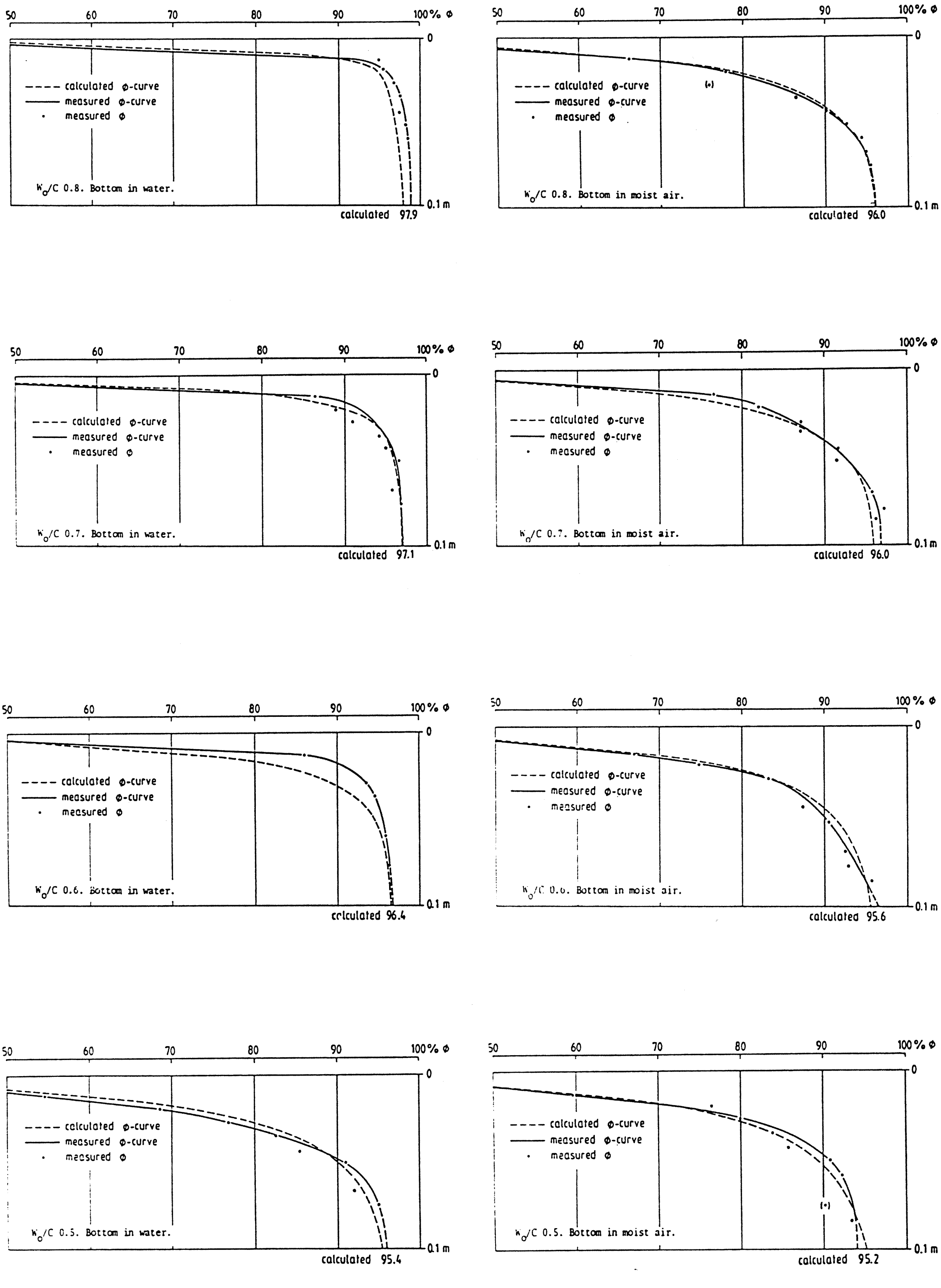

Figure 13: Distributions of the relative humidity in specimens with a hight of 0.10 m.

W_o/C	g from specimen where the bottom is in water $kg\ m^{-2}\ s^{-1}$	g from specimen where the bottom is in moist air $kg\ m^{-2}\ s^{-1}$	$g_{water}/g_{most\ air}$
0.5	$65 \cdot 10^{-9}$	$62 \cdot 10^{-9}$	1.05
0.6	$105 \cdot 10^{-9}$	$71 \cdot 10^{-9}$	1.48
0.7	$165 \cdot 10^{-9}$	$84 \cdot 10^{-9}$	1.96
0.8	$297 \cdot 10^{-9}$	$82 \cdot 10^{-9}$	3.62

Table 3. Flows from 0.1 m high specimens.

Evaluated moisture permeability

The moisture permeability is evaluated according to Eq. (9) and is shown in Table 4.

ϕ %	$\delta_v \cdot 10^6 (m^2/s)$									Coefficient of variation
	W_o/C 0.5		W_o/C 0.6		W_o/C 0.7		W_o/C 0.8		mean val.	
	bott. in water	bott. in moist air	bott. in water	bott. in moist air	bott. in water	bott. in moist air	bott. in water	bott. in moist air		
33-70	0.19	0.18		0.19				0.16	0.18	0.08
70	0.19	0.18		0.27				0.26	0.22	0.21
75	0.38	0.18		0.31				0.39	0.32	0.31
80	0.49	0.42		0.45		0.69		0.60	0.53	0.21
84	0.62	0.61		0.73		1.04		0.80	0.76	0.23
86	0.71	0.80		1.19		1.13		0.93	0.95	0.22
88	0.77	1.05	0.70	1.62	0.91	1.40		1.12	1.08	0.31
90	0.93	1.45	1.15	2.12	1.69	1.71		1.49	1.51	0.26
91	1.10		1.60	2.41	2.43	1.93		1.76	1.87	0.27
92	1.40		2.15	2.79	3.29	2.13		2.02	2.30	0.29
93	1.82		3.02	3.07	4.12	2.52	1.96	2.47	2.71	0.29
94	2.86		4.99	3.27	5.49	3.01	3.12	3.06	3.69	0.29
95	5.37		9.48		7.06		5.20		6.78	0.29
									estimated mean values	
96			23		14		9		23	
97							17		60	
98									130	
98.8									250	

Table 4. δ_v as a function of W_0/C and ϕ.

In Table 4 it is seen that there is no influence on δ_v with W_0/C for ϕ up to about 95%. δ_v is not evaluated for higher ϕ than 95%, because it is very difficult to evaluate the steep sloops of the ϕ-distribution curve. In the calculated ϕ-distribution curve, δ_v are assumed above $\phi = 95\%$.

The reason for estimating values above $\phi = 95\%$ lies in the fact that the largest pores in the cement paste (about 200-500 nm in diameter) remaining unfilled with liquied water until ϕ approaches its maximun value, retard water transport, which increases considerably upon filling of these pores. As the volume of the largest pores is greater in concrete with high W_0/C as compared to concrete with low W_0/C, such concrete has a higher δ_v when the pores are filled.

Calculations of drying

Can the evaluated δ_v:s, which are determined at steady state conditions, be used in none steady state computer simulations? To investigate this, computer simulations were made with the above moisture permeabilities for tests made by Pihlajavaara [6] and Nilsson [7]. The desorption isotherms which were used are published in [7]. For both the tests 160 mm long specimens were used, which dried uniaxially. ϕ in the surrounding air was about 40%. Pihlajavaara measured the moisture content by volume after 68, 179 and 293 days. Nilsson measured ϕ after 6 and 260 days. Pihlajavaaras specimens were seal cured for 10 months. Nilssons specimens was seal cured for 28 days. The results are shown in Figure 14

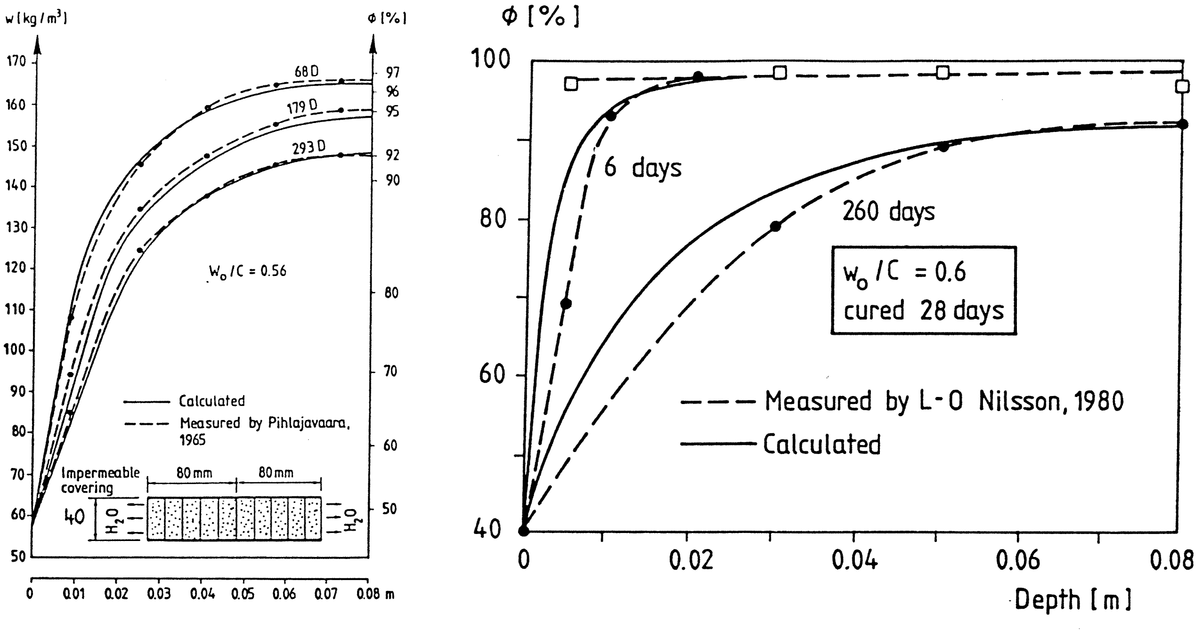

Figure 14. Comparison between measured and calculated moisture distributions.

REFERENCES

[1] Hillerborg A. Application of Fracture Mechanics to Concrete. (Lund Institute of Technology, Div. of Building Materials, Lund 1988), Report TVBM-3030.

[2] Petersson P-E. Crack Growth and Development of Fracture Zones in Plain Concrete and Similar Materials. (Lund Institute of Technology, Div. of Building Materials, Lund 1981). Report TVBM-1006

[3] Hassanzadeh M. et. al Tests of Material Properties in Mixed Mode I and II. (Proc. of International Conference on Fracture of Concrete and Rock, pp 353-358. June 17-19, 1987 Houston, U.S.A.)

[4] Hassanzadeh M. Determination of Fracture Zone Properties in Mixed Mode I and II. (to be published)

[5] Hedenblad G. Effect of Soluble Salt on the Sorption Isotherm, (Lund Institute of Technology, Div. of Building Materials, Lund 1987). Report TVBM-3035.

[6] Pihlajavaara S.E. On the Main Features Methods of Investigation of Drying and Related Phenomena in Concrete, (University of Helsinki, 1965).

[7] Nilsson L-O. Hygroscopic Moisture in Concrete - Drying, Measurements and Related Material Properties, (Lund Institute of Technology, Div. of Building Materials, Lund 1980) Report TVBM-1003.

METHODES D'ETUDES DE LA CORROSION DANS LES BETONS EN MILIEU CHLORURE

par : CHAIEB Mohamed Tahar, TRIKI Ezzeddine, HACHANI Leila

RESUME :

La présence d'ions chlorures dans le béton entrave, à partir d'un certain seuil de concentration, la corrosion par enrouillement des armatures pouvant aboutir à la ruine complète de l'ouvrage. L'évaluation de la vitesse de diffusion des ions agressifs à travers la matrice est primordiale pour prévoir les risques encourus. Les méthodes électrochimiques classiques (mesure du potentiel d'électrode, mesure de la résistance de polarisation et de l'impédance) peuvent être adaptées à l'étude de la dégradations des bétons; elles fournissent conjointement aux essais de diffusion, des renseignement précis sur le comportement électrochimique des armatures, sur leur vitesse de corrosion et sur le rôle des chlorures dans le processus de dégradation et de passivation des armatures.

ESSENTIAL DATA FOR SERVICE LIFE PREDICTION

Göran Fagerlund

CEMENTA AB, P.O. Box 144, S-182 21 DANDERYD, Sweden

ABSTRACT

Durability design based upon old experience-codes of good practice etc - is still widely used. It is, however, a dangerous method that has led to a lot of durability problems; examples are given in the report. A design based upon a service life calculation has many advantages but is very complex. A lot of data concerning functional requirements, environment, deterioration mechanism and material are needed. Examples of relatively elaborate methods for the estimation of the service life of concrete are presented briefly. The use of the service life concept means that the traditional accelerated test methods must often be abandoned in favour of non-accelerated tests.

1 TODAY'S SITUATION

When a building designer selects the materials that shall be included in a certain building component - e.g. a floor, an external wall, a roof etc - and when he selects the way to combine the different materials to form the finished component, it is fairly easy for him to satisfy the required function of the component at "time zero"; i.e. at the time of delivery of the finished building. He can base his choice of materials and his design on reasonably welldefined properties that are listed in product brochures from the producer or utilize general data listed in handbooks etc; such properties include the 28-day strength of the concrete or the heat transfer coefficient of the heat insulation. The considerably more complex properties that describe the "ageing" of the material in situ, i.e. the time-dependent interaction between two adjacent materials, or the interaction between the material and the surrounding environment, or the effect of possible changes in the structure or in the environment, are of no importance for the function at time zero. Those properties are also very seldom accounted for by the producer or in handbooks. In many cases, the producer and the designer do not even know which material properties are of importance for the long-term function.

Carpets to be used on concrete floors on the ground can be taken as trivial examples of products for which important information is still lacking to a great extent. Properties such as colour, thickness etc are accounted for by the manufacturers but properties that are extremely important for the long term function are normally unknown; e.g. the (possibly time -dependent) relation between the relative humidity (RH) and the moisture diffusivity of the carpet, or the interaction between the carpet and different glues and putties in the presence of alkaline moisture from the concrete. The effect of the permeability of the carpet on the moisture state of the glue and putty is shown in Fig. 1. The chart is valid for one-family houses with a concrete slab directly on the ground, /1/. The RH at the interface will be 90% if the carpet has a diffusivity at its present moisture state that is 1/50 of that of the concrete slab but only 82% if the diffusivity ratio is 1/5 (assuming a heat insulation of the floor that gives a temperature drop of 1.5°C and an RH value in the room of 40%). This difference in RH is dramatic; most putties and glues are durable at RH = 82% but very few at RH = 90% (in fact, however, the effect of the RH on the durability of glues and putties is also unkown to a large extent. There are certainly materials (organic) that do not even endure an RH as low as 80% for a very long time as has been experienced in Sweden).

Another example of missing information, valid for the same type of structure, deals with the moisture absorption in the heat insulation that should normally be laid beneath the concrete in order to lower the RH value of the flooring material; Fig. 1. It is very important that this layer does not absorb water. If it does, the RH value of the concrete could reach too high a value. A material often used in Sweden is expanded clay granules. A layer of about 25 cm should theoretically lower the RH value in the floor to about 80% providing there is no capillarity in the layer. Previously, there were very few problems in Sweden with such layers. Nor did simple capillarity tests with layers of expanded clay give reason to believe that the material absorbed water to a height of more than a few centimetres. The manufacturer therefore stated that his material had "no capillary suction", and this was believed by the designers. Then, over a period of some years, a large amount of moisture-induced damage occurred in floors with that type of insulation and covered with plastic carpets. All measurements indicated that moisture must have been transferred from the ground to the concrete slab via the insulation. A theoretical analysis /2/ showed that even an extremely slow capillary suction, for example in dust grains on the surface of the granules, was enough to raise the RH value of the floor to an unacceptable level for the flooring material; the diffusion downwards caused by the thermal gradient and the drying upwards through the very dense carpet was not enough to compensate for even a slow capillarity. This slow capillary suction could not be detected by the rather coarse method used for testing the capillarity. Consequently the producer could be said to have been in "good faith". Quite a new measurement principle was suggested by which even a very slow capillary suction could be observed /2/. Unfortunately, this method has never come into use and the manufacturer still claims that his material has "no suction". Fortunately, however, the material is very little used due to the poor experience obtained, but obtaining that experience, which could have been predicted if the material had been correctly tested, has cost a lot of money and caused much suffering among residents.

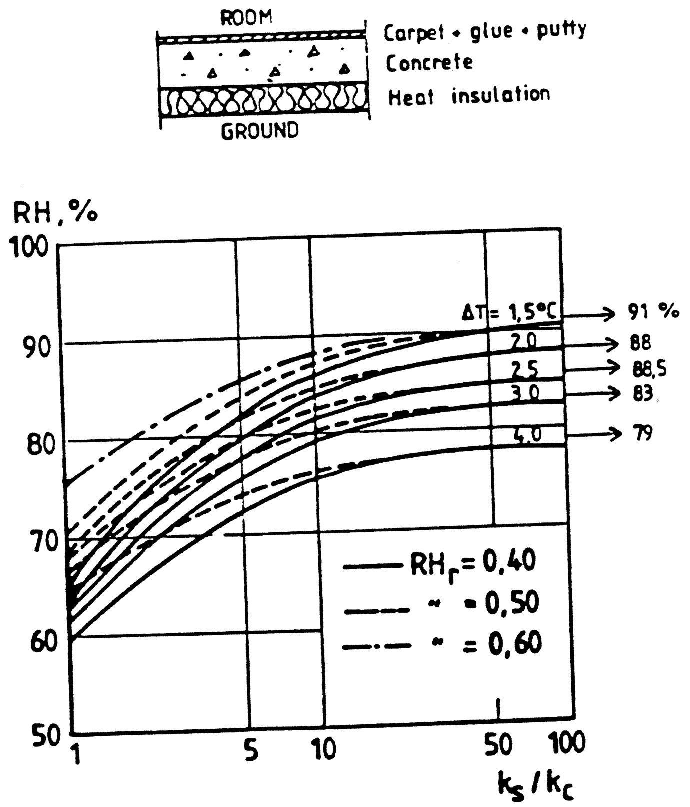

Fig. 1 The equilibrium relative humidity at the interface between a carpet and a concrete slab on the ground /1/. (ΔT = the temperature drop across the floor, RH_r = RH in the room above the floor, k_s and k_c are the moisture diffusivities of the concrete slab and the carpet respectively).

There are of course many more examples to give of durability problems that have been caused by ignorance of data, lack of data or even misleading data.

This evident lack of interest in the long term performance of a building during its design phase is rather remarkable. It reflects the considerable complexity involved in dealing with durability and service life predictions, especially the very great difficulties in making accurate service life calculations. Instead of actually designing the building with regard to its durability one simply turns to experience of the behaviour of similar buildings in similar environments. This experience is normally expressed in terms of simple rules in different official standards or in codes of good practice. Such rules are certainly quantitative but do not deal with service life directly but merely with maximum or minimum values of certain substituting properties that are supposed to be coupled to service life.

Concrete can be used as an example of a material for which substituting properties are widely used. The durability requirements are normally expressed in terms of requirements for:

- compressive strength
- water-cement ratio
- permeability to water (sometimes to air)
- air-content of the fresh concrete
- concrete cover over the reinforcement
- cement type

Many of those properties are measured on specially manufactured specimens and not on the concrete in the erected structure. This is also typical of materials other than concrete. In many cases, the specimens used for quality control are not even very representative of the structure. The consequences of a design based upon experience only will be discussed below after which the possibilities of an alternative design based upon the service life concept will be presented.

2 EXPERIENCE AS A BASIS FOR SERVICE LIFE DESIGN

A design based solely upon experience of the behaviour of similar structures has many drawbacks. It is very defensive and dangerous in a situation where the design principles are often changed more or less radically and where more and more new building materials and components are marketed and utilized rather uncritically.

In Sweden, there are many examples of changes in building construction that have caused great problems during the last decades, simply because no-one ever analyzed the consequences of such changes on the service life. Therefore the old design rules were kept. In many of those cases it was rather small changes that caused the troubles, because the previously used design principle had a very low factor of safety against damage; the small change transferred the structure from the "durable side" to the "non-durable". Some examples will be given:

* Concrete floor slabs in one-family houses were built directly on moist ground without changing the design that was previously used - with fairly good results - for floors on well-drained ground. Thus, no heat insulation was used in the floor. Even a very elementary moisture mechanics analysis had shown that this design meant great risks of damage (decay, bad smell, loosening) in conjunction with certain types of organic flooring materials. A change in RH from perhaps 90% in a well-drained ground to 100% in a moist ground is often disastrous. But such analyses were never made by the designers and the material producers did not point out the risks, simply because they did not realize that the environment in which their material should function was radically changed. Consequently, thousands of one-family houses in Sweden are now more or less damaged by moisture, due to a design based upon old, but irrelevant, experience.

* For concrete, the concept "quality" has normally been synonymous with the strength. Thus, in a more severe environment a higher strength level has been required. Strength has been used as a substituting property for W/C ratio which is in turn a measure of such properties as permeability, amount of freezable water, OH concentration of the pore water which effects the protection of the reinforcement, etc.

  The use of strength as a quality criterion is based upon the assumption of a relative well-defined relation between strength and W/C ratio. During the last decades there has been a gradual change in this relation, however, towards higher strength levels for the same W/C ratio; the cement strength has increased and the ready-mix concrete industry has become more skilled. Consequently, the same requirement with regard to strength means a higher W/C ratio and a lower durability today than it did 20 years ago. The mean relations for Swedish ready-mix concrete in the beginning of the 1960's and to-day are shown in Fig. 2. The change is rather drastic since even a small change in W/C ratio might have a very great effect on the durability.

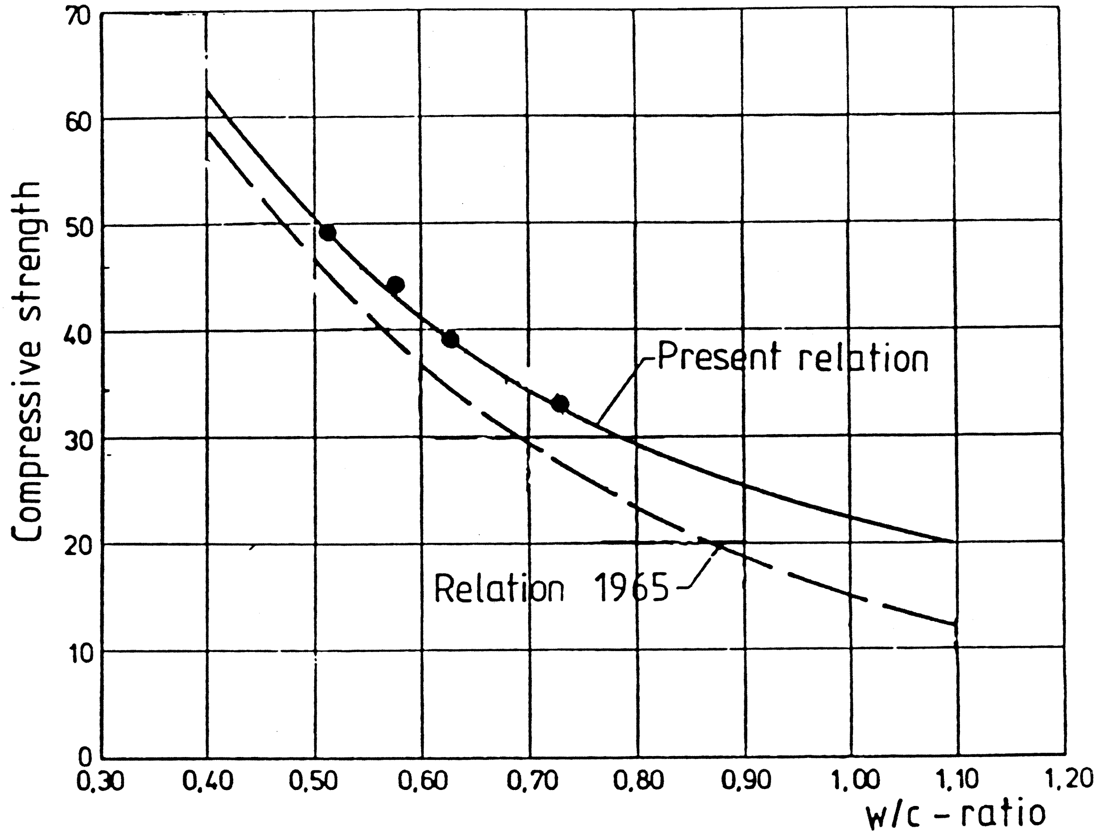

Fig. 2 The mean relation between water-cement ratio and compressive strength at 28 days for Swedish ready-mix concrete.

Similar cases can also be expected to occur in the future. Some Swedish examples of current changes in building design, in building materials and in environment that will have a great, but so far unexplored, effect on the service life of buildings will be described below. Some of them are certainly of current interest in many more countries.

* The transition from concrete floors directly on the ground to well insulated wooden floors separated from the ground by an aerated space. The risk of moisture induced damage in such structures is imminent unless the choice of materials and design are made with great care. This choice must be based on detailed analyses of the microclimate in the floor, and on functional analyses and tests of the durability of the materials used.

* Increased use of glued wooden fiber beams in highly insulated walls, floors and roofs instead of solid wooden girders. The reason for this is, of course, to reduce the building costs but it may also result in reduced durability. The effect of moisture and temperature on the mechanical and physical behaviour of that type of building element has not been studied very much.

- Additional heat insulation of older buildings. This means a change of the moisture state in the old part of the structure, eventually leading to incipient decay. Relatively small changes in the climate could be disastrous.

- Utilization of the possibility of heat accumulation in heavy building components; e.g. in thick concrete slabs on the ground. This will lead to new temperature and moisture fields that might reduce the service life if precautions are not taken in the design.

- Utilization of industrial wastes in the production of building materials, especially the use of different fly-ashes in cement and concrete. The effect on strength is often marginal and can be easily compensated for. The effect on durability, on the other hand, could be drastic. There are no reasons to believe that the "normal" relation between strength and durability should hold true. It is often claimed that materials such as fly-ash from coal burning or silica-fume should reduce the water permeability at equal strength and that this should be favourable for durability. This is nonsense because water permeability is only one parameter affecting durability. Such parameters as the pH-value of the pore water, base reserve, air content, air-pore structure, gas diffusivity are often influenced in a negative manner by the use of fly-ashes. Besides, concrete with fly-ashes are much more sensitive to bad curing than are normal concretes. Consequently, one cannot be sure that the low permeability of laboratory specimens will be reproduced in the surface layer of the real structure.

- Energy saving in the burning of ceramic products - tiles, bricks. This could reduce the frost-resistance and the chemical resistance; e.g. the resistance against alkali attack from the mortar. Old experience could not be relied upon in such cases.

- Increased acidification of the environment, which might affect the service life of underground structures - foundations, pipes etc.

All those examples show that one cannot rely upon experience or upon qualitative assessments of durability. It is quite clear that we must try to find quantitative methods of analyzing durability, preferably expressed in years of expected service life calculated during the design stage. It is then necessary to analyze not only each material separately but also the time-dependent interaction between all materials in the building component.

In the same manner, it is important that the service life concept be regarded more consciously in official standards and norms. The authorities must be aware of the fact that the fixation of a certain minimum quality level (e.g. the required strength or W/C-ratio of concrete in a certain environment) means that they have also settled the average service life of the whole future population of that type of concrete structure. Today such quality levels are settled on the rather defective information gained by "old experience" and unreliable simplified laboratory tests.

3 THE CONCEPT "SERVICE LIFE" - DEFINITION AND FACTORS TO CONSIDER

The service life of a building material or a building component is the space of time during which it fulfils all functional requirements. The concept service life is therefore meaningless unless it is possible to express the functional requirements in a perceptible, quantitative way. Consequently, considerable effort must be devoted to expressing the functional requirement in terms of measurable properties such as loadbearing capacity, deformation, strength, surface spalling, discoloration, emission of dangerous substances etc. Such functional requirements, although quantitative, are often very complex and composed of a number of more basic properties; e.g. the loadbearing capacity of a reinforced concrete beam exposed to frost attack is determined by such time-dependent factors as, (i) the long-term compressive strength of the concrete, (ii) the spalling depth of the concrete surface, (iii) the corrosion depth of the reinforcement bar /3/. All these basic properties must be analyzed if a service life estimate is to be possible. In the case of a reinforced concrete beam, therefore, at least three different deterioration mechanisms must be known /3/.

In many cases it is enough to study the interaction between the material or component and the external environment. In other cases it is also necessary to investigate the internal interaction between different materials. One example is the system "concrete on ground - putty - glue - carpet" which must be treated as a unity; the service life - e.g. the degradation of bond - could be quite different for different material combinations despite the fact that the external climate is constant.

The service life of a given structure is of course a function of the environment, as is illustrated by the following two examples:

Example 1;

Fig. 3 shows the degradation of bond between a plastic carpet and a concrete slab on the ground. The functional requirement is a bond of at least 0.2 MPa. This value is reached after

1 month when RH = 95% at the interface between the concrete and the carpet. It is reached after 3 months when RH = 90% but it is never reached when RH = 85%. In many practical cases, a high RH prevails only during a few months before the concrete slab has dried downwards towards a harmless equilibrium moisture content. Therefore no problems occur. In other cases the equilibrium moisture is high enough to give a low service life, or the time to reach a low equilibrium RH is so long that moisture-induced damage has time to develop.

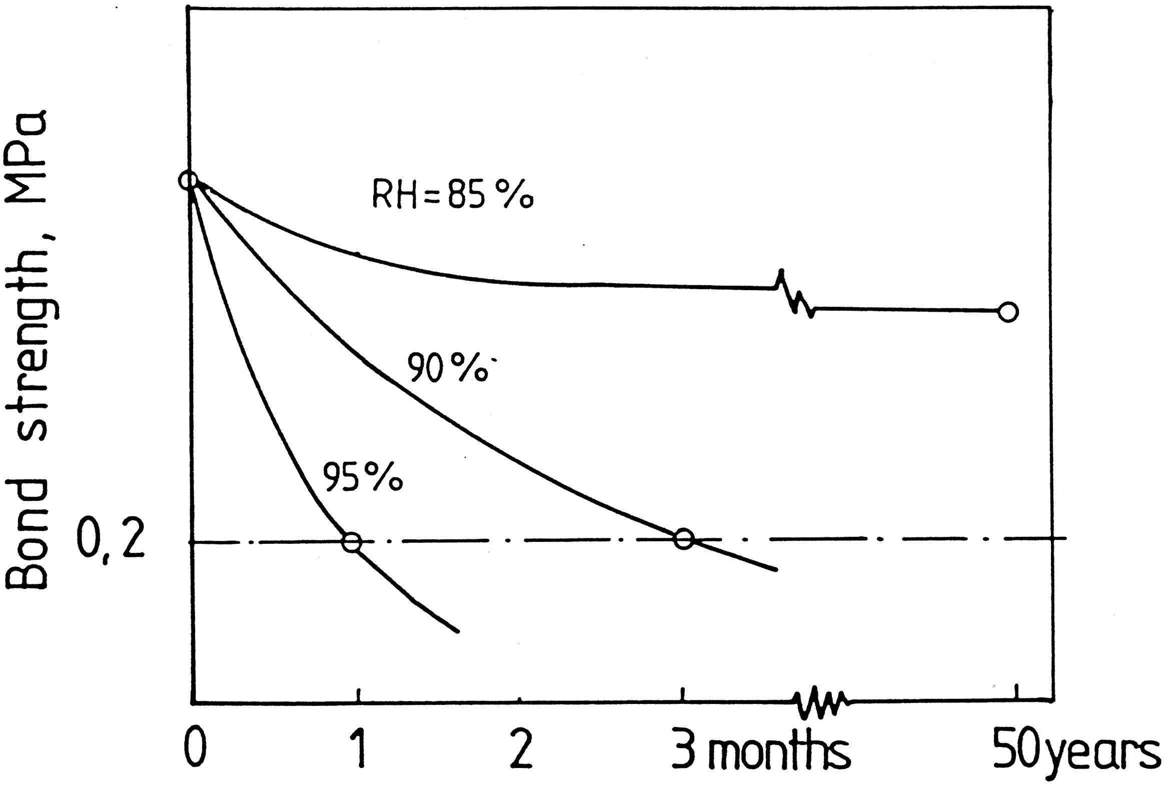

Fig. 3 Hypothetical curves over the degradation of bond between the carpet and the concrete slab.

Example 2;

Fig. 4 shows an outdoor parking deck in two different environments. The destruction curves are indicated. Environment 1 is completely "free of salts" while environment 2 contains both de-icing salts and freeze/thaw cycles. Loadbearing capacity is the function under consideration. In environment 1, no damage occurs until the carbonation front has reached the reinforcement bars (point A) at which point these start to corrode with a speed that is controlled by the oxygen diffusion into the bars. At a certain stage (point B) the concrete cover is spalled off and the function fails. The increase in serviceability until point A depends on the continued hydration. The service life is t_1.

In environment 2, a certain spalling occurs already during the first freeze/thaw cycles due to the de-icing salts. After one or two years (point C) chlorides of a dangerous concentration have reached the reinforcement bars at which point the passivation fails and the bars start to corrode. The serviceability diminishes right from the start; at first as a consequense of the spalling of the surface; after point C mainly due to corrosion. The minimum acceptable loadbearing capacity is already reached before the concrete cover is spalled off (which occurs at point D) as a consequence of the reduction of concrete and reinforcement cross-sections. The service life is t_2 which is much shorter than t_1.

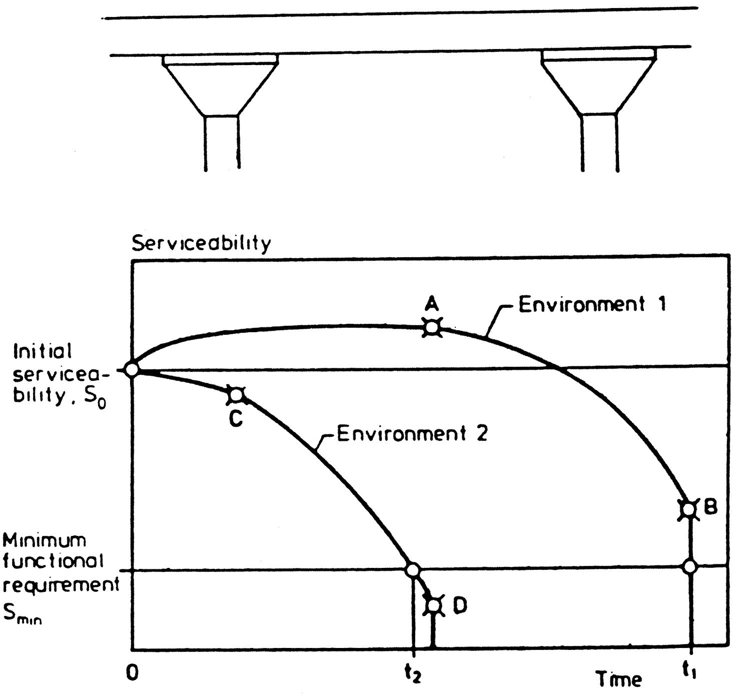

Fig. 4 Hypothetical serviceability-time curves of an outdoor parking deck. o indicates a change in the deterioration mechanism; see the text.

Some important (and some trivial) conclusions can be drawn from these two examples;

1: Different types of materials, e.g. different types of flooring materials, will have different serviceability - time curves in the same environment. The reason could very well be that quite different destruction mechanisms are acting. By utilizing the concept "service life" it is, however, in theory at least, possible to make a fair judgement between the different materials. Materials with the same service life have equal durability despite the fact that they are different in many other aspects, chemically and physically. Such a conclusion cannot be drawn on the basis of information from ordinary durability tests. These tests are often accelerated - see below - and quite different types of tests are often used for different types of materials. The interpretation problems are therefore considerable.

2: The functional requirement(s) must be clear and quantified. In Example 1 bond strength was used as the criterion for function. Another, equally important (or more important) criterion is "bad smell" which might appear long before the bond fails. This is caused by the decay of organic substances beneath the plastic carpet. Decay will follow other time-curves for each value of RH. Consequently, the service life will be different also.

The breaking down of a functional requirement into basic, measurable properties is often very complicated but is necessary for a reliable service life calculation.

3: The service life is highly dependent on the properties of the environment. This must therefore be known in detail - RH, temperature, precipitation, concentration of aggressive media etc. Possible future changes in the environment must also be considered; for example the recent use of large quantities of de-icing salts on concrete structures that were once designed for normal frost attack has created overwhelming problems on bridges in many countries; severe scaling, reinforcement corrosion.

4: The main destruction mechanism is often different during different periods. For example in Example 2 (Fig. 4), at point C, there is a change-over from frost attack to reinforcement corrosion as the most important destructive mechanism. Consequently, the serviceability - time curve changes its slope drastically. Such jumps between two mechanisms frequently occur in practice and must therefore be known in conjunction with the service life design. They also imply that one can seldom base a service life calculation upon simplified durability tests in which one type of destruction at a time is studied. Results of such tests - even if extrapolated correctly in time - will only yield a value of the service life of the actual specimen under the actual test conditions, but not of the real structure in the real environment. The complex, often synergetic, action of many simultaneous destructions might be analyzed theoretically on the basis of results of separate tests of each destruction, or on the basis of knowledge of the destruction mechanisms.

5: A service life prediction can only be made when the destruction mechanism is known in detail. For example, the induction period before the chloride corrosion starts in the parking deck in Fig. 4 is a function of numerous parameters connected in an intricate manner, which are still partly unknown. The basic properties are the OH^--concentration of the capillary water in the concrete and the diffusivity of Cl^--ions in the concrete cover /4/. But these two parameters are a function of many other properties; the W/C ratio, the cement content, the cement type, the type and amount of residual materials, the curing, the temperature etc. A mistake in the assessment of the effect of one of those properties will lead to great errors in the estimated service life.

6: Example 1, Fig. 3, shows that it is very useful if one single fundamental property could be found - in this case RH - which determines the degradation curve as well as the environment. This makes it much more easy to make a service life estimate. In order to find this fundamental property it is of course, as was mentioned above, necessary to know the destruction mechanism. Frost destruction of porous materials is an example of a durability problem that could be described sucessfully by one single fundamental property; viz the degree of water saturation S of the pore system. Each material has a certain critical (maximum allowable) value of S and each environment imposes a certain actual value of S in the material. The frost damage is a function of the probability that S_{ACT} exceeds S_{CR} /6/. The fact that S_{CR} exists is also predicted by the two most plausible destruction mechanisms, /6/.

So far, the serviceability - time curves have been assumed to be continuous; i.e. the destruction increases gradually with time. However, for some types of attack, the curves are discontinuous and severe destruction occurs more or less instantanously after a time of almost constant serviceability. A typical example of this feature is frost destruction; see Fig. 5.

The serviceability in the representative unit volume V in the material is constant or grows as long as the environmental conditions are such that the critical degree of saturation S_{CR} is not transgressed in the volume. S_{CR} is almost constant with time. Then, suddenly, at point B, the external conditions are very wet and S_{ACT} exceeds S_{CR} in conjunction with a freezing period. The destruction in the unit volume is then very large /5/ and its serviceability immediately drops to a low value. A real material consists of numerous unit volumes (size 1 -> 5 mm^3) for which reason destruction of one volume will not necessarily affect the material very much. Normally, however, a very large number of volumes are damaged simultanously, and a measurable drop in the serviceability of the material is therefore obtained.

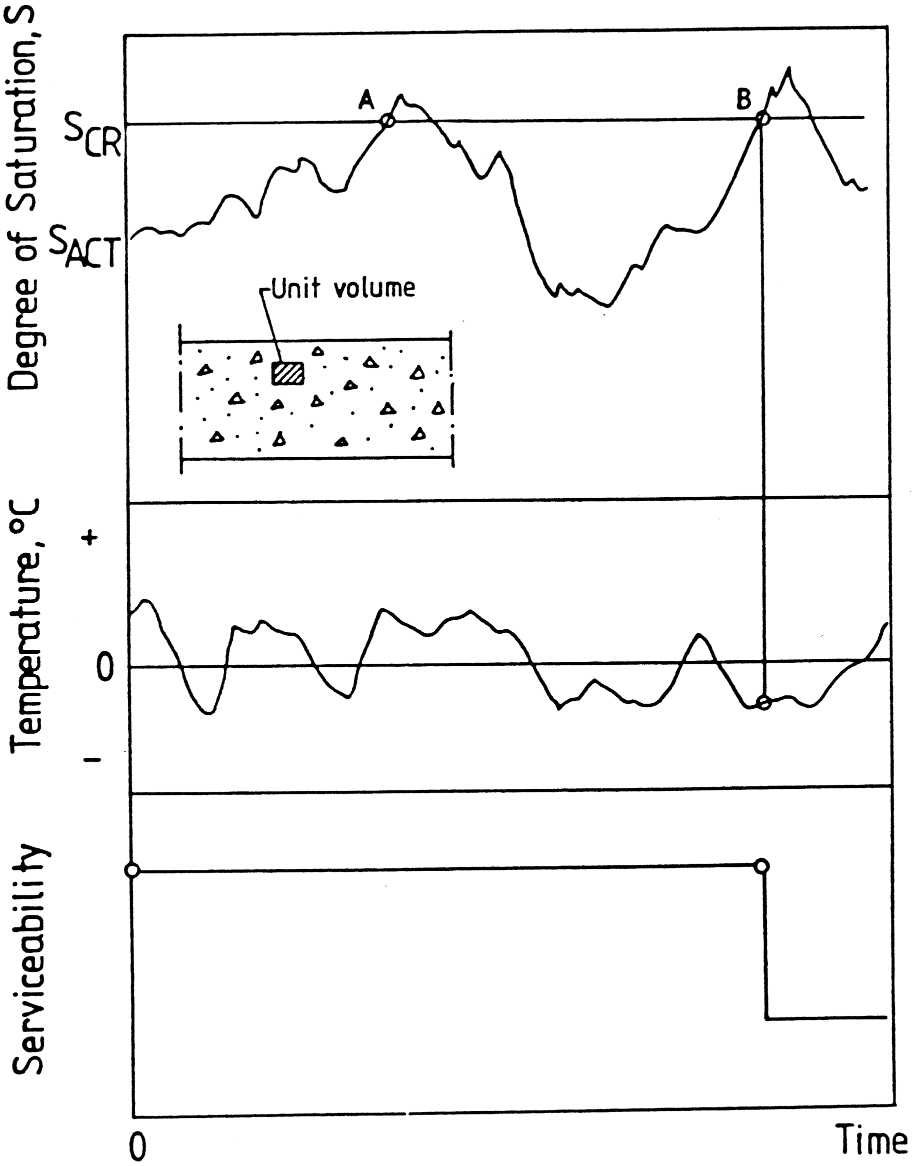

Degree of Saturation, S
S_{CR}
S_{ACT}
A
B
Unit volume
Temperature, °C
+
0
-
Serviceability
0
Time

Fig. 5 Example of a discontinuous serviceability-time curve. The frost attack on a unit volume inside a porous material.

The frost destruction is a good example of the statistical character of service life. The very unlucky combination of too high a moisture content over a large material volume and freezing temperatures might occur as easily in the first year as in the fiftieth. Thus, it becomes very difficult to make a safe service life calculation. It is quite clear, however, that a long service life requires that the material or structure is designed in such a way that the probability that S_{ACT} should exceed S_{CR} becomes very low. I shall return to the frost attack below.

4 INFORMATION REQUIRED FOR A SERVICE LIFE PREDICTION

The information and methods that are needed for a reliable service life prediction can be summarized in the following way:

1: The functional requirements must be known and be expressed quantitatively in terms of one or more measurable basic material properties.

2: The environment around and inside the material, must be known as exactly as possible. It should also be expressed in quantitative terms. This part of the service life design requires, in almost all cases, a detailed analysis of the moisture-temperature field in the structure.

In most cases it is impossible to gain full knowledge of the environment; see Fig. 5 according to which one must predict the future moisture fluctations in all parts of the material in order to predict the risk of frost damage. Therefore, it is often necessary to employ some sort of standard environment which is intended to represent the real environment in a fair way. Then, one will not get the true service life but a potential service life; see below.

3: The interaction between the environment and the material - i.e. the destruction mechanism - must be known. A misconception concerning the destruction mechanism could lead to the use of a completely irrelevant durability test or to the stressing of an irrelevant material property. Such mistakes are frequent and examples are easy to find. Tests of frost resistance are often based upon the hypothesis that destruction is a consequence of fatigue. Therefore, a large number of freeze/thaw cycles are performed under uncontrolled moisture conditions. The gradual destruction is monitored. A typical example is the ASTM-test C 666 for concrete. Such a test will only give a qualitative value of frost resistance and cannot be used for a service life estimate. In reality, frost destruction is not caused by fatigue but by "single-load fracture" when freezing occurs at too high a moisture level. By utilizing the real mechanism, it is possible to design a test method by which the service life can be predicted, /6/. Another example is corrosion of reinforcement in a chlorine environment. Service life is often assumed to be a function of the diffusivity of Cl^--ions in the saturated concrete cover; a concrete with low diffusivity is considered to have a long service life. Therefore, the durability testing is often restricted to Cl-diffusivity only. In reality, however, there is a threshold concentration of Cl^--ions around the bar before corrosion can start. This concentration is very different for different concretes and has nothing to do with diffusivity. It is just as important as the diffusivity but is seldom measured.

4: All the information from points 1 - 3 must be merged together and used in the design of non-accelerated tests - see below - on the basis of which it is possible to assess the required serviceability - time curves after extrapolation of the results. Preferably, such tests should be excluded, however, in favour of theoretical models for describing the interaction between the material and the environment. The data to be put into the models are normally not based upon traditional durability tests but consist of structural, physical and mechanical properties of the material and of some environmental data. A theoretical calculation is considerably more rapid than an assessment based on durability tests. As examples of relatively elaborated theoretical service life models could be mentioned the reinforcement-corrosion model by Tuutti /4/ and the frost-attack model by the author /6/. As an example of a service life model based upon extrapolation of a single non-accelerated test could be mentioned the theory for acid attack on concrete elaborated by Rombén /7/.

The frost-destruction and the corrosion models are worked out in such great detail that it should, in theory, at least, be possible to calculate the service life on the basis of material and environmental data only; no durability test should be needed. The models are, however, not perfect. Many important parameters are still uncertain. Nevertheless, the models can already be used for a quantitative analysis of the effect on the expected service life of a change in different material properties or in the climate around the structure, see Fig. 6 and 7 below.

The requirements for a reliable service life prediction are clearly very high. This may be the reason for the limited use of the service life concept in building design. It is, however, quite clear that much more of the durability studies made must be directed towards destruction mechanisms and towards developing service life models. Today most studies unfortunately consist of rather rough investigations by accelerated durability tests yielding very little information of universal applicability.

5 THE POTENTIAL SERVICE LIFE

As has been mentioned above, it is very difficult to express the real environment in quantitative terms or to reproduce it in a non-accelerated test. Therefore, one often has to exchange the complicated real environment for a simpler "standard" environment which is easy to reproduce in the laboratory or to treat theoretically but which is still as similar to the real environment as possible.

By using the standard environment one will not get the true service life but merely a sort of "potential" service life. This concept has been used for frost attack /6/ and for reinforcement corrosion /4/. In the first case, the real condition has been exchanged for simple isothermal water absorption of a thin material slab put in contact with a free water surface. The potential service life is the space of time during which the degree of saturation reached during the capillary suction is lower than the critical value; see above. Thus, one has to extrapolate the measured absorption curve by a factor of 10 to 1000. An extrapolation of this magnitude can only be made if the mechanism is known by which the coarse pores in the material become water-filled. So far, the absorption has been assumed to be proportional to the logarithm of suction time. This is a considerable over-simplification and has in fact no physical significance.

Fig. 6 presents a chart for estimating the potential service life of concrete, exposed to freezing without salts. It is calculated theoretically on the basis of a destruction mechanism that leads to the existence of a so-called critical spacing between air-filled pores /6/. The air-void system - pores larger than 5 µm - is assumed to have the following frequency function of radii.

$$F(r) = k \cdot \frac{\ln 1.025}{1.025^{r}}$$

k = constant
r = pore radius

The W/C-ratio is 0.60 or 0.45. The chart shows that a potential service life of 20 years (1,7 · 10^5 hours of uninterrupted water storage) requires an air content of about 5.5% at a W/C-ratio of 0.45. The same air-content will only yield about 2 months of service life when the W/C-ratio is 0.60. The diagram is by no means exact due to difficulties in describing the water absorption process. Research is, however, now under way in order to clarify this problem.

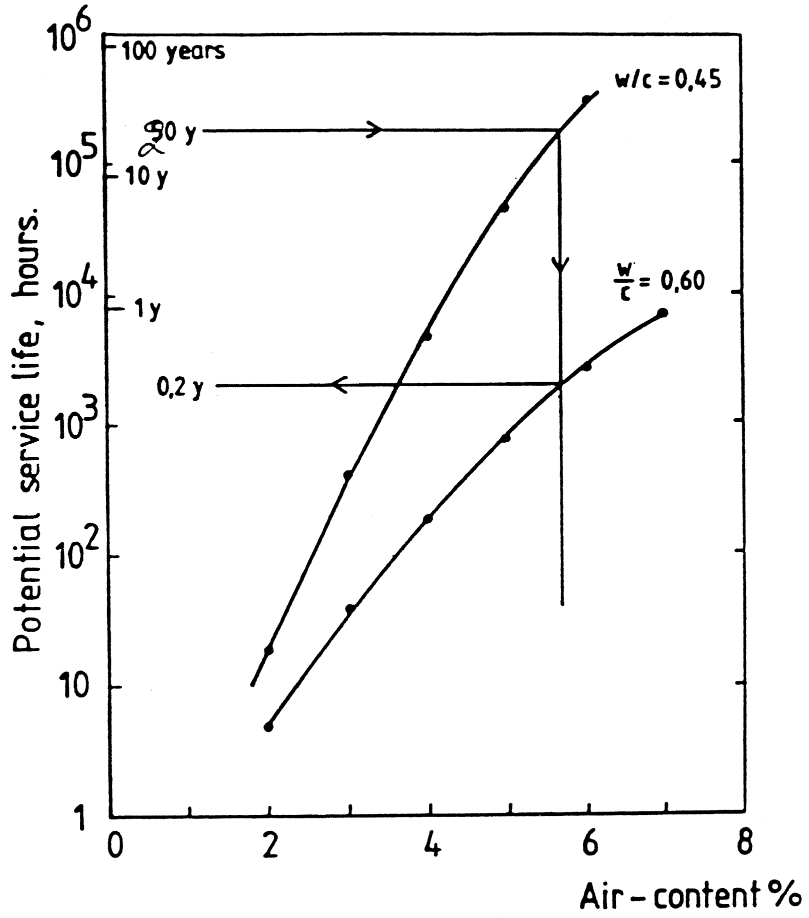

Fig. 6 The service life of Portland cement concrete subjected to uninterrupted water absorption followed by freezing.

In the case of reinforcement corrosion induced by carbonation of the concrete, the RH profile of the concrete cover is of major importance. The higher the RH, the lower the carbonation rate. Thus, a concrete which is constantly moist has a very low rate of carbonation and consequently a long service life. The same concrete placed outdoors but protected against rain has a rapid carbonation but is in most countries wet enough to have a rapid corrosion rate once the carbonation front has reached the bars. Thus, it has a low service life. The different types of environment can be divided in different classes, each with its own characteristics. Every class of environment will produce a certain RH profile in the concrete cover. It could be estimated by means of moisture mechanics analyses and will be different for different types of concrete depending on its W/C-ratio etc. On the basis of this information, it is possible to calculate the rate of penetration of the carbonation front /4/. Fig. 7 shows the results of such calculations valid for concretes with pure Portland cement and placed in two different Swedish environments; "outdoors protected from rain" and "outdoors exposed to rain". The figure is slightly adjusted in order to fit field data. It gives the maximum carbonation depths which can be expected. A W/C-ratio of 0.75 will only give a service life of 7 years for a rain-protected structure with a concrete cover of 20 mm. The W/C-ratio must be lowered to 0.50 if a service life of 50 years is required. The wetter structure has a service life of about 50 years and >100 years for those two W/C-ratios.

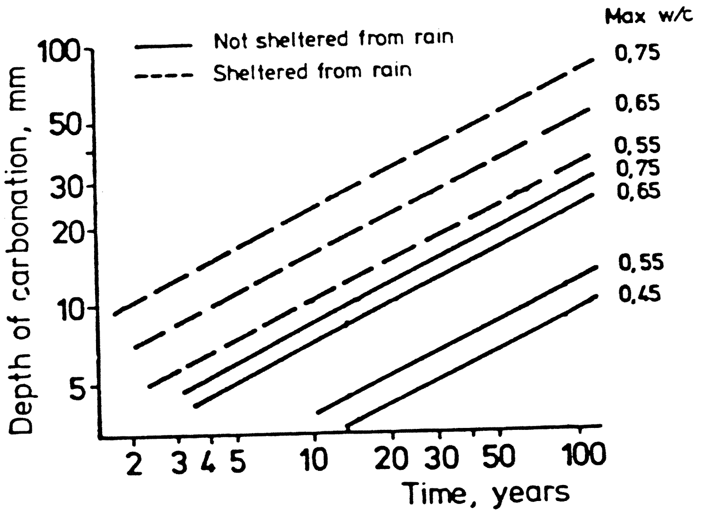

Fig. 7 Maximum carbonation depths of Portland cement concretes exposed to two different classes of environment /4/.

Tuutti /4/ has treated chloride-induced corrosion in a similar manner. Fig. 8 shows the result of his calculations. It gives the service life for the start of corrosion as a function of the diffusivity of Cl^--ions in the concrete cover and the threshold concentration of Cl^- in order to start corrosion. Those two factors are functions of the composition and curing of the concrete /4/.

The concept "potential service life" could probably be applied with success to many other types of destruction processes even outside the concrete field.

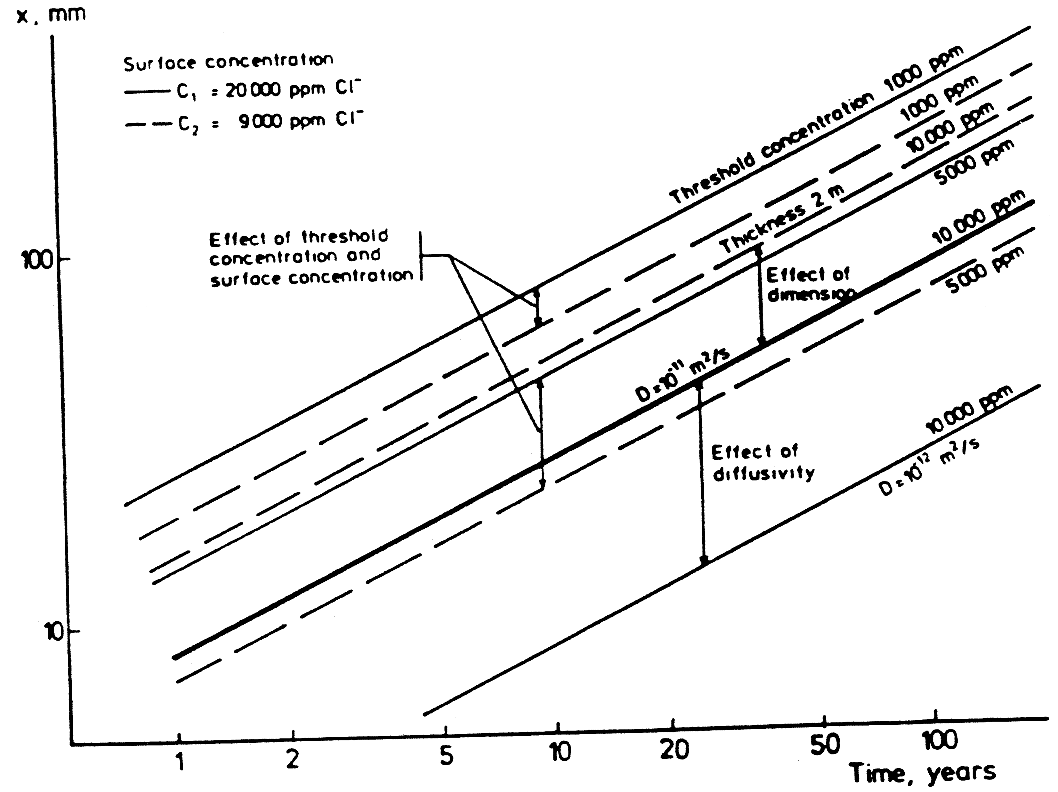

Fig. 8 The "incubation time" before start of reinforcement corrosion as a function of the Cl^--diffusivity and the threshold Cl^--concentration /4/.

6 INDIVIDUAL STRUCTURES VERSUS POPULATION OF STRUCTURES

The service life of one particular structure depends on the individual characteristics of exactly that structure and of its environment. All those characteristics have certain discrete values which, if known, make it possible, in principle at least, to calculate a discrete value of the service life of the actual structure, assuming that we know the destruction mechanism. The principle is shown in Fig. 9 (a).

In practice, however, we will never get access to all the information needed in order to calculate the exact value of the service life; all properties are afflicted with uncertainties. Therefore, we can only expect to predict the service life of the actual structure with a certain degree of uncertainty. However, if we know the mean value and the spread in all relevant properties it should be possible to estimate also the mean value and spread in the service life; see Fig. 8 (b). Such stochastical methods for concrete structures have been eleborated by Sentler /8/ among others.

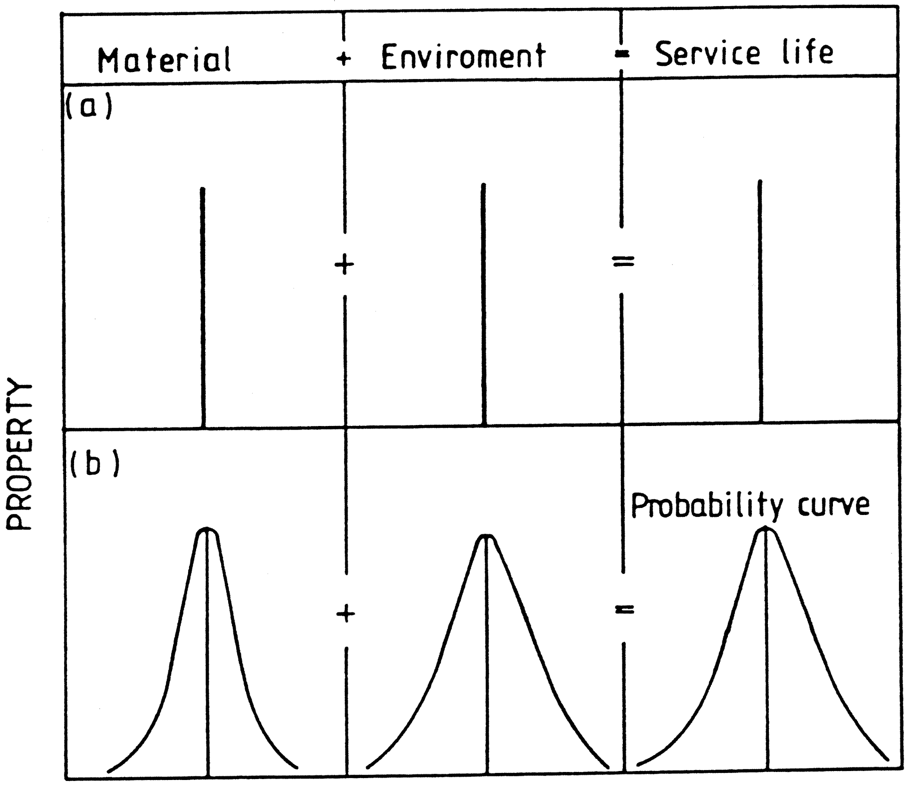

Fig. 9 The service life of a given structure.
(a) Exact data is available for material and environmental properties.
(b) Only the range of variation of all properties are available.

The same principles could be used for a whole population of similar building structures; e.g. all road bridges to be built in a country. In this case we have a much wider spread in material and environmental properties in connection with which parameters such as "quality" of the building work and climate during the building phase must also be considered since they considerably affect the properties of the finished building. By stochastical methods it should then be possible to estimate a frequency function of the service life for the whole population in which all parameters are considered.

Stochastical methods of this type ought to be used by authorities in connection with the establishment of quality requirements for different types of structures. This should result in considerably more rational requirements than the normal ones which are based upon "old experience" without any service life assessment.

Hypothetical examples of calculated frequency functions for two types of concrete structures; bridges and external walls - are shown in Fig. 10. For bridges, a characteristic service life of 100 years is required by the authorities, which means that only 5% of all bridges are allowed to have a service life shorter than 100 years. In order to achieve this, it is necessary according to the calculation to select concrete properties and design that give an average life of 150 years; a lower concrete quality will theoretically give an unacceptably low service life for a large fraction of all bridges. Similarly, for external walls, the required average life will be 75 years if the required characteristic value of 50 years should be achieved.

It is highly probable that the use of such methods has resulted in much higher quality requirements than those used in the majority of concrete standards in the world.

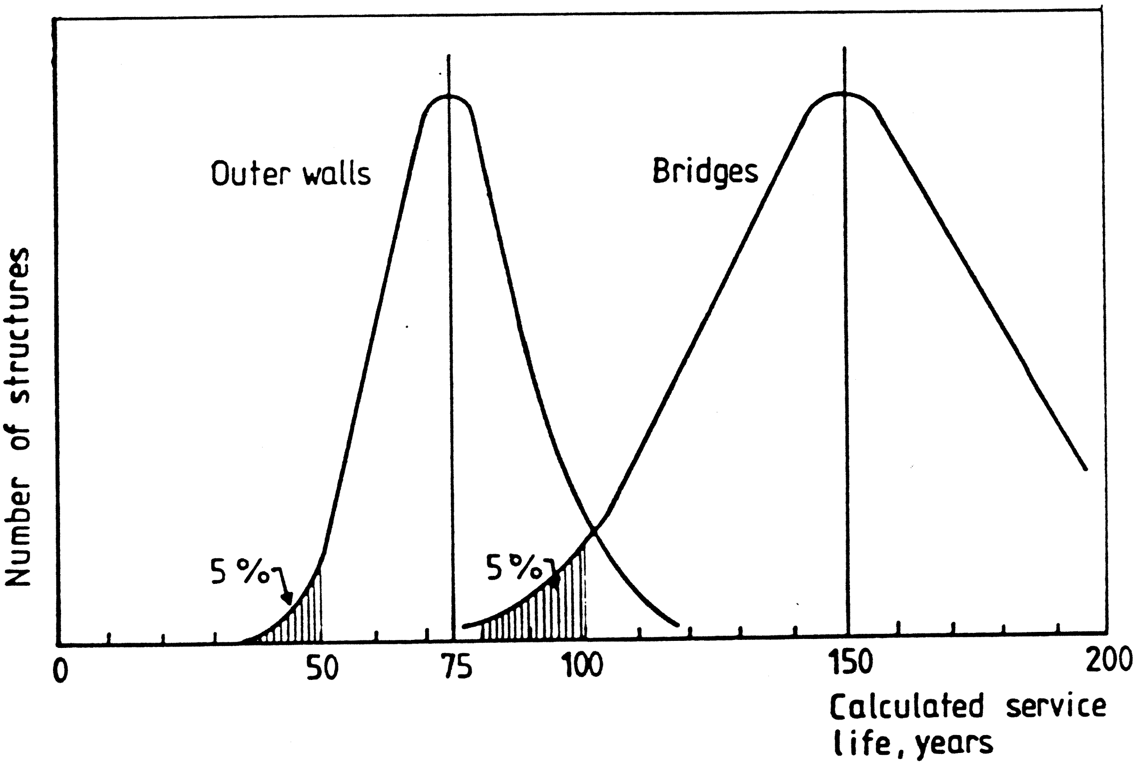

Fig. 10 Hypothetical frequency functions of service life for external concrete walls and concrete bridges. The curves are calculated on the basis of certain assumed material and environmental properties.

7 A "SENSITIVITY ANALYSIS"

It is characteristic for the durability problem that very small changes in the material properties or the design can cause problems and substantial reductions in service life. In many cases, it is easily neglected details in the design that turn out to be decisive for the service life; for example, the exchange after some years of the original flooring material for another type which has a lower moisture diffusivity or which has a lower critical RH - see Fig. 3 - might create moisture-induced damage in floors on the ground because the moisture state in the floor is changed - see Fig. 1.

One should of course not build houses that are that sensitive also to very small and natural changes. Therefore, the design should include a sensitivity analysis in which the effect on serviceability of imaginable future changes in the design is considered as well as the effect of maltreatment of the materials during the building phase, uncertainties in material properties and future accidents (e.g. water leakage).

A sensitivity analysis is nothing else but a service life analysis based on different assumptions. Materials for which relevant information is missing or is uncertain will be "punished" since they are either rejected or require a much more expensive design in order to be used safely. Thus, the use of sensitivity analyses of service life will hopefully stimulate the manufacturers to produce essential data.

8 DURABILITY TESTS AS A BASIS FOR SERVICE LIFE PREDICTIONS

It has already been said - Chapter 4 Subsection 4 - that the prediction of service life requires either a purely theoretical model for describing the interaction environment-material or some sort of durability test of the material or component followed by a translation of the test result into the expected service life.

Durability testing can be done according to two different principles:

1: Accelerated testing in which the environment is concentrated in such a way that the whole service life is run through during a short time in the laboratory.

2: Non-accelerated testing in which the actual environment is transferred unchanged into the laboratory. The material changes, which are normally very small, are monitored by sensitive methods, whereupon the whole destruction curve is extrapolated.

Accelerated tests are widely used, but are very unsuitable as a basis for service life predictions for the following reasons; see Fig. 11.

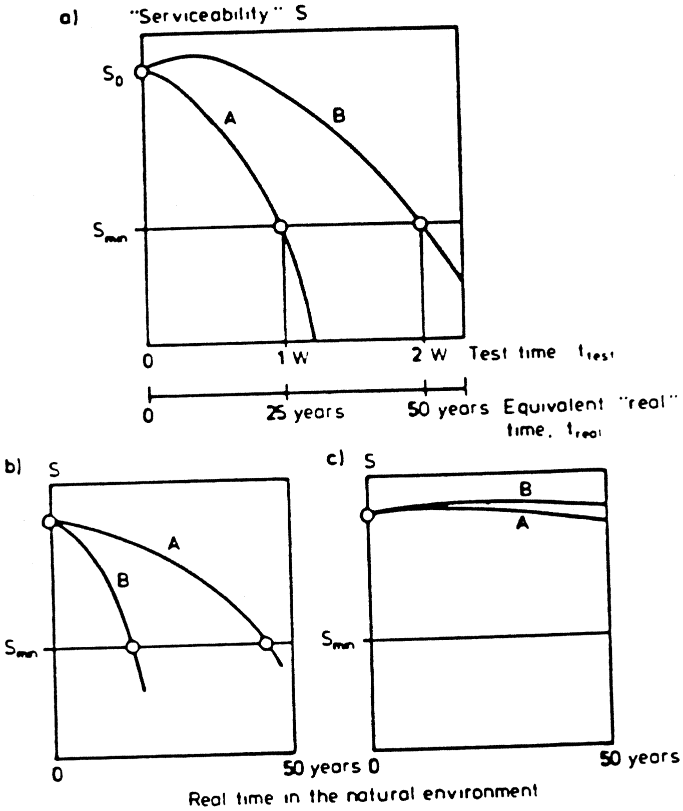

Fig. 11 Problems with accelerated tests
(a) The time scale
(b) In reality; A is better than B. In the test; B is better than A.
(c) In reality; both materials are highly durable. In the test; both materials are damaged.

1: It is almost always impossible to translate the exposure time in the test to a real exposure time in the real environment; in Fig. 11 (a) the time scale is supposed to be 1 week for each 25 years.

2: The acceleration sometimes changes the destruction mechanism. Consequently, it might very well be that material A is better than B in reality - Fig. 11 (b) - although, it was inferior in the test - Fig. 11 (a).

3: The acceleration is sometimes so large that destruction occurs although it would never happen in practice - Fig. 11 (c). In such a case the test is completely misleading.

4: In reality, one often has a synergetic effect between two or more destructive actions or time-dependent jumps between one action to another - see Fig. 4 above. This will not be revealed in a normal accelerated test since only one destruction type at a time is studied.

Non-accelerated tests can be used for service life predictions. This makes them very attractive: The problems with such tests are

1: Selection of the test environment which implies a careful analysis of the aggressive parts of the real environment.

2: Detection of the damage which is always very low due to the non-accelerated conditions and the short testing time.

3: Extrapolation of the measured destruction - time curve by a time factor 10^2 to 10^3.

The extrapolation problem is the most severe one because it requires full knowledge of the destruction mechanisms. One must also know about all mechanism changes that might occur in the future. A typical example of the use of a non-accelerated test for extrapolation of service life is the method elaborated by Rombén for assessing the service life of concrete pipes exposed to acid attack /7/. Rombén makes a thorough analysis of the destruction mechanisms and shows that the rate-determining process changes on two occasions. He shows that the service life will be considerably over-estimated if the last mechanism change occurring after some months is not considered in the extrapolation.

9 CONCLUSIONS

The present situation in which the building design with regard to durability is often based upon old experience and defective data concerning materials and environment is not desirable. It has been shown by many examples above that this design procedure could lead to considerable over-estimations of the durability. Besides, it does not stimulate the material producers to investigate their materials thoroughly or the designer to analyse the effect of a new design with regard to durability.

It would be much better if the qualitative concept "durability" was abandoned in favour of the quantitative concept "service life". Thus, each design should include a service life prediction. A safe service life prediction requires a lot of data, however; the functional requirements and the environment must be expressed in quantitative terms; the destruction mechanism must be known in detail; the interaction between environment and material must be calculated theoretically or extrapolated by a non-accelerated test, which means that a lot of material data must also be known.

The difficulties in making an accurate service life prediction are great. Examples from concrete research do, however, show that those difficulties might be coped with successfully if more durability research is directed towards really developing models for a theoretical description of the deterioration mechanism.

It has been shown that the real service life can often be exchanged for a potential service life which is valid for the component subjected to a reproducible standard environment which in turn is intended to represent the real environment in a satisfactory way.

The service life concept should always be used in connection with the elaboration of official standards in which the minimum quality levels of different types of structures are determined. This ought to lead to a higher probability that the required service life of the actual population of structures is reached than does the usual, more arbitrary, way of determining quality requirements.

The effect of uncertain material or environmental data on the service life can always be analyzed by a "sensitivity" analysis. This will "punish" materials for which relevant data are missing and will therefore stimulate the material producers to measure and present data that are of importance to the designer.

REFERENCES

1. Fagerlund G, Floors on the Ground. (Stockholm; BPA Byggproduktion AB, Handl Nr 32, 1980). (In Swedish)

2. Fagerlund G, A Theoretical Analysis of a Test Method for Capillary Suction of Granular Materials. (Stockholm; Swed. Res. Inst. for Cement and Concrete, Report Nr 7726, 1977). (In Swedish)

3. Fagerlund G, Predicting the Service Life of Concrete Structures, in J.F. Young, Ed., Characterization and Performance Prediction of Cement and Concrete. (New York: Engineering Foundation, 1982), pp 187-198.

4. Tuutti K, Corrosion of Steel in Concrete. (Stockholm; Swed. Res. Inst. for Cement and Concrete, Research Fo 4:32, 1982).

5. Fagerlund G, The Critical Degree of Saturation Method of Assessing the Freeze/Thaw Durability of Concrete. Materials and Structures 10(1977):58 pp 217-230.

6. Fagerlund G,. Prediction of the Service Life of Concrete Exposed to Frost Action, in Studies on Concrete Technology (Stockholm; Swed. Res. Inst. for Cement and Concrete, 1979).

7. Rombén L, Aspects of Testing Methods for Acid Attacks on Concrete - Further Experiments. (Stockholm, Swed. Res. Inst. for Cement and Concrete, Research Fo 9:29, 1979).

8. Sentler L, Statistical Evaluation of the Durability of Concrete. (Lund; Div. of Build. Techn., Lund Inst. of Technology, 1982).

ETUDE DE LA DEGRADATION DES BETONS

Chaieb M.T. Triki E. Ben Cheikha M.

INTRODUCTION

La dégradation du béton résulte d'actions d'orgine soit mécanique et physique, soit chimique:

- Les dégradations mécaniques sont diverses et suitent les conséquences d'une su restimation de la résistance mécanique mesurée sur éprouvettes standards.
- Les dégradations physiques sont dues à des surcharges, aux sollicitations excessives, aux chocs thermiques, aux gonflements et aux retraits. Toutes entraînent l'érosion et la fissuration du béton.
- Les dégradation chimiques sont dues aux acides, aux bases et aux solution salines. Elles entraînent presque toujours la dissolution de la chaux et le plus souvent, en association avec cette dissolution, la formation de composés nouveaux.

MECANISMES D'ALTERATION CHIMIQUE DU BETON

Les altérations du béton peuvent être dues à des agents extérieurs (solutions acides, sols gypseux, agressifs vis-à-vis de la pâte du ciment) où à des agents internes (hydratation de CaO et de MgO libres dans le ciment).

Les altérations sont de deux types: soit érosion, qui entraîne une partie du liant, soit gonflement et éventuellement fissuration, par formation de composés expansifs.

A) Dégradation par dissolution et érosion

De tous les constituants hydratés du ciment, la chaux est le plus soluble [5]. Elle peut être dissoute par attaque superficielle ou par percolation à travers le béton.

La chaux qui émerge de la structure par des fissures forme des efflorescences blanches de $Ca(OH)_2$ et de $CaCO_3$.

Cette dissolution s'accompagne de la formation de composés nouveaux, solubles ou insolubles. S'ils sont solubles, les sels formés diminuent la résistance du béton, sinon ils peuvent au contraire se substituer à la chaux et former une couche protectrice sur la surface du béton [3].

B) Dégradation par foisonnement

- Actions des sulfates. Parmi les modes de dégradation les plus importants pour le béton, intervient l'action des sulfates dissouts dans l'eau. La chaux libre peut se transformer par les sulfates en formant ainsi du gypse secondaire qui attaque à son tour les aluminates du ciment pour former l'ettringite ($3CaO\ Al_2O_3\ CaSO_4\ 32H_2O$) suite à la présence d'une quantité d'eau de cristallisation [7].
- Action de l'eau de mer. Les éléments présetns dans une eau de mer sont: chlorure de sodium (NaCl), chlorure de magnésium ($MgCl_2$), sulfate de magnésium ($MgSO_4$), sulfate de calcium ($CaSO_4$), sulfate de potassium (K_2SO_4) et (Co3H)2Ca, dont les plus agressifs sont les sels de magnésium $MgSO_4$ et $MgCl_2$.

L'attaque du béton par l'eau de mer résulte de réactions séparées mais plus ou moins simultanées entre les sulfates et les chlorures et les costituants du ciment.

* Le sulfate de magnésium réagit avec Ca(OH)2 et en raison de la substitution de $Mg^{2+} \Rightarrow Co^{2+}$, il y a formation simultanée du gypse secondaire $CaSO_4$ et du brucite $Mg(OH)_2$. Le gypse attaque les aluminates en formant alors un précipité d'ettringite provoquant ainsi le gonflement et l'éclatement du béton.

* Les ions "chlore" dus à la dossociation de $MgCl_2$, réagissent avec les aluminates pour former le "monochloroaluminate" ou "sel de Friedel" ($3CaO\ Al_2O_3\ CaCl_2\ 10H_2O$) qui est un produit instable et se transforme, en présence des sulfates, en ettringite.

* De plus, les ions CO_3^- peuvent jouer un triple rôle:
  - Ils colmatent la surface du béton en précipitant un mélange de calcite et d'aragonite ($4CaCO_3$) à partir de la réaction avec la chaux.
  - En diffusant dans les bétons armés, ils diminuent le pH du milieu et concourent à la corrosion des aciers qui ne sont plus protégés par le liant basique.
  - En présence de SiO_2 à l'état actif, ils transforment l'ettrengite en thaumasite ($CaCO_3\ CaSO_4\ CaSiO_3\ 15H_2O$).

ETUDE EXPERIMENTALE

Les dégradations sont variables selon que le béton est totalement immergé, en immersion alternée ou en semi-immersion: c'est en immersion alternée que les détériorations sont les plus importantes [3].

Dans le but d'étudier le comportement de certains ciments tunisiens agressés par ce mode de dégradation, la laboratoire des matériaux de construction a implanté un banc d'essai expérimental composé d'un réservoir contenant la solution et lié, d'une part à une pompe pour le remplissage du bac recevant les éprouvettes et, d'autre part à une électrovanne permettant le retour de la solution vers le réservoir après vidange du bac. La pompe et l'électrovanne sont reliées à une commande automatique qui assure le déroulement répétitif de cycle.

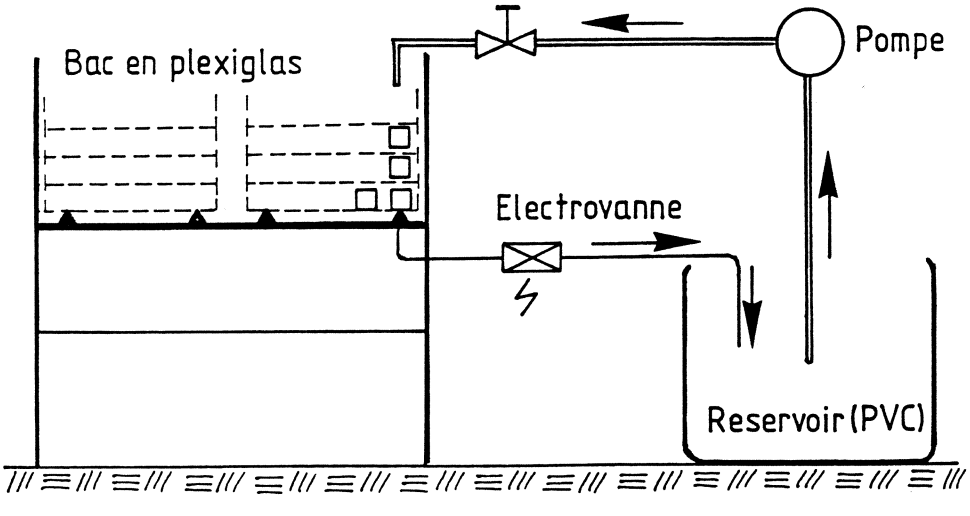

Figure 1. Schéma du dispositif d'immersion-séchage.

Essai

Cet essai consiste à faire subir aux éprouvettes en béton des cycles immersion-séchage à raison d'un cycle par 48 heures, 24 heures d'immersion et 24 heures séchage.

Description des éprouvettes

Les éprouvettes sont cubiques de 7·7·7 cm en béton.

La composition est la suivante:

- ciment	370 kg/m^3
- sable (0-3 mm)	700 kg/m^3
- gravier (3-7 mm)	330 kg/m^3
- gravier (7-12 mm)	730 kg/m^3
- eau	170 l/m^3

Pour cette étude, trois ciments tunisiens sont utilisés chacun pour la confection d'une série d'éprouvettes, à savoir:

- le C.P.A. du C.A.T. (Kharrouba)
- le C.P.A. de Bizerte
- le ciment preise mer de C.A.T. (Kharrouba)

Les données des analyses chimiques et des compositions calculées (d'après Bogue [1]) sont reportées dans le tableau 1 suivant.

Ciment	SiO_2	Al_2O_3	Fe_2O_3	MgO	K_2O	CaO	SO_3	C_3S	C_2S	C_3A	C_4AF
Prise mer	22.97	3.13	3.76	1.09	0.53	63.17	1.94	59.0	21.34	1.93	12.44
C.P.A. (C.A.T.)	18.91	6.71	2.69	0.15	0.48	53.36	2.19	24.57	42.75	8.75	10.62
C.P.A. (Bizerte)	21.12	4.86	3.65	0.15	0.50	59.87	2.38	45.33	27.87	6.73	11.23

Tableau 1.

Mesures

Dans le tableau 2, nous indiquons respectivement dans une première et deuxième série de colonnes, les valeurs des chutes de masse et de résistance en compression moyenne en % après 15, 30 et 45 cycles.

Sure la figure 2 on a reporté, sous forme de diagrammes, les chutes en pourcentages de résistance à la compression dues à l'attaque par les eaux sulfatées.

L'échantillon A, à savoir le ciment prise mer, s'est montré le plus résistant. L'aluminate tricalcique est pratiquement faible.

Les échantillons B et C ont un comportement semblable à savoir, le ciment B de faible teneur en silicate tricalcique est de résistance mécanique et chimique élevée par rapport au ciment C.

	$\frac{\Delta m}{m}$ %			$\frac{\Delta \sigma_c}{\sigma_c}$		
	Aprés 15 cycles	Aprés 30 cycles	Aprés 45 cycles	Aprés 15 cycles	Aprés 30 cycles	Aprés 45 cycles
Ciment A Prise mer	0.38	1.23	2.22	6.09	17.5	11.3
Ciment B C.A.T.	0.14	0.923	1.93	0.47	11.47	25.15
Ciment C Bizerte	0.08	0.922	1.74	2.20	31.60	43.0

Tableau 2.

Courbe

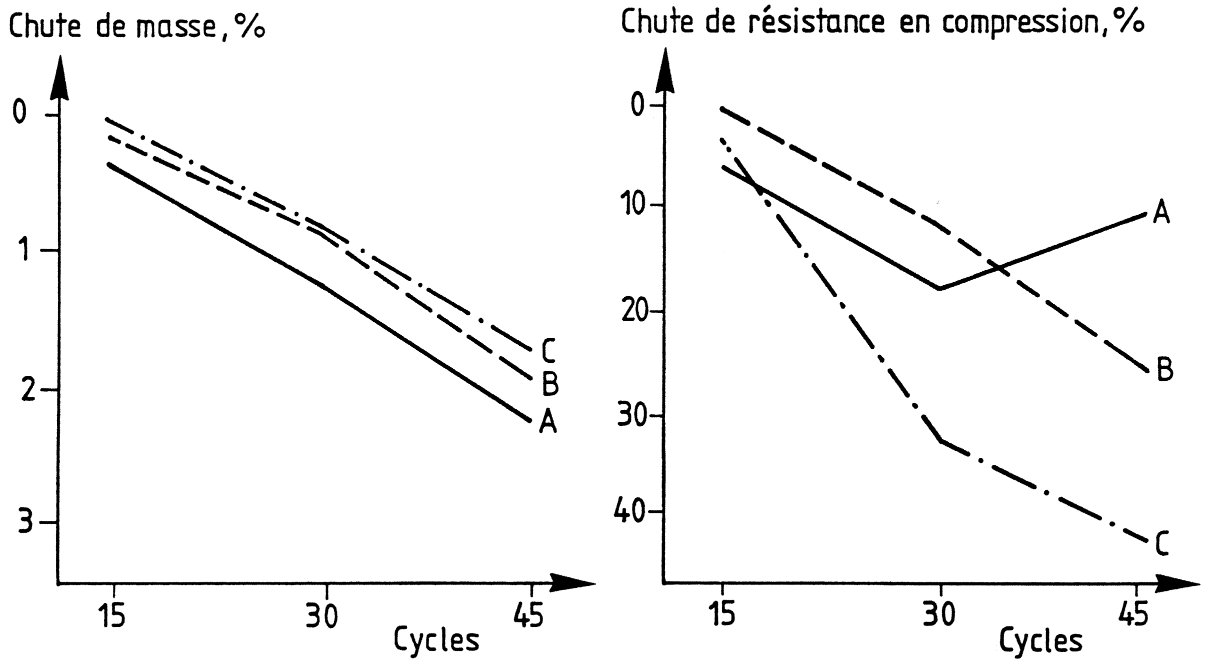

Figure 2.

Avant de conclure, nous pensons qu'il est bon d'attirer l'attention sur le fait que notre classification; pour laquelle on s'est proposé de présenter, par l'examen, des dégradations provoquées par une solution sulfatée agissant de l'extérieur, est insuffisante du fait, entre autres, des compositions de béton incontrôlables sur le plan commercial.

BIBLIOGRAPHIE

[1] R.H.Bogue. La chimie du ciment portlaud. Paris,Eyrolles 1952.

[2] C.Goria, L.Cussino. Bétons exposés à l'agression dans les dépôts de sels marins à haute concentration. Colloque RILEM, Palerme Mai 1965.

[3] M.Regourd. La résistance du béton aux altérations physiques et chimiques. Presse de l'ENPC 1982.

[4] A.M.Paillere, M.Raverdy, J.Millet. Influence du ciment sur la dégradation du béton en milieu marin. Paris, Bull. liaison, Labo P. et Ch. Janv-Févr 1985.

[5] R.Sierra. L'hydratation des ciments portlaud. Paris, Bull. des laboratoires routiers, spécial 0, Juin 1970.

[6] M.Venaut, M.Papadakis. Manuel du laboratoire d'essais des ciments, mortiers, bétons. Paris, Eyrelles 1969.

[7] M.Venaut. La pratique des ciments et des bétons. Paris, Le Moniteur 1976.

Transfert d'humidité dans le béton

R.Mensi

Résumé

Le séchage naturel du béton est un phénomène très lent qui a des conséquences importantes sur son comportement physique et mécanique plus particulièrement sur deux aspects spécifiques de ce matériau: les déformations différées (retrait, fluage) et sa durabilité (fissuration superficielle, pénétration d'agents agressifs). En plus de la modification des caractéristiques mécaniques et physiques locales qui résultent des variations de teneur en eau, la non-uniformité de ce paramètre au cours du temps induit un effet de structure particulièrement important (effet d'échelle pour le retrait et le fluage de dessiccation, et fissuration de retrait). A partir de l'analyse physique des mécanismes qui régissent les mouvements d'eau dans le matériau, on a développé un modèle de diffusion non-linéaire qui a été validé, grâce à la détermination expérimentale des distributions spatiales de teneur en eau, et de leur évolution au cours du temps, par la méthode de densimétrie par absorption des rayons gamma, au moyen d'un banc gamma rotatif. Le modèle ainsi validé permet d'une part d'extrapoler, dans certaines limites, les rsultats expérimentaux, et d'autre part, il aide à exploiter et interpréter les essais de retrait et de fluage.

BETONS A BASE DE SABLE DU DESERT

par : CHAIEB Mohamed Tahar, AOUIDIDI Abdessalem

RESUME :

Dans une construction, on prévoit habituellement l'utilisation du béton de granulats légers pour en abaisser le coût global. La construction peut être moins onéreuse vu la réduction du poids mort. C'est la raison principale de l'emploi du béton de sable du désert comme béton cellulaire.

L'économie réside alors dans une recherche d'équilibre entre le prix du métre cube de béton, sa densité et ses qualités mécaniques.

Ce béton fait partie des bétons de faible densité qui sont légers et employés principalement à des fins d'isolation.

Notre étude comporte les étapes suivantes:

- analyse intrinsèque du sable de désert;
- étude du béton ordinaire;
- mise au point d'un procedé de fabrication du béton cellulaire à base du sable désert.

INTRODUCTION

Les régions présahariennes ne disposent pas de matériaux de construction classiques mais possèdent des gisements importants de sable fin, non utilisé dans la confection des bétons.

Au moment où la Tunisie lance un vaste projet de constructions dans le sud, il a été jugé utile d'entreprendre des études sur ce sable de désert afin de déterminer les proprietés d'un béton "classique" l'utilisant et d'envisager la réalisation d'éléments légers présentant de bonnes qualités thermiques.

LE SABLE DE DESERT : ANALYSE - PROPRIETES

Dans cette première partie, les analyses et les essais ont porté sur le sable du désert et à titre comparatif, sur le sable normal et celui de Khélidia.

Tous ces essais visent à identifier et caractériser le sable de désert et d'en préciser son éventuel interêt comme matériau de construction.

Caractèstiques morphologiques et dimensionnelles

type de sable sable	sable AFNOR	sable du désert	sable de Khélidia
masse volumique apparente (kg/m3)	2.625	1.445	1.551
masse volumique absolue (kg/m3)	2.625	2.650	2.604
porosité	39.2%	45.5%	40.4%
equivalent de sable	98	90	92

Tableau 1: Propriétés physiques des sables

Comme le montrent les résultats des essais, le sable de désert parait moins dense que le sable normal ou celui de Khélidia. Ceci peut être expliqué soit par une grande porosité, soit par la densité intrinséque des grains qui le constituent. La mesure de la compacité et l'analyse physique vont nous permettre de mieux interpréter ces résultats.

Les valeurs des masses volumiques absolues et apparentes nous ont permis de déduire la compacité et la porosité de ces sables.

Le tableau ci dessus montre bien la grande compacité du sable de désert et par consèquent sa faible porosit. Ceci ne peut être expliqué que par la finesse apparente de ses particules: plus les grains sont fins plus le volume des vides interstitiels est faible. D'ailleurs cette finesse des grains de ce sable va être confirmée, dans ce qui suit grâce l'analyse granulométrique.

La propreté du sable de désert ne diffère pas de manière nette de celle des sables usuellement connus (les cahiers de charges recommandent un équivalent de sable supérieur à 80 % pour l'élaboration des bétons).

Analyse granulométrique

Vu la finesse apparente du sable étudié, nous avons fait l'étude granulométrique grâce â un tamisage par voie humide.

Nous nous proposons dans ce qui suit de déterminer les fractions pondérales que contient chaque classe pour pouvoir étalonner chaque type de sable et surtout pour comparer les résultats avec la granulométrie de refêrence â savoir celle du sable AFNOR.

L'étude de la granulométrie du sable de désert avec les autres sables permet de confirmer la finesse relative du premier. En effet, sa courbe granulométrique, qui ne présente pas de discontinuité, est décalée vers la gauche par rapport â celles des autres sables.

Les modules de finesse sont déterminés â partir de la somme des refus cumuéls (exprimés en pourcentages pondérals) sur les tamis dont les ouvertures en mm sont 0.16; 0.315; 0.63; 1.25; 2.5; 5; 10. Ces valeurs ne font que confirmer ce qui a été dit auparavant â savoir le sable de désert est le plus riche en éléments fins.

	ouvertures des tamis (mm)						
type de sable	2.5	1.25	0.63	0.32	0.16	0.08	MF
AFNOR R.C. %	0	12.5	62.1	76.5	84.2	95.1	2.35
T.C. %	100	87.5	37.9	23.5	15.8	4.9	
Désert R.C. %	0	0.1	1.1	8.7	76.0	94.3	0.9
T.C. %	100	99.9	98.9	91.3	24.0	5.7	
Khélidia R.C. %	0	2.8	31.2	59.2	76.2	92.9	1.7
T.C. %	100	97.2	68.8	40.8	23.8	7.1	

* voir courbes granulométriques des sables

MF = moule de finesse

R.C. = refus cumulés

T.C. = tamisats cumulés

Tableau 2: Granulométrie des sables (*)

ETUDE DE LA COMPOSITION DU BETON

Présentation des compositions

L'étude d'une composition de béton consiste presque toujours rechercher conjointement deux qualitès essentielles: résistance et ouvrabilité. Or ces deux qualités sont étroitement liées l'une â l'autre du fait qu'elles dépendent des mêmes facteurs, mais varient en sens inverse comme indiqué dans le tableau 3 suivant.

La qualité des agrégats (propreté, forme et dureté, le rapport entre le gros agrégat et l'agrégat fin et la détermination du dosage en eau en fonction de la consistance désirée sont les bases d'étude de la composition du béton.

facteur de composition du béton	pour une bonne ouvrabilité	pour une bonne résistance
tailles des grains	plutôt fin	plutôt gros
rapport gravier/sable	à diminuer	à augmenter
dosage en eau	à augmenter	à diminuer
granularité	continue	discontinue
dimension maximale des grains	plutôt petite	plutôt forte

Tableau 3: Critères de choix des bétons

Le béton qu'on se propose de confectionner sera dosé à 350 kg/m^3 avec une consistancéegale à 6 cm. Les agrégats disponibles sont:

G1 : 12/20 concass

G2 : 5/12 concass

On considèrera les bétons à base de deux sables différents: celui du désert et à titre comparatif celui de Khélidia.

En appliquant la méthode de Dreux, qui tient compte des différentes caractéristiques des composants du béton, nous obtenons les compositions suivantes:

bétons à base de sable	de Khélidia (kg)	du désert (kg)
poids de S (sable)	582	473
poids de G1 (12-20)	910	1019
poids de G2 (5-12)	327	327
poids de C (ciment)	350	350
poids de E (eau)	175	175

Tableau 4: Composition calculées par mètre cube des bétons ordinaires.

A titre comparatif, et pour mettre en valeur l'interêt de calculer pour chaque type de sable et d'agrégats la composition du béton fait à base de ces derniers, on a confectionné des bétons faits à base des sables considérés précedemment avec les mêmes agrégats G1 et G2. Toutefois il s'agit maintenant de la même composition pour chacun d'eux (celle qu'on utilise généralement sur chantier sans calculs préalables).

poids de S (sable)	650 kg	(37%)
poids de G1 (12-20)	753 kg	(42%)
poids de G2 (5-12)	377 kg	(21%)
poids de C (ciment)	350 kg	(E/C=0.5)
poids de E (eau)	175	

Tableau 5: Composition classique par mètre cube de béton

Résultats des essais

Les résultats des résistances mécaniques des diffèrents bétons ont été récapitulés dans le tableau suivant:

	a - bétons à composition calculée					
type de sable	résistance à la flexion			résistance à la compression		
Temp	7 jour	14 jour	28 jour	7 jour	14 jour	28 jour
Désert	3.3	4.4	6.0	25.5	33.5	44.6
Khélidia	4.4	5.8	8.0	27.0	35.0	47.3
	b - bétons à composition classique					
Désert	2.2	3.0	4.0	14.5	20.3	27.0
Khélidia	2.4	3.5	4.5	17.6	23.3	31.0

Tableau 6: Résistances mécaniques des bétons

Interprétations

En considérant les bétons faits à base des différents sables, on constate une perte de la résistance mécanique du béton lorsqu'on substitue le sable couramment utilisé (sable de Khélidia) par le sable de désert.

Pour expliquer ces faits, il est nécessaire de reprendre les résultats obtenus dans la première partie de notre travail, concernant l'étude comparative des proprietés physiques, morphologiques et dimensionnelles des sables considérés:

- en granulométrie: on a constaté que les grains de sable de désert sont plus fins que ceux du sable de Khélidia. Or plus les grains sont fins, plus la quantité d'eau nécessaire pour mouiller ces derniers est grande.
- autre raison possible de la différence entre les résistances trouvées est la contenance en impuretés poussièreuses, vaseuses et argileuses et en matières organiques qui est plus grande pour le sable de désert que pour celui de Khélidia. Ces éléments sont nuisibles pour le béton du fait qu'ils diminuent sa résistance en entrant en réaction avec le ciment au cours de son durcissement.
- Enfin, en comparant les résultats des compositions classique et calculée, on constate à quel point le calcul de la composition du béton pour chaque type d'agrégats et de sable est fructueux. En effet, par ce calcul, on a pu augmenter la résistance de chaque béton de l'ordre de 65 %. Il faut noter que ce n'est pas seulement le changement du pourcentage de sable qui a été bénéfique mais c'est surtout la prise en compte de la granulométrie des agrégats qui a été déterminante.

MISE AU POINT D'UN BETON CELLULAIRE

Le béton cellulaire est une varieté du béton léger à pores uniformment répartis (atteignant jusqu'à 85 % du volume total du béton). Il est obtenu par durcissement d'un mélange expansé à l'aide d'un gonflant et comportant un liant, de l'eau et un composant de silice sous forme de sable broyé.

On classe les bétons cellulaires suivant:

- la nature du liant utilisé (bétons au gaz et bétons mousses fabriqus, bétons silico-calcaires au gaz et les mousses de laitier);
- le mode de durcissement (traités à la vapeur ou durcis en autoclave);
- l'utilsation: les bétons d'isolation thermique de masses volumi ques en relations avec les classes de résistances.

La structure du béton cellulaire est constituée d'alvéoles fermés, de dimension allant de 0.4 à 1.5 mm. L'uniformité des dimensions des pores fermés, réduit la concentration des contraintes au sein de l'enveloppe en ciment des alvéoles, les contraintes se répartissant de facon régulière suivant la section de l'élément et augmente la résistance du béton cellulaire.

Si la structure n'est pas parfaite, à côté des petits pores fermés, apparaissent de grandes alvéoles pouvant communiquer entre elles ainsi qu'avec le milieu environnant. Cette structure du béton cellulaire réduit la résistance mécanique et augmente la conductibilité thermique et l'absorption d'eau.

L'introduction dans la composition du béton cellulaire du sable non broyé ou la réduction de la quantité d'eau de gâchage ainsi qu'une technologie de fabrication des pièces plus sophistiquées, gonflement avec vibration suivi d'un traitement en autoclave, permet de réduire sensiblement les déformations de retrait.

Béton cellulaire à base du sable de désert

Les raisons pour lesquelles nous avons décidé d'étudier le béton cellulaire à gaz à base de sable du désert sont les suivantes:

- la mise au point d'un tel matériau et de son mode de préparation serait d'une grande utilité pour la construction d'habitations rurales, aussi bien du point de vue économique que d'isolation thermique.
- le sable de désert présente une finesse exceptionnelle en comparaison avec les autres sables étudiés;
- la surface spécifique du sable de désert est acceptable, pour que ce dernier puisse être utilisé sans broyage préalable dans le béton cellulaire.
- le sable de désert a un équivalent de sable acceptable ainsi qu'une teneur en matières organiques et argileuses faibles, ce qui n'élimine pas la possibilité de l'utiliser dans les bétons à base de ciment portland et en particulier dans le béton cellulaire.

Principe de base

Le béton cellulaire au gaz est obtenu à partir d'un mélange de liant (ciment portland), d'un composant de silice et d'un agent de dégagement de gaz, la poudre d'aluminium par exemple, qui entre en réaction avec une solution aqueuse de l'hydroxyde de calcium en dégageant de l'hydrogène.

$2\,Al + 3\,Ca\,(OH)_2 \Rightarrow 3\,CaO \cdot Al_2O_3 + 3\,H_2$

L'hydrogène qui se dègage provoque le gonflement de la pâte de ciment qui, en durcissant, garde une structure poreuse.

Dans les bétons au ciment portland, l'hydroxyde de calcium se forme par hydrolyse du silicate tricalcique.

La poudre d'aluminium est introduite sous forme de suspension aqueuse afin d'assurer sa meilleure répartition au sein du mélange. Comme la poudre d'aluminium est soumise en usine à un paraffinage, on ajoute à la suspension d'aluminium une quantité de poudre de lessive pour enlever la couche de paraffine.

Le mode de préparation du béton cellulaire est le suivant:

a. préparation de la suspension liquide de la poudre d'aluminium;

b. préparation du mélange de béton cellulaire à la température 32°C-45°C;

c. confection des éprouvettes;

d. durcissement:

Il nous a fallu faire les essais multiples pour aboutir à un béton cellulaire à structure homogène et à des proprietés mécaniques acceptables.

Essais et résultats

On constate que pour la composition du béton cellulaire calculée, la résistance du béton obtenu s'est avérée faible et le béton ná pas suffisament gonflé ce qui nous a incité à prendre un rapport C/S plus grand et ajouter une quantiré de soude (1% du poids de ciment) à laquelle on peut substituer par une quantité de chaux vive, dosée à 10% du poids de ciment, qui, en contact de l'eau donnera du $Ca(OH)_2$ suivant la réaction suivante.

$$CaCO_3 + H_2O \Rightarrow Ca(OH)_2 + CO_2$$

et en chauffant l'eau de gâchage jusqu'à une température de l'ordre de 80°C de maniére à ce que son mélange avec les autres constituants donne une température de 40°C.

Tenant compte de ces remarques, les résultats obtenus sont trés bons:

- le gonflement du béton est suffisant et uniforme;
- la masse volumique à sec de ce béton est trés satisfaisante $P_m = 750$ kg/m^3;
- la structure de ce béton parait homogène;

Les résultats de ces essais effectuées 28 jours aprés la confecti de ce béton sont présentés dans le tableu ci-aprés:

Type de matériaux	masse volum (kg/m^3)	conductivité thermique (W/mC)	résistance à la compresion (MPa)
brique cuite	1200	0.46	2.5 - 3.5
aggloméré	1200 - 1600	1.30	6.0 - 8.0
pierre	2700	2.00	variable
terre stabilisée	2600	1.80	3.0 - 4.5
plâtre	1000	0.35	5.0
béton cellulaire	600 - 800	0.25 - 0.35	2.5 - 5.0

Tableau 7: Résistances en fonction d'agents gonflants

	Béton avec soude	Béton avec chaux vive
Résistance à la compression (MPa)	2.73 2.50 3.05 2.77 3.00 Moyenne = 2.81	2.70 2.85 2.96 2.58 3.00 Moyenne = 2.82

Tableau 8: Comparison du béton cellulaire aux autres matériaux

Le béton cellulaire est avec le plâtre le meilleur matériau du point de vue isolation phonique. Cette caractéristique résulte de la porosité de ce dernier qui fait partie de la famille des ma tériaux poreux à ossature rigide.

Substitution du ciment par d'autres matériaux

La substitution du ciment par un autre matériaux est possible dans la mesure ou :

- il s'agit d'un liant hydraulique;
- il contient un pourcentage suffisant de $Ca(OH)_2$;
- son durcissement n'est pas trés rapide pour permettre au béton de gonfler convenablement.

L'un des matériaux qui répond le mieux à ces conditions est la chaux hydraulique ce qui nous permettra d'envisager par la suite l'étude du béton cellulaire à base de:

- lait de chaux + laitier de hauts fourneaux;
- lait de chaux + brique broyée.

CONCLUSION

De l'étude qu'on a effectuée, il ressort que le béton à base du sable de désert ne diffrèe pas trop de celui usuellement connu. Son utilisation dans la construction est donc possible.

De plus ce sable, par ses proprietés spécifiques, s'est averé bon pour être utilisé comme élément de base d'un béton léger: le béton cellulaire.

L'étude de la faisabilité d'un tel béton, habituellement sophistiqué, a abouti à la mise au point d'un procedé technique d'une grande simplicité.

Tous ces résultats, quoi qu'encourageants, sont loin d'être les plus concluants sur toutes les possibilités qu'offre ce sable de désert.

Néanmoins, ils incitent à se lancer dans d'autres recherches éventuelles, concernant le sable de désert et les matériaux locaux d'une manière générale.

BIBLIOGRAPHIE

- Américan Concrete Institute A.C.I.Commitee 213. Guide pour le béton de structure à-base de granulats légers.
- V.MICHEL. La pratique des ciments et des bétons. Edition du moniteur des travaux publics et du bâtiment 1976.
- G.DREUX. Guide pratique du béton. Societé de diffusion des techniques du bâtiment et des travaux publics. Paris 1972
- P.CORMON. Bétons légers d'aujourdhui. Eyrolles.Paris 1973
- N.BEN AZOUZ. & S.GUERMAZI. Elaboration du béton à base du sable du sable de désert. Projet de fin d'étude. E.N.I.T. Tunis 1987
- E.OLIVIER. Technologie des méthodes de construction: Les bétons Paris 1980

UDC 624.073.01245 : 624.04

The advanced strip method – a simple design tool

Arne Hillerborg*

UNIVERSITY OF LUND : LUND INSTITUTE OF TECHNOLOGY

SYNOPSIS

The advanced strip method is a method for the design of slabs which are partly supported on columns, re-entrant corners or other point supports. On the basis of this general method, it is possible to formulate simple and straightforward rules for the design of most slabs met with in practice. The calculation of the design moments is then reduced to a simple application of ordinary beam theory, supplemented by taking into account a few rules regarding moment distribution and curtailment of reinforcement. The procedure is illustrated by examples, covering supports on interior columns, exterior columns, corner columns, a wall extending under part of the slab and a re-entrant corner. The method is simpler and safer than design based on yield-line analysis, and just as economical as regards reinforcement.

Introduction

The strip method of design for reinforced concrete slabs was first proposed in 1956(1) and further developed in 1959(2), when the 'advanced' method was first presented. These first papers were written in Swedish and the presentation to the English-speaking world is due to Crawford(3), Blakey(4), Wood(5,6), Armer(6) and many others. In 1975 a book(7) was published, in which the complete theoretical background was presented and also many examples of different practical applications were given.

Nowadays the strip method is referred to in many text-books, but the author has found that in most books only the 'simple' strip method is described. The reason for this seems to be that the 'advanced' method has been supposed to be complicated. In the author's opinion this is a mistake, which may have been caused by the perhaps too scientific, rigorous and complete treatment given in the book(7).

For most practical cases, the advanced method is rather simple and straightforward. It is far simpler than a correct application of the yield-line theory, in spite of the fact that it always gives safe results. From the point of view of economy, the advanced strip method is virtually equivalent to the yield-line theory or in practice even better (see reference 7).

As the simplicity of the advanced strip method seems to have been overlooked by the authors of text-books, the present author has felt a challenge to demonstrate this simplicity by means of a few examples.

The corner-supported element

The advanced strip method is meant to be applied when a slab is point-supported on a column, a re-entrant corner or some other support where it is reasonable to assume that there will be concentrated support reactions.

The most fundamental concept of the advanced strip method is the corner-supported element. In its simplest form, which will be treated here, this is a rectangular part of a slab, characterized by the following properties:

(1) the edges are parallel to the reinforcement directions;
(2) it carries a uniform load q per unit area;
(3) it is supported only at one corner;
(4) no shear forces act along the edges;
(5) no twisting moments act along the edges;
(6) all bending moments along an edge have the same sign (or are zero);
(7) the bending moments along the edges are the design moments for the reinforcing bars.

---

*Professor Arne Hillerborg, Division of Building Materials, Lund Institute of Technology, Box 725, S–220 07, Lund, Sweden.

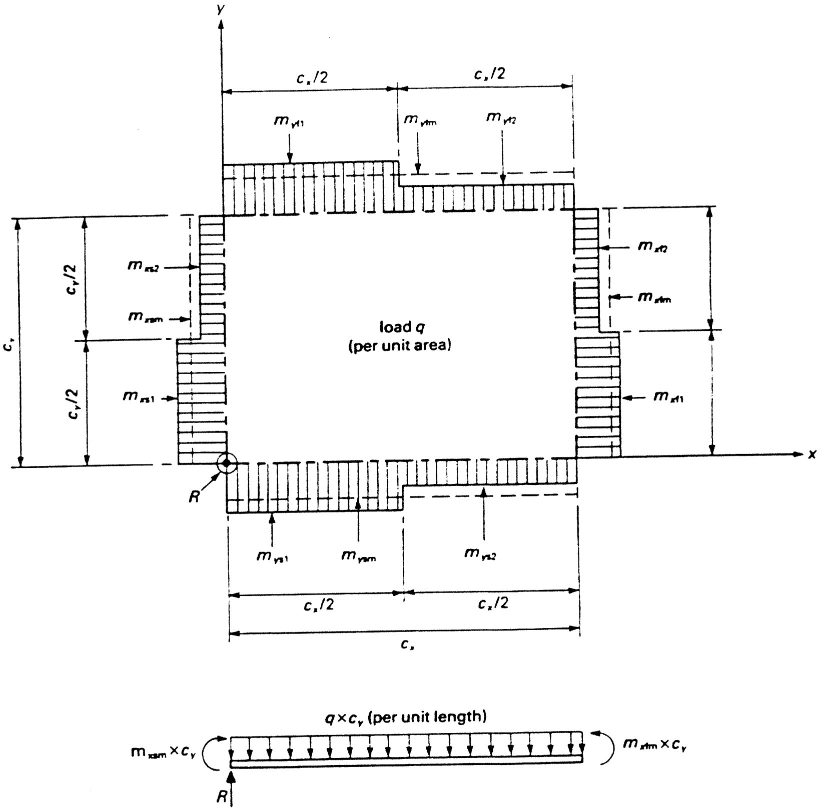

Figure 1: A corner-supported element with assumed distribution of moments along the edges. The edges of the element are shown in chain-dotted lines, indicating zero shear forces. Subscripts x and y stand for directions, s and f for support and field (span), and m for mean.

We will here further limit ourselves to the case where we assume that:

(8) the bending moment is constant along each half of each edge.

Figure 1 shows the forces and moments acting on a corner-supported element according to the above description.

From vertical equilibrium, we directly get the corner reaction

$$R = qc_xc_y \quad \text{.......................(1)}$$

Moment equilibrium around the y-axis gives

$$m_{xfm} - m_{xsm} = qc_x^2/2 \quad \text{.................(2)}$$

where m_{xfm} and m_{xsm} are the mean span and support moments per unit width respectively, corresponding to the reinforcement in the x-direction.

In the same way we may write

$$m_{yfm} - m_{ysm} = qc_y^2/2 \quad \text{.................(3)}$$

Equation 2 is identical with the condition for a corresponding part of a simple strip, spanning in the x-direction, supported at the y-axis and carrying the load q. Thus, if the corner-supported element forms part of a strip, that part should carry the whole load q. The same is true in the y-direction according to equation 3.

Thus, where a corner-supported element forms part of strips in the x- and y-directions, *the full load q should be carried in both directions.* This fact has sometimes astonished people, when they compare it with the simple strip method, where the load is divided between the two directions. The difference is that, in the simple strip method, each strip is supported over its whole width, so that a load has only to be carried in one direction to reach a support; however, for a corner-supported element, the whole load at each point has to be carried in both directions in order to reach the supported corner. In order to indicate that the whole load is carried in both directions in a corner-supported element, such an element is marked with crossing arrows in the plan showing the load distribution (see Figures 3 to 9 below).

One essential point in the description of the corner-supported element is that the edge moments, given in Figure 1, are the design moments for the reinforcing bars. This means that no bar will meet a greater design moment inside the element. In order to fulfil this condition, a limitation must be put on the moment distribution along the edges(7). For the type of moment distribution shown in Figure 1, the restriction can be given in the following simplified form

$$m_{xf2} - x_{xs2} = \alpha qc_x^2/2 \quad \text{.................(4)}$$

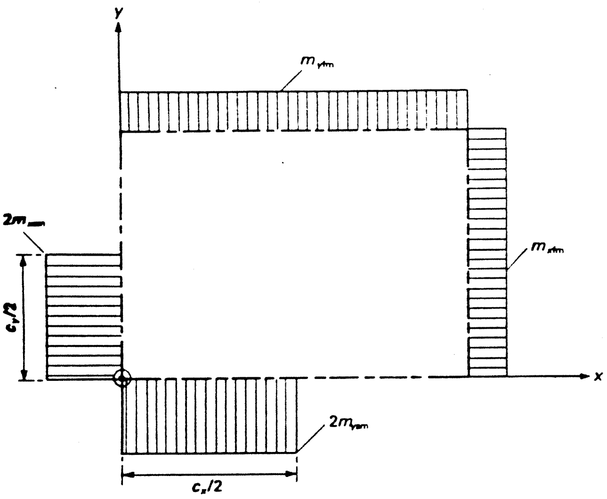

Figure 2: Recommend moment distribution to be used in all cases where this is possible with respect to equation 5.

with

$$0{\cdot}25 \le \alpha \le 0{\cdot}7 \quad\ldots\ldots\ldots\ldots(5)$$

and a corresponding expression for the y-direction.

For most practical applications, it is suitable to choose (cf. Figure 2)

$$m_{xf1} = m_{xf2} = m_{xfm} \quad\ldots\ldots\ldots\ldots(6a)$$

$$m_{xs2} = 0 \quad\ldots\ldots\ldots\ldots(6b)$$

and

$$m_{xs1} = 2m_{xsm} \quad\ldots\ldots\ldots\ldots(6c)$$

The span reinforcement must always be carried through the whole corner-supported element.

The support reinforcement corresponding to $m_{xs1} - m_{xs2}$ must be anchored more than 0·6 c_x from the support. The remaining support reinforcement must be carried through the whole corner-supported element. Where equation 6b is fulfilled thus, only the first rule applies.

Rules for practical application

The corner-supported elements are combined with each other and with parts of one-way strips to form a system of strips, in which each strip carries the total load q over its whole length – see the examples below. In a strip may also be included an ordinary simple strip along the corner-supported element, having the same load and mean moments.

The concentrated corner support may be assumed to be situated at the edge or corner of a supporting concrete column or column head. If the support is made of some weaker material, e.g. masonry, the point of support should be assumed with regard to permissible compressive stresses (see reference 7).

The mean moments in the strips are calculated by means of ordinary rules for beams. The moment distribution can thus be based on the theory of elasticity or on some other choice. In the examples below, a value of about 1·5 to 2·0 has been chosen for the ratio between support and span moments. The choice of this value will not be further commented upon here, as it is of no importance for the understanding of the method.

Moment transfer to the columns has been neglected in the examples (just as it is usually neglected when yield-line theory is applied). Some comments on this are made at the end of the paper (Figure 9).

The positions of the moment maxima (zero shear forces) give the sizes of the corner-supported elements, and thus the widths of the strips in the perpendicular directions.

The distributions of bending moments across the width of the strips are made according to Figure 2, where possible, or else with regard to the more general Figure 1. Condition 5 (equation 5) has to be fulfilled. Where a narrow simple strip is included parallel to corner-supported elements (see, for instance, Example 1), the width of this strip may be looked upon as included in the corner-supported elements when moment distributions are determined.

In the corners of the slabs, some parts are not covered by the strips described above ('main strips'). The reinforcement within these parts may be designed for one-third of the span moments in the adjoining parts of the parallel main strips. This is strictly somewhat on the unsafe side, but the error is small in comparison with what is accepted in applying the yield-line theory.

The curtailment of the reinforcement in the corner-supported elements is made according to the rules given after equation 6 above. The curtailment of the reinforcement in the simple strips follows normal rules. In the parts at the corners of the slab, all reinforcement has to be carried to the supports.

Examples

For all the Examples, the following conditions are valid:

////////// denotes a fixed edge
– – – – – – denotes a simply supported edge
———— denotes a free edge
▨ denotes a column
—— - —— denotes a line of zero shear force

All sizes are given in metres (in the smaller numerals). The design load is 8 kN/m². Moments are given in kNm/m. Moment curves show mean moments in the strips.

The numerical calculations of moments are not shown, as it is quite evident how they are performed, and the values can easily be checked by anyone who is familiar with the calculation of bending moments in beams.

All columns are supposed to be made of concrete, which means that the supports are assumed to be situated at the column edges.

EXAMPLE 1

Figure 3 shows the size and support conditions of a slab, the chosen moment curves for the main strips, the corresponding widths of the main strips and the resulting design moments, all according to the rules given above.

The total width of the y-strip is $2{\cdot}65 + 0{\cdot}3 + 3{\cdot}1 = 6{\cdot}05$ m. The central portion of width 0·3 m, corresponding to the width of the column, is divided between the two corner-supported elements when it comes to the distribution of support moment. This gives the values $(2{\cdot}65 + 0{\cdot}15)/2 = 1{\cdot}40$, $(3{\cdot}1 + 0{\cdot}15)/2 = 1{\cdot}625$ and $1{\cdot}40 + 1{\cdot}625 = 3{\cdot}025$ given in the Figure.

A check of the α-values according to equation 5 gives the following four results, which are all within the limits:

$$7{\cdot}28/\ (7{\cdot}28 + 20{\cdot}8) = 0{\cdot}26$$
$$17{\cdot}64/(17{\cdot}64 + 20{\cdot}8) = 0{\cdot}46$$
$$11{\cdot}36/(11{\cdot}36 + 20{\cdot}0) = 0{\cdot}36$$
$$16{\cdot}0\ /(16{\cdot}0\ \ + 20{\cdot}0) = 0{\cdot}44$$

The load carried by the column is

$$R = 8 \times 6{\cdot}1 \times 6{\cdot}05 = 296 \text{ kN}$$

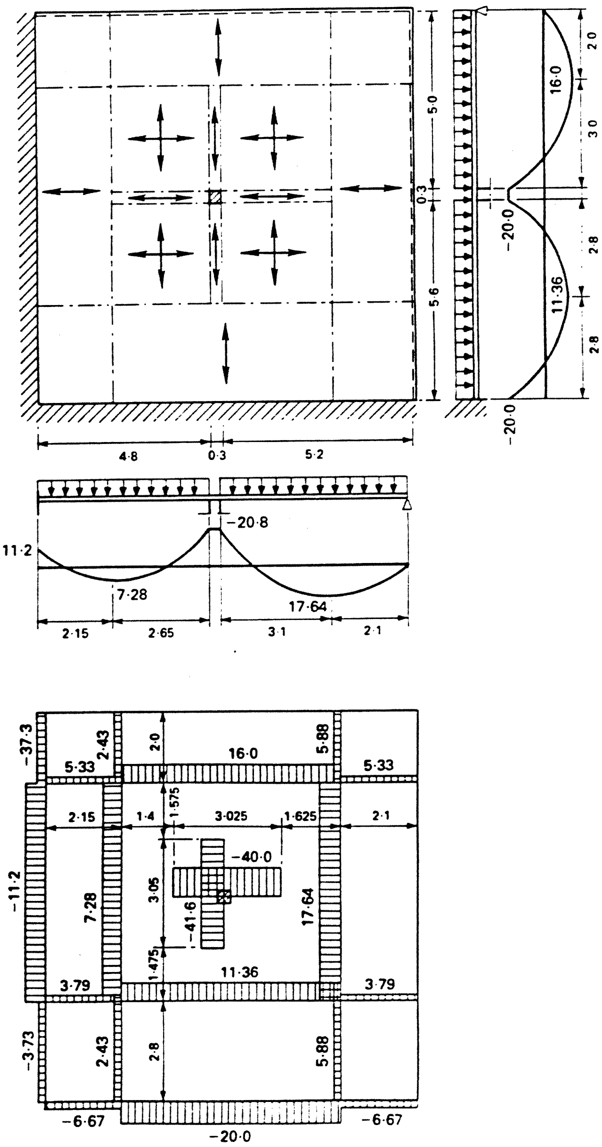

2·0
3·0
2·8
2·8
16·0
-20·0
11·36
-20·0
5·0
0·3
5·6
4·8
0·3
5·2
-20·8
-11·2
7·28
17·64
2·15
2·65
3·1
2·1
-3·73
2·43
5·33
2·0
16·0
5·88
5·33
1·575
2·15
1·4
3·025
1·625
2·1
-40·0
-11·2
7·28
3·05
-41·6
17·64
1·475
11·36
3·79
3·79
-3·73
2·43
2·8
5·88
-6·67
-6·67
-20·0

Figure 3: Example 1.

EXAMPLE 2

This slab (Figure 4) is identical with the previous one except that the simple support along one edge is replaced by a column. The moment curves in the main strips are therefore identical with those chosen for Example 1.

When it comes to the distribution of moments, the simple rules according to Figure 2 and equations 6a to c cannot be followed in the x-direction for the elements supported on the edge column, as there is no support moment. Therefore an uneven distribution of span moment must be used with regard to

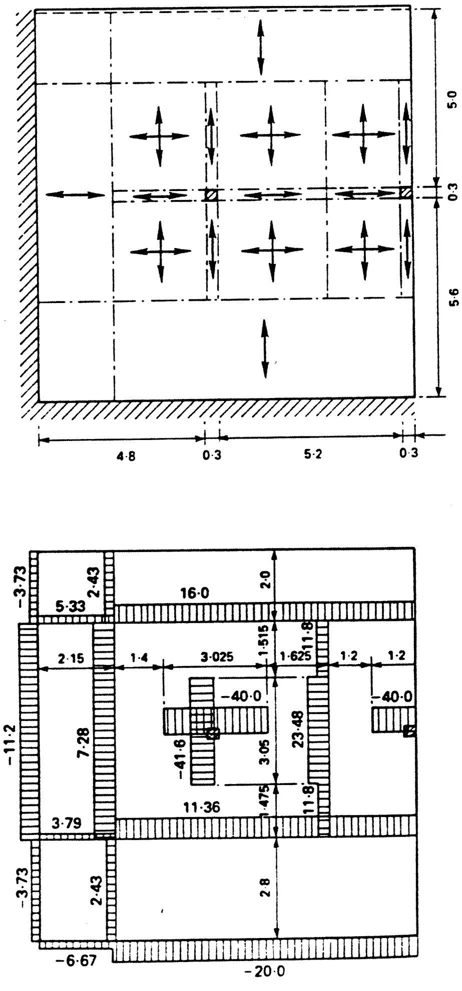

5·0
0·3
5·6
4·8
0·3
5·2
0·3
-3·73
2·43
5·33
16·0
2·0
2·15
1·4
3·025
1·515
1·625
11·8
1·2
1·2
-40·0
-40·0
-11·2
7·28
-41·6
3·05
23·48
11·36
1·475
11·8
3·79
-3·73
2·43
2·8
-6·67
-20·0

Figure 4: Example 2.

condition 5. For the moment m_{xf2}, we have to fulfil the following condition with regard to the edge column:

$$0{\cdot}25 \leq m_{xf2}/17{\cdot}64 \leq 0{\cdot}70$$

and the following with regard to the inner column:

$$0{\cdot}25 \leq m_{xf2}/(17{\cdot}64+20{\cdot}80) \leq 0{\cdot}70$$

In order to fulfil both these conditions, we find that

$$9{\cdot}61 \leq m_{xf2} \leq 12{\cdot}35$$

and we can thus choose $m_{xf2} = 11{\cdot}8$.

EXAMPLE 3

This is the slab of Example 2, but extended 2 m to the right (Figure 5). This changes the moment curves in the x-direction, giving a statically determinate support moment over the column next to the free edge. In order to fulfil condition 5, at least 0·25 of this support moment has to be distributed over the whole width of the corner-supported element.

EXAMPLE 4

This is the slab of Example 1, but with a wall extending from the left to the position of the column (Figure 6). This will mean that the left part of the slab can be treated by means of the simple strip method, e.g. with the load distribution shown. The mean strip moments in the y-direction can be taken to be the same as in Example 1. For the load carried in the x-direction only, the sum of mean design moments is (with the chosen size 2·4 m) $8 \times 2{\cdot}4^2/6 = 7{\cdot}68$, which has been divided into a span moment of 3·0 and a support moment of 4·68.

The support reinforcement in the x-direction from the corner-supported elements has to be safely anchored into the slab, which means a distance of the same order as the length in the element, i.e. about $0{\cdot}6 \times 3{\cdot}1 = 1{\cdot}9$ m. The support moment in the y-direction over the wall may be more concentrated towards the end of the wall.

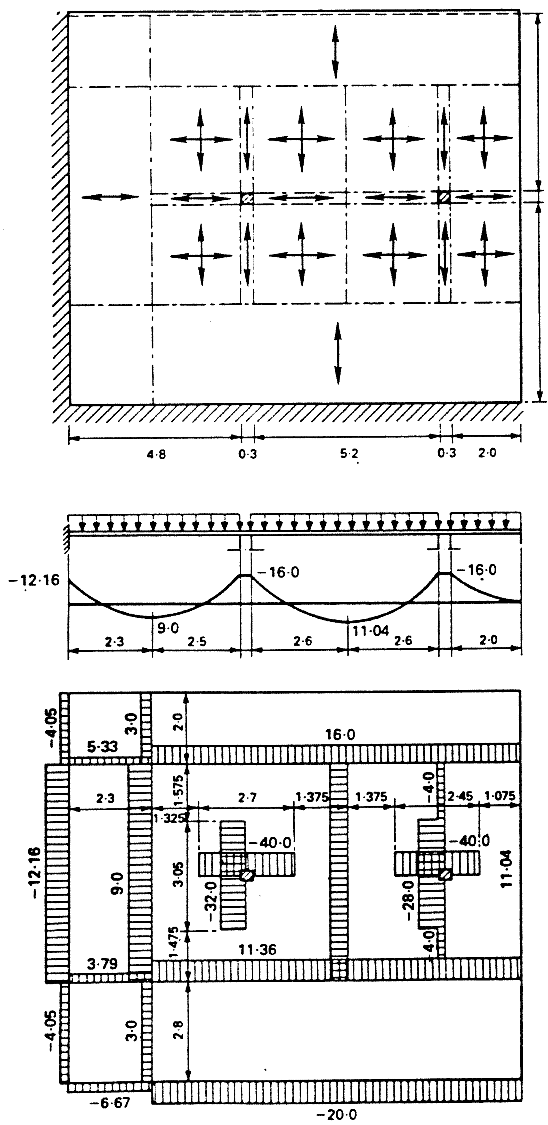

5·0
0·3
5·6
4·8
0·3
5·2
0·3
2·0
−12·16
−16·0
−16·0
9·0
11·04
2·3
2·5
2·6
2·6
2·0
−4·05
3·0
2·0
16·0
5·33
2·3
1·575
2·7
1·375
1·375
4·0
2·45
1·075
1·325
−40·0
−40·0
−12·16
9·0
3·05
−32·0
−28·0
11·04
1·475
11·36
4·0
3·79
−4·05
3·0
2·8
−6·67
−20·0

Figure 5: Example 3.

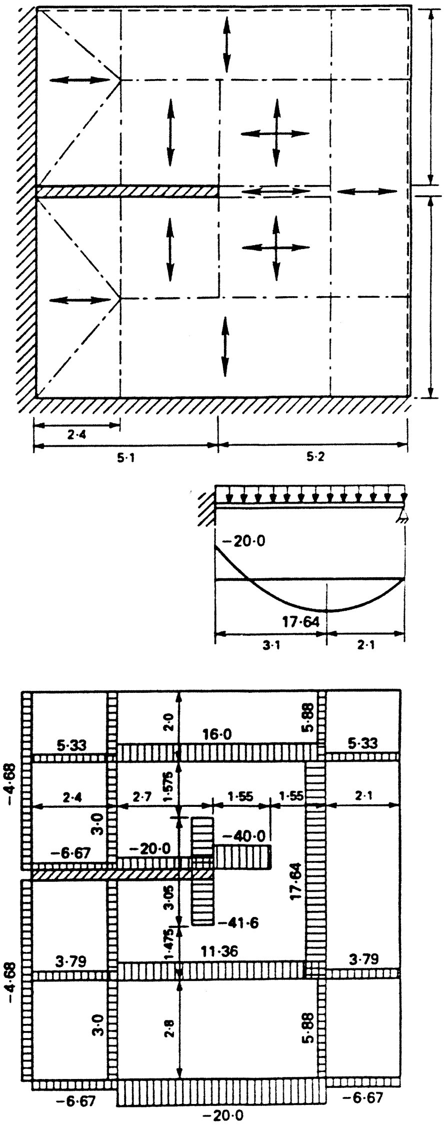

5·0
0·3
5·6
2·4
5·1
5·2
−20·0
17·64
3·1
2·1
2·0
16·0
5·88
5·33
5·33
−4·68
2·4
2·7
1·575
1·55
1·55
2·1
3·0
−40·0
−6·67
−20·0
3·05
17·64
−41·6
1·475
11·36
3·79
3·79
−4·68
3·0
2·8
5·88
−6·67
−20·0
−6·67

Figure 6: Example 4.

A very similar technique can be applied to the slab in Figure 7, which can be looked upon as the slab of Figure 6 with another wall meeting the first one at the position of the column in Example 1.

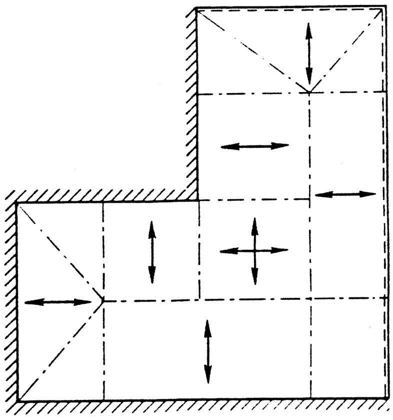

Figure 7: Slab with re-entrant corner.

EXAMPLE 5

This slab (Figure 8) has two free edges, one corner column and one edge column. A special problem in this case is that the span moment in the y-direction must be unevenly distributed in order to fulfil condition 5. On the other hand, it should be evenly distributed in order to agree with the conditions in the one-way-spanning part of the strip. It has, however, been demonstrated(7) that the latter condition does not have to be rigorously fulfilled, but that a permissible moment field can be found in that part of the slab also with an uneven distribution of bending moment in the span. The moment distribution should then be chosen as even as possible with regard to condition 5; thus

$$m_{xf2} \simeq 0{\cdot}7\, m_{xfm} = 0{\cdot}7 \times 16 = 11{\cdot}2$$

The value chosen should not be higher than this, but it may be a little lower, e.g. 10 or 11.

OTHER APPLICATIONS

The examples above are all based on the assumption that the load is evenly distributed and the moment distribution follows Figure 1. Where the load is not evenly distributed, the same method can also be applied, at least where one of the following conditions is fulfilled:

(1) the load varies only in one direction (e.g. water pressure);

(2) the unevenly distributed load is small compared with the evenly distributed load (e.g. a point load of 20 kN in the examples).

Sometimes there may be a reason for choosing a narrower band of support reinforcement than indicated in Figures 1 and 2. This is possible, but the limits of condition 5 have to be changed. When the band has zero width, the condition can be written.

$$0{\cdot}5 \leq \alpha \leq 0{\cdot}6 \qquad \text{.....................(7)}$$

For other widths, a linear interpolation between equations 5 and 7 can be used.

One example of a case where a narrower reinforcement band should be used is where the moment transfer to a column is taken into account. Assume, for instance, that the columns in Example 5 are to be designed to take a mean support moment of 3·2 kN/m for reinforcement in the y-direction and

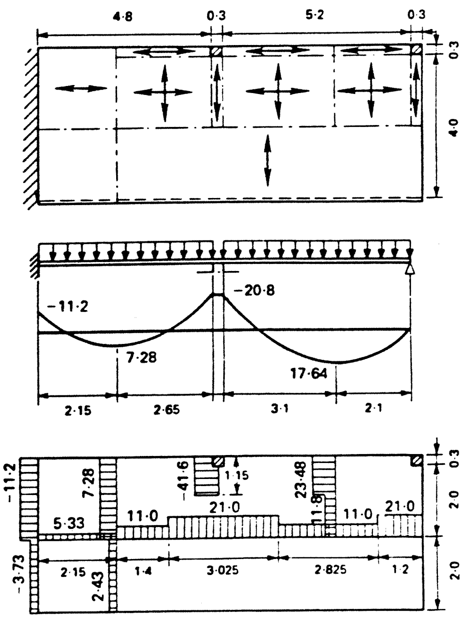

Figure 8: Example 5.

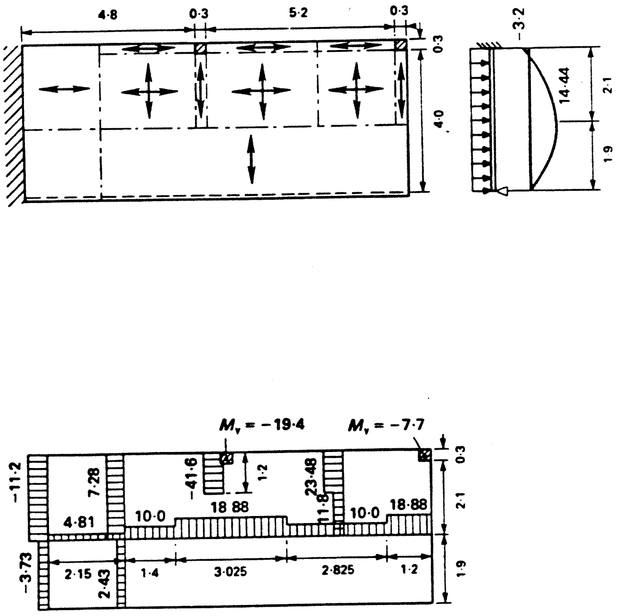

Figure 9: Example 5, but with support moments in columns.

that this moment is to be carried on a width corresponding to that of the column. This leads to a possible moment distribution according to Figure 9. If we, on the safe side, disregard the width of the column, condition 7 in this case gives

$$0{\cdot}5\times 17{\cdot}64 \le m_{xf_2} \le 0{\cdot}6\times 17{\cdot}64$$

$$8{\cdot}82 \le m_{xf_2} \le 10{\cdot}58$$

The moment in the corner column is

$$M_y = -3{\cdot}2(2{\cdot}1+0{\cdot}3) = -7{\cdot}7\,\mathrm{N\,m}$$

and in the edge column

$$M_y = -3{\cdot}2(2{\cdot}65+0{\cdot}3+3{\cdot}1) = -19{\cdot}4\,\mathrm{N\,m}$$

In this case it has been assumed that the moment is taken only on the column width, i.e. that the top reinforcement is bent down into the column. If the moment is taken on a greater width, the edge must also be reinforced with regard to torsion.

It must be noted that the above moments refer to the edges of the columns. In order to get the moments with respect to the centre of a column, the influence of the eccentric reactions has to be taken into account. For the edge column this eccentric reaction is

$$8\times 2{\cdot}1(2{\cdot}65+0{\cdot}3+3{\cdot}1) = 101{\cdot}64\,\mathrm{kN}$$

which gives an additional moment of

$$101{\cdot}64\times 0{\cdot}15 = 15{\cdot}2\,\mathrm{kN\,m}$$

The total column moment is thus 34·6 kN m. The total column force is:

$$8(2{\cdot}1+0{\cdot}3)(2{\cdot}65+0{\cdot}3+3{\cdot}1) = 116\,\mathrm{kN}$$

The advanced strip method can be applied to many cases other than those demonstrated here, e.g. to non-rectangular slabs, slabs with irregularly situated supports, slabs with non-orthogonal reinforcement etc., but of course these more complicated cases need some special treatment, which is outside the scope of this paper.

Comparison with the yield-line theory

The main theoretical difference between the strip method and the yield-line theory is that the former gives results on the safe side, whereas the latter gives results on the unsafe side. This means that it is necessary to be very careful when the yield-line theory is used for design, as any mistake regarding the assumed yield-line pattern results in an unsafe design. No corresponding risk exists with the strip method.

A practical difference between the two approaches is that the strip method is a design method which directly gives the design moments and forces, whereas the yield-line theory is a method for checking the strength of a given structure. This check must often be made for many possible yield-line patterns. In complicated cases, the design will therefore involve an iterative process in order to find the best reinforcement distribution.

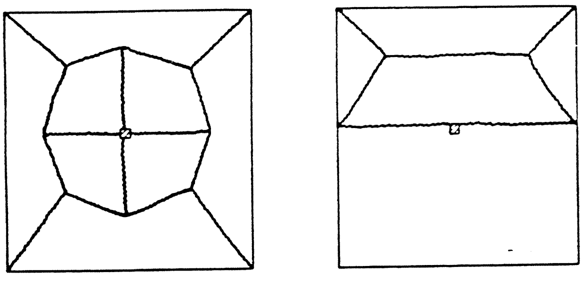
(a) *(b)*

Figure 10: Two possible yield-line patterns for Example 1.

If, for example, we wish to design the slab of Example 1 by means of the yield-line theory, we have to start by assuming a complete moment distribution and check the corresponding load-carrying capacity by means of at least one total yield mechanism according to Figure 10a and four partwise yield mechanisms of the type shown in Figure 10b. We also have to check for local failure around the column. The check for possible curtailment of reinforcement is very laborious.

A design by means of the yield-line theory for the types of slabs treated here is thus very complicated, if it is done in a correct way, so that the results are not too much on the unsafe side. The economic result, measured as the amount of reinforcement required, is practically the same with the two approaches.

REFERENCES

1. HILLERBORG, A. Jämviksteori för armerade betongplattor. (Equilibrium theory for concrete slabs.) *Betong*. Vol. 41, No. 4. 1956 pp. 171–182.
2. HILLERBORG, A. *Strimlemetoden för plattor på pelare, vinkelplattor mm.* Stockholm, Svenska Riksbyggen, 1959.
3. CRAWFORD, R. E. *Limit design of reinforced concrete slabs.* Thesis submitted to the University of Illinois for the degree of PhD. Urbana, 1962.
4. BLAKEY, F. A. *Strip method for slabs on columns, L-shaped plates etc.* Translation of reference 2. Melbourne, CSIRO, 1964. D.B.R. Translation No. 2.
5. WOOD, R. H. The reinforcement of slabs in accordance with a predetermined field of moments. *Concrete.* Vol. 2, No. 2. February 1968. pp. 69–76.
6. WOOD, R. H. and ARMER, G. S. T. The theory of the strip method for design of slabs. *Proceedings of the Institution of Civil Engineers.* Vol. 41, No. 10. October 1968. pp. 285–311.
7. HILLERBORG, A. *Strip method of design.* In Swedish 1974. English translation: Wexham Springs, Cement and Concrete Association, 1975. pp. 256. Viewpoint Publication 12.067.

Contributions discussing the above paper should be in the hands of the Editor not later than 30 June 1983.

APPLICATION OF FRACTURE MECHANICS TO CONCRETE

with emphasis on the work performed at Lund Inst. of Tech.

Arne Hillerborg, Div. of Building Materials, Lund Inst. of Tech.,
Lund, Sweden.

Abstract

Different approaches to the application of fracture mechanics to concrete are discussed, with an emphasis on the models based on strain softening and strain localization, particularly the fictitious crack model. Examples of results of the theoretical analyses are demonstrated, and some practical conclusions are drawn. Future research is also commented.

Introduction

Conventional fracture mechanics is mainly based on the theory of elasticity and it is used for studying the stability and propagation of existing cracks. The modern form of application of fracture mechanics to concrete, which was first developed in Lund, differs from the conventional fracture mechanics in both these respects.

In the basic form of conventional fracture mechanics it is assumed that the stresses and strains tend towards infinity at a crack tip, Fig. 1. This is of course not realistic. In spite of this the theoretical results based on this assumption in many cases lead to realistic conclusions. In other cases this is not the case. This has since long been recognized, and in conventional fracture mechanics many methods have been advised to overcome this problem. Some of these methods are similar to the methods now applied to concrete, even though there are fundamental differences.

The most important practical difference between conventional fracture mechanics and the modern application to concrete is that conventional fracture mechanics has never been applied to structures without any initial crack, whereas the modern model can also be applied to this case. It is now possible not only to study the stability and propagation of a crack, but also its formation. Thus the complete development of fracture can be analysed by means of one model as a continuous process. This is an expansion of fracture mechanics, which opens quite new possibilities to analyse fracture of real structures, as will be demonstrated by means of examples.

This circumstance has been emphasized here, because it has not always been fully appreciated. Thus for example the new approach is sometimes described as a variant of the so called Dugdale-Barenblatt model. Dugdale and Barenblatt never realised the possibility to use this type of model for the analyses of uncracked structures. They only intended their models as explanations of the stress situation in the vicinity of the tip of an existing crack.

Conventional fracture mechanics

As a background for the understanding of the new model a short description will be given of conventional fracture mechanics, particularly linear elatic fracture mechanics, often written LEFM for short.

If a stress is applied perpendicular to a crack with a sharp tip, the linear elastic solution shows that a stress concentration will appear at the tip, such that the stress approaches infinity, Fig. 1. Close to the crack tip the stress distribution is approximately described by the equation

$$\sigma_y = \frac{K}{\sqrt{2\pi x}}$$

In this equation x is the distance from the crack tip and K is called the **stress intensity factor.** This factor can be calculated from the equation

$$K = Y\sigma\sqrt{a}$$

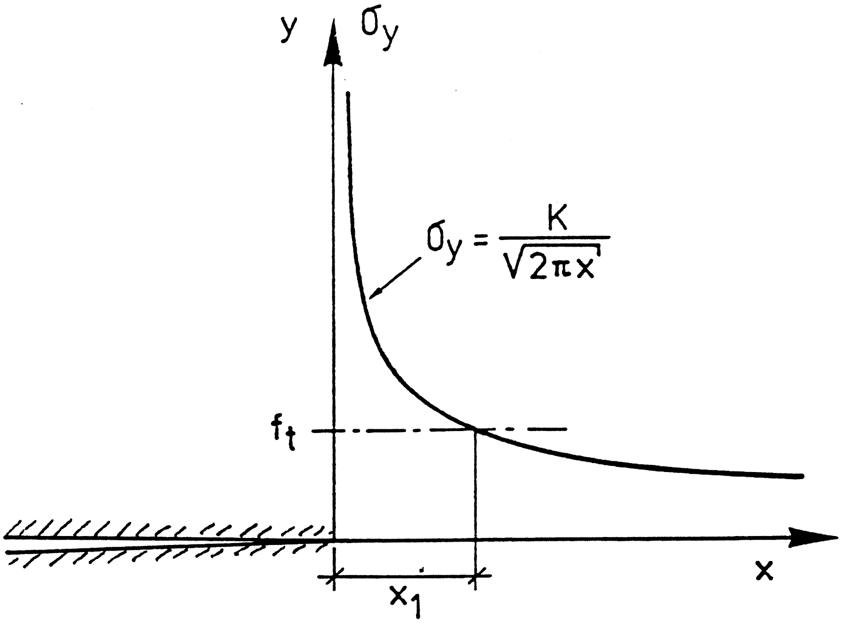

Fig. 1 Stress distribution according to the theory of elasticity.

where a is the crack length (for a crack at an edge, or half the crack length for an interior crack), σ is the stress which would have acted if there had been no crack, and Y is a dimensionless factor, which depends on the type of structure, the loading conditions, and to some extent to the crack length. The value of Y is often approximately 2.

According to this formal stress distribution the stress within a distance x_1 exceeds the tensile strength f_t. The stress distribution cannot be valid within this part. The larger the value is of x_1, the less accurate are the conclusions drawn by means of LEFM.

As the stress approaches infinity, the analysis of crack stability and crack propagation cannot be based on a comparison with the strength of the material. Instead it is necessary to introduce a new criterion, which says that the crack will start propagating when the stress intensity factor K reaches a critical value, **the critical stress intensity K_c**, which is assumed to be a material property.

It can be noticed that conventional fracture mechanics can only treat problems concerned with an existing crack, as K becomes zero when the crack length a is zero. For uncracked material the ordinary theory of strength of materials has to be used, with a comparison between a stress and a strength as fracture criterion. This means that different models have to be used for cracked and uncracked material, with different fracture criteria and two different material properties, K_c and strength. This lack of continuity is a drawback, at least for materials like concrete.

An alternative treatment according to LEFM is based on the stress release rate when a crack propagates, i e the amount of energy which is released in the structure per unit crack area when the crack propagates. An **energy release rate G** is theoretically calculated. The crack i assumed to propagate if G reaches a critical value, **the critical energy release rate G_c**, which is equal to the amount of energy that is absorbed in the fracture zone per unit area when the crack grows. It can be demonstrated that the approaches by means of stress intensity factors and energy release rates are equivalent, and that they are coupled by means of the following relation for the case of plane stress conditions.

$$K^2 = EG$$

It has long been recognised that the unrealistic assumption that the stress and strain approaches infinity can lead to erroneous results. Many methods are used to make corrections in order to take into account the limited strength of the material. These methods will not be discussed here, as they as a rule give results, which are not accurate enough for concrete structures of normal sizes.

The basis of the new approach.

The basic idea of the new approach is best demonstrated by means of a discussion of the stress-deformation behaviour of a specimen in a tension test, Fig. 2. It is assumed that complete stress-deformation curves are recorded simultaneously by means of four gauges. Gauges B, C, and D are of the same length and situated immediately after each other, whereas gauge A has a length which is equal to the sum of gauges B, C, and D.

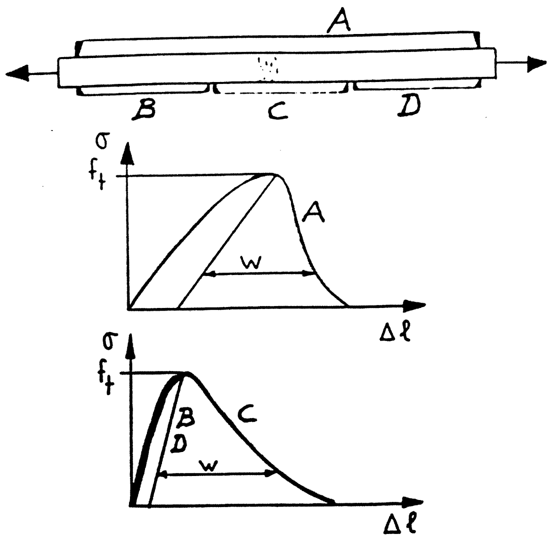

Fig. 2. Deformations along different gauge lengths in a tensile test.

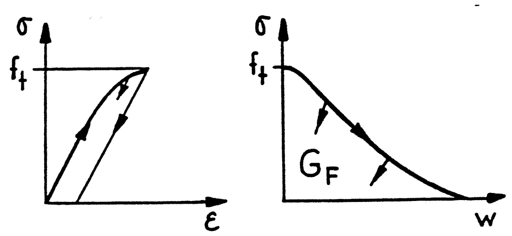

Fig. 3. General deformation properties.

The test is assumed to be performed in deformation control, which means that the deformation is slowly increased. During the first phase of the test, the stress increases as the deformation increases. This is said to be the ascending branch in the stress-deformation diagram. If the specimen is assumed to be homogenuous, the relative elongation during this phase is the same along the whole specimen. This means that the deformation can be described by means of a strain ε, defined as the deformation divided by the gauge length. The same stress-strain diagram is valid for the whole specimen at this stage.

After the peak stress has been reached, the **post-peak** stage, a further increase in deformation means that the stress decreases. We are now on the **descending branch** in the diagram. The cause for the decreasing stress is that the damage (microcracks) somewhere along the bar has become so high, that any increase in deformation leads to a decreasing ability to transfer stresses. Within this **damage zone** or **fracture zone** an increase in deformation takes place, at the same time as the damage increases and the transferred stress decreases.

As the stress decreases due to the increasing damage within the fracture zone, the parts outside this zone are unloaded, and they thus contract. At the post-peak stage an increase in the total deformation corresponds to a decrease in deformation for most parts of the specimen, but an increase in the deformation within the fracture zone. The term **strain localization** is often used to characterize this behaviour. The increase in deformation is localized to the fracture zone, whereas no further increase in strain takes part outside this zone.

Another term, which is often used to describe the stress-deformation at the post-peak stage is **strain softening**, which means that the stress decreases as the average strain (or rather the deformation) increases.

In Fig. 2 the stress-deformation curves from the four gauges are shown on the assumption that the fracture zone is situated within gauge-length C. The sum of the deformations in gauges B, C and D is equal to the deformation in gauge A.

From the figure it is evident that the curves from the different gauges are different, with the exception of gauges B and D, which are equal. Thus the stress-deformation relation cannot be expressed by a single curve, as this relation depends on the gauge-length and on the position of the gauge with respect to the fracture zone. It is thus not possible to find a general stress-strain curve for a material, including the descending branch. This fact is often neglected. Many examples can be found in the litterature, where equations for such stress-strain curves for concrete have been proposed.

A general description of the stress-deformation properties can be given by means of two curves according to Fig. 3, one stress-strain (σ-ε) curve for strains smaller than the stress at the peak point, and one stress-deformation (σ-w) curve for the additional deformation w within the fracture zone, caused by the damage within this zone. The general equation for the deformation Δl on a gauge length l is then given by

$$\Delta l = \varepsilon l + w$$

where ε is taken from the σ-ε-curve and w from the σ-w-curve. The latter value is only used where there is a fracture zone within the gauge length in question. In other cases it equals zero. In the post-peak region the value of ε is taken from the unloading branch.

One essential property of the σ-w-curve is the area below the curve, as this area is a measure of the energy which is absorbed per unit area of the fracture zone during a test to failure. This value is usually called the **fracture energy** (more correct fracture energy per unit area), and is denoted by $\mathbf{G_F}$.

For the behaviour of a specimen it is of importance how much of the deformation that is due to the σ-ε-curve, and how much that is due to the σ-w-curve. In other words it is important how these curves are related to each other. One way of defining this relation is by taking the ratio between a deformation equal to G_F/f_t from the σ-w-curve and a deformation f_t/E from the σ-ε-curve. This yields a value which is called the **characteristic length $\mathbf{l_{ch}}$** of the material

$$l_{ch} = EG_F/f_t^2$$

G_F/f_t corresponds to the maximum deformation w if the shape of the curve had been a rectangle, whereas f_t/E is the maximum strain if the σ-ε-curve were a straight line, see Fig. 4. The characteristic length l_{ch} is a material property, which cannot be directly measured, but which is calculated from the measured values of E, G_F and f_t.

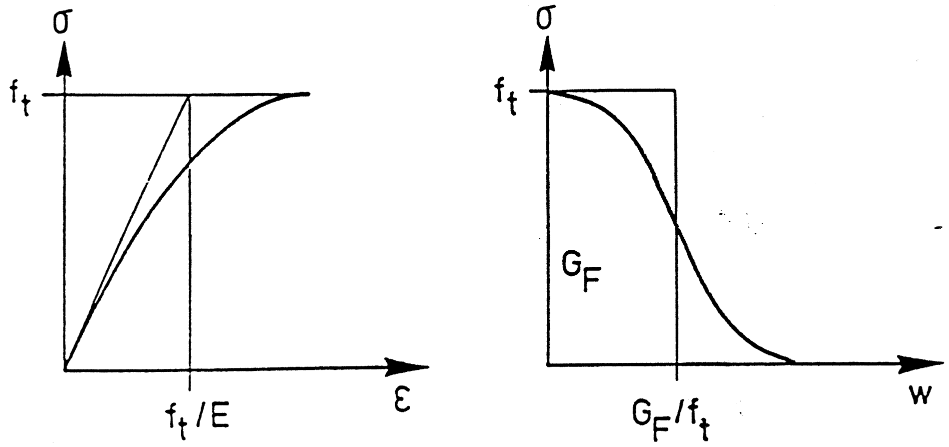

Fig. 4.

The fracture zone.

The development of the fracture zone starts by the formation of microcracks, which make this zone weaker. At this first stage the zone may comprise a certain length in the stress direction, and the additional deformation corresponds to the the sum of the additional deformations within these microcracks.

As the deformation increases, it gets more and more localized, and in reality practically all the additional deformation happens within a narrow zone, which may best be described as an irregular crack, which changes direction, bifurcates etc, depending on the inhomogenities of the material. Thus the width of the fracture zone (the size in the stress direction) can be assumed to be practically zero.

One way of expressing this is simply to assume as a formal model that the fracture zone is a crack with the width w and with the ability to transfer stresses according to the σ-w-curve. A crack with the ability to transfer stresses is of course no real crack, but just a hypothetical model. It can therefore be said that the crack is "fictitious". This model has been called the "fictitious crack model". The model was first published by Hillerborg et al (1976), and it has later been further developed and applied in many publications, e g by Petersson (1981) and Gustafsson (1985).

However from the point of view of practical application it does not matter whether the additional deformation in the fracture zone is assumed to take part in a "fictitious crack" or if it is assumed to be distributed on a certain length, as long as this length is small in comparison with other dimensions of the structure. Thus there is hardly any practical difference between the "fictitious crack model", and the "crack band model" proposed by Bazant and Oh (1983), where they assume a distribution on a length equal to 3 times the maximum aggregate size. These models are often implemented into a finite element scheme in different ways, but this is another question, which will be commented upon later.

The concentration of the fracture zone to a thin band or a single crack is typical for tensile fracture of concrete. It is not accompanied by any significant lateral deformations or stresses, and thus it corresponds to a very simple one-dimensional stress and deformation state. Therefore the σ-w-curve can be assumed to be a material property, which is rather insensitive to the shape of the structure and the general stress state, as long as all other stresses (e g a possible perpendicular compressive stress) are low compared to the strength.

For metals the stress state is much more complicated, as the yielding of metals gives rise to a complicated three-dimensional stress state and lateral deformations. Fracture mechanics of metals cannot be treated with the same model that is used for concrete.

For concrete in compression the fracture zone also develops in another way than in tension, as crushing is accompanied by lateral deformations. The compression fracture is much more complicated than tensile fracture. Some kind of descending σ-w-curve exists, but probably it cannot be regarded to be a well defined material property. The maximum stress as well as the shape of the curve can be expected to depend on e g confinement through stirrups or strain gradients. The application of the fracture mechanics ideas to compressive fracture is still an unexplored but interesting domain. It will only be very shortly commented upon at the end of this paper.

Material properties.

The stress-strain curve in tension for ordinary concrete deviates rather little from a straight line. Thus for most practical applications this relation can be assumed to be a straight line. All applications so far seem to have been based on this assumption.

The stress-deformation curve corresponding to the descending branch can be measured by means of modern test equipment. The shape of this curve is now relatively well known. It has the general shape shown in Fig. 5. One important parameter of the curve is the enclosed

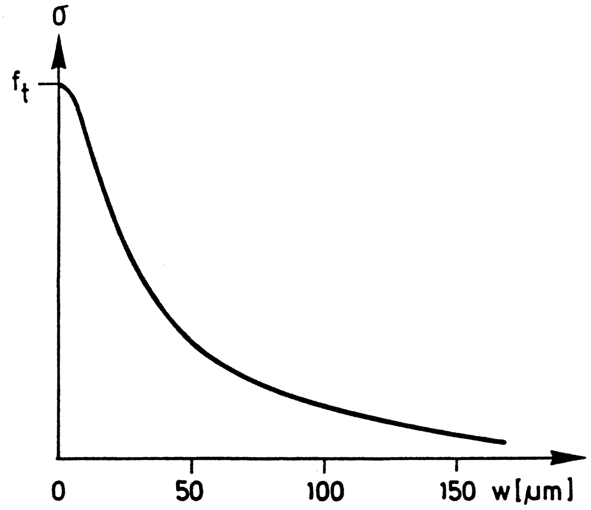

Fig. 5. Ordinary shape of the σ-w-curve for concrete.

area, which equals the fracture energy G_F. Another important property may be the initial slope of the curve. This property and its practical significance has not hitherto been studied in detail.

The fracture energy G_F can suitably be determined by means of a simple bending test on a notched beam according to a RILEM recommendation, Fig. 6. The load-deformation curve is recorded in the test. The total energy, that is absorbed during the test, is equal to the sum of the areas A_1, A_2 and A_3. A_1 is measured in the diagram, A_2 is calculated as $F_1 \cdot \delta_o$, where F_1 is a central force giving the same bending moment as the weight of the beam and the loading equipment. A_3 is assumed to be equal to A_2. This total energy is divided by the area b(h-a), that has been fractured, in order to get the value of G_F.

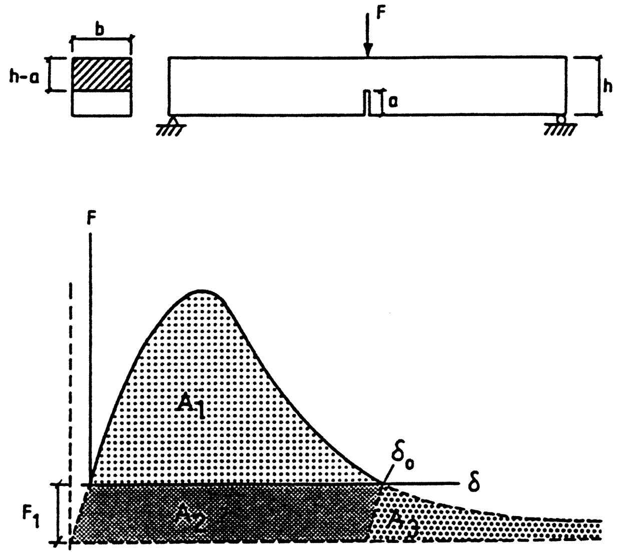

Fig. 6. Test for the determination of the fracture energy G_F according to RILEM Recommendation (1985).

For normal concrete qualities the material parameters are within the following ranges:

$E = 20 - 40$ GPa
$G_F = 65 - 200$ N/m
$f_t = 2 - 4$ MPa
$l_{ch} = 0.1 - 1$ m

The value of l_{ch} can be expected to be lower for high strength concrete and for light weight concrete than for ordinary concrete, which means that these materials are more brittle.

For fibre reinforced concrete the shapes of the σ-ε- and σ-w-curves may differ much from those for plain concrete. These curves then have to be determined and introduced into the analyses for the particular materials in question.

Application, principles.

Wherever tensile strains appear, which tend to pass the strain corresponding to the peak point in the tensile stress-deformation curve, a fracture zone starts to develop. Then the model outlined above can be applied, which means that the σ-w-curve is applied to the additional deformation in the fracture zone.

Let us as an example look at the bent beam in Fig. 7. At low loads the simple beam theory can be used, which means that the strains and stresses vary linearly across the section, with a maximum stress equal to

$$\sigma_{max} = 6M/bd^2$$

where M is the acting moment, b the width and d the depth of the beam. When the maximum stress reaches the tensile strength f_t a fracture zone starts developing if the deflection of the beam is increased. As the deflection increases, the fracture zone grows into

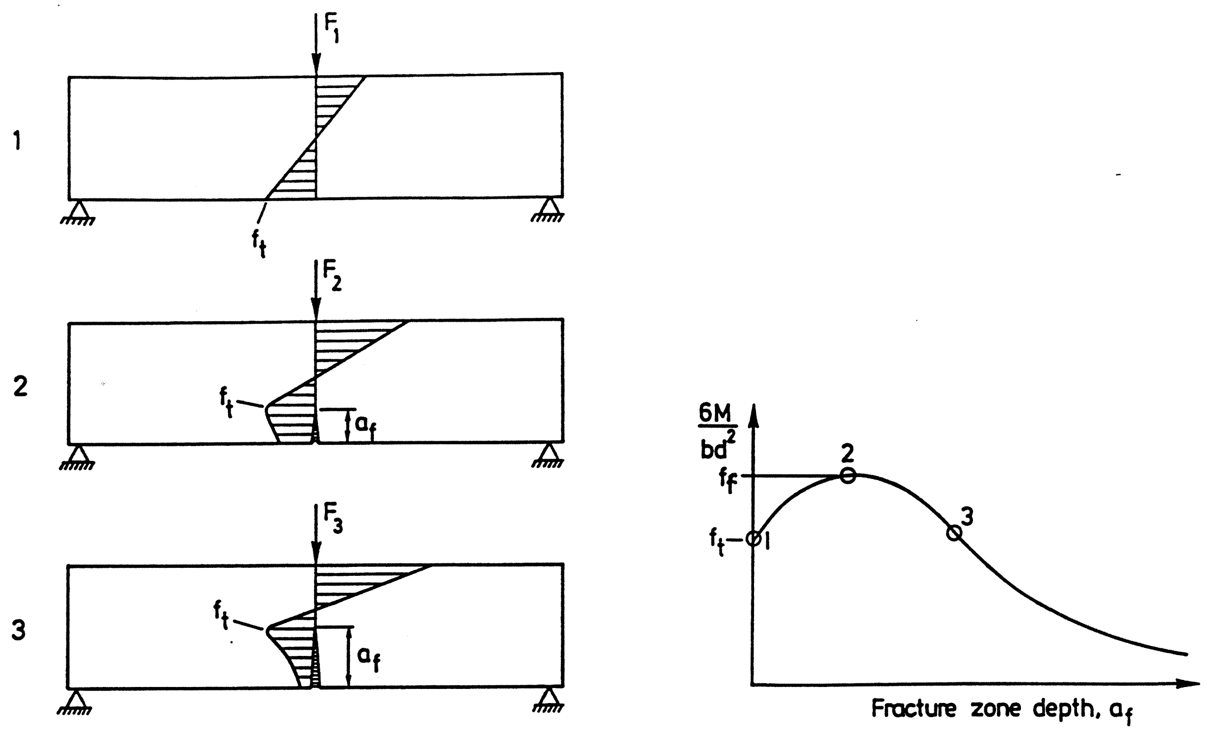

Fig. 7. Stress development in an unnotched beam.

the beam. At the same time the stress across this zone decreases, as the additional deformation increases. At the upper end of the fracture zone the stress is equal to f_t.

By means of a suitable numerical analysis the development of the stress distribution in the beam can be followed as the fracture zone grows. The corresponding development of the bending moment can be calculated, as it is shown in Fig. 7, as well as the deflection.

Exactly the same procedure can be followed also if the beam contains a crack from the beginning, Fig. 8, which is the case treated by conventional fracture mechanics. In that case the fracture zone start to grow already as soon as a load is applied, due to the stress concentration at the crack tip. The growth is however slow in the beginning. It can be shown that the depth of the fracture zone at low loads in this case is approximately proportional to the square of the moment.

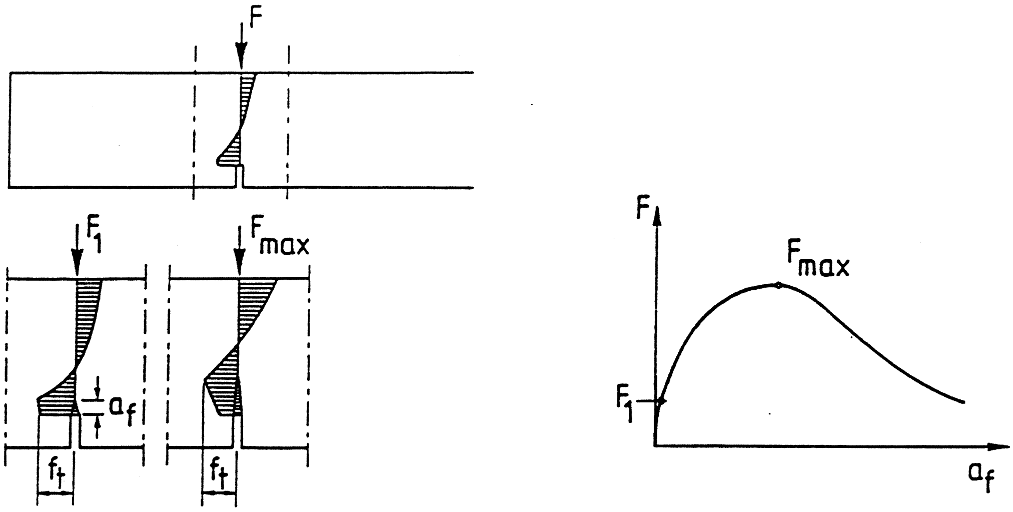

Fig. 8. Stress development in a notched beam.

In more complicated cases it is possible that the fracture zone starts inside a structure and grows in two directions. This may for instance happen with some shear cracks in reinforced beams or with splitting cracks under concentrated forces, like end anchors for prestressing tendons.

Size parameters. Brittleness number.

The characteristic length l_{ch} is a material property. If a characteristic size of a structure is divided by l_{ch}, this gives a dimensionless ratio, which relates a property of the structure to a property of the material. For a beam the depth d is often chosen as the characteristic size, and the ratio then is d/l_{ch}. This ratio is sometimes called **brittleness number**, as it gives an indication of the brittleness of the structure. The higher the brittleness number, the more brittle the structure.

As will be demonstrated later, the relative strength of a structure, expressed as a ratio between a formal stress at maximum load and f_t, is a function of d/l_{ch}. In this way many results of the theoretical analyses can be given in dimensionless general diagrams.

Application by means of finite element analysis.

The application by means of the finite element method (FEM) is rather straightforward if the fracture zone follows the direction of the element boundaries. The fracture zone then can be modelled either as a separation between elements (the fictitious crack model) or as a change in stress-strain properties of a row of elements (the crack band model).

In the fictitious crack model it may for instance be suitable to calculate the forces in the node points between the elements. When such a force reaches a value corresponding to the tensile strength, a separation between the elements is assumed, Fig. 9. Forces are introduced between the separated node points. The values of these forces depend on the separation distances w according to the σ-w-curve for the material, see Fig. 3. In this way the development of the fracture zone and the corresponding forces and deformations can be followed.

In the crack band model the formal stress-strain-curve for an element, where the fracture zone passes, is simply determined according to the general formula

$$\varepsilon_1 = \varepsilon + w/l$$

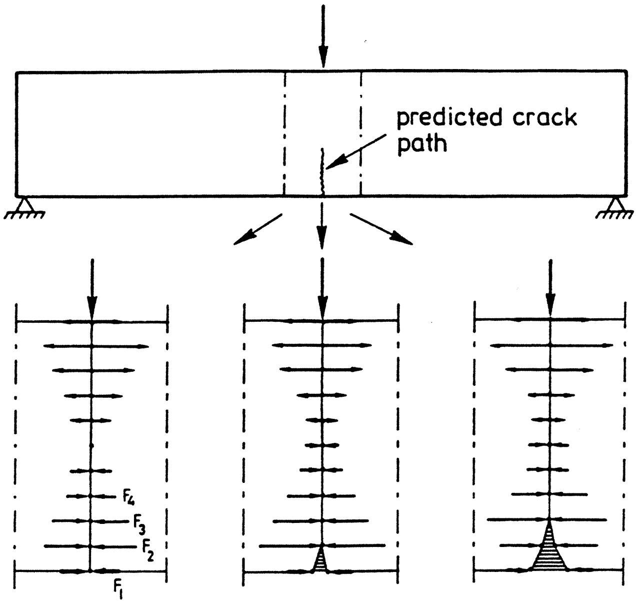

Fig. 9. The formation and growth of a fracture zone, modelled by means of a successive separation of node points.

where ε_1 is the formal average strain in the element, ε and w are in accordance with the properties of the material, and l is the size of the element in the direction of the tensile stress.

In the types of analyses described above, the fracture zones and the cracks propagate along discrete cracks or bands. Therefore this type of approach is called the **discrete crack approach**. This approach is more difficult to apply when the fracture zone does not follow along the direction of the element boundaries, but crosses the elements at skew angles. Certain possibilities exist for the application of the discrete crack approach to such cases, but these are complicated, and will not be discussed here.

When the direction of the fracture zone does not follow along the element boundaries it is easier to apply the **smeared crack approach**. In this approach a formal stress-strain relation is assumed for the material, just like in the crack band model described above. Even though this approach may be formally easier to apply, it involves some problems and risks of misinterpretations.

When the formal stress-strain relation shall be calculated the value of the length l is not well defined when the direction of the tensile stress forms a skew angle with the element directions. This leads to an uncertainty in the determination of this relation, which gives rise to an uncertainty in the results.

Still worse, however, is that the properties of many types of finite elements are not suitable for describing the growth of a fracture zone in a realistic way. When the strain in an element reaches the descending branch in the stress-strain curve, this corresponds to a negative modulus of elasticity for further deformations. Such an element may then be coupled more or less in parallell with an adjoining element with a positive modulus of elasticity. The result may be very discontinuous stress and strain distributions, which are unrealistic. In order to avoid large mistakes it is necessary to be very careful when the smeared crack approach is used. An uncritical application may lead to quite unreliable results. After this warning has been given, the smeared approach will not be discussed any further in this paper.

Application to the bending of beams.

All the results which will be shown beolw are based on the application of the fictitious crack model. The assumed σ-ε-relation is always a straight line, whereas two different relations have been used for the σ-w-relation according to Fig. 10. The single straight line, denoted "SL", is the simplest possible assumption for the numerical analyses, whereas the bilinear relation is meant to be a good approximation for the real shape. It is denoted "C" for concrete.

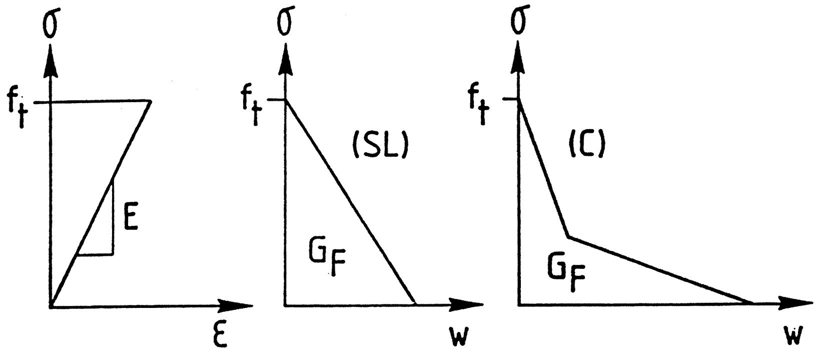

Fig. 10. Simplified assumptions regarding material properties.

A simple example is the bent unreinforced beam, without or with a notch (crack) on the tensile side. Figs. 11-14 show results of such analyses. The strength of the beam is expressed as a formal bending stress at failure, for the unnotched beam

$$f_f = 6M/bd^2$$

and for the notched beam

$$f_{net} = 6M/b(d-a)^2$$

where M is the maximum moment and a is the notch depth.

The value of the ratio f_f/f_t can be taken from diagrams of the type shown in Fig. 7, and the ratio f_{net}/f_t from Fig. 8.

Fig. 11 shows the variation of the flexural strength (modulus of rupture, MOR) with d/l_{ch}. From this diagram it can e g be seen that the ratio between flexural strength and tensile strength for a 100 mm deep beam with l_{ch} = 400 mm can be expected to be about 1.6, which is in a reasonable agreement with experience.

With the model it is also possible to study the influence of shrinkage stresses. Fig. 12 shows an example of this, where the shrinkage strains have been assumed to have values of an order which can be expected in a normal interior structure.

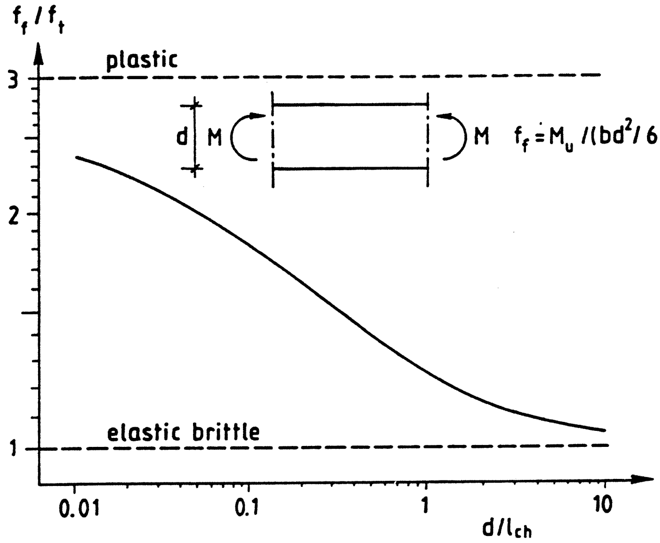

Fig. 11. Ratio between flexural strength and tensile strength.

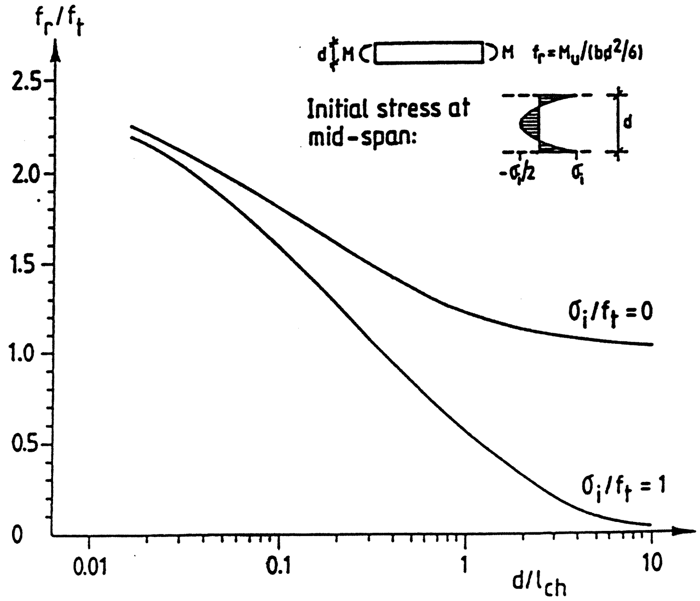

Fig. 12. Influence of shrinkage stresses on the ratio between flexural strength and tensile strength.

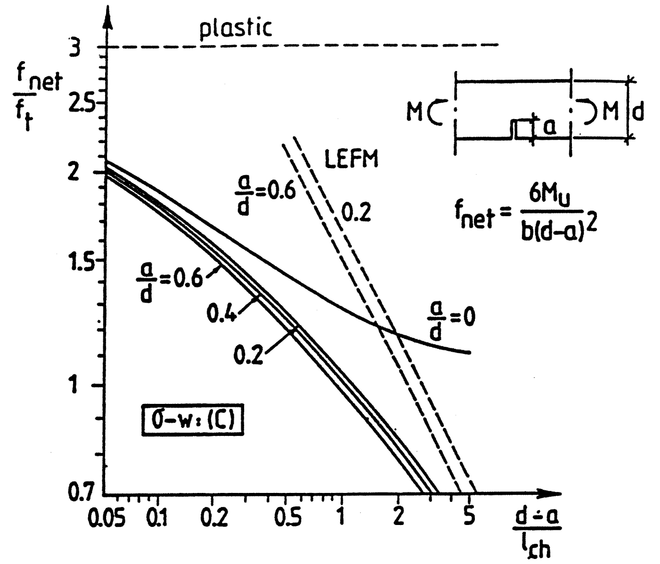

Fig. 13. Ratio between net bending strength of a notched beam and the tensile strength.

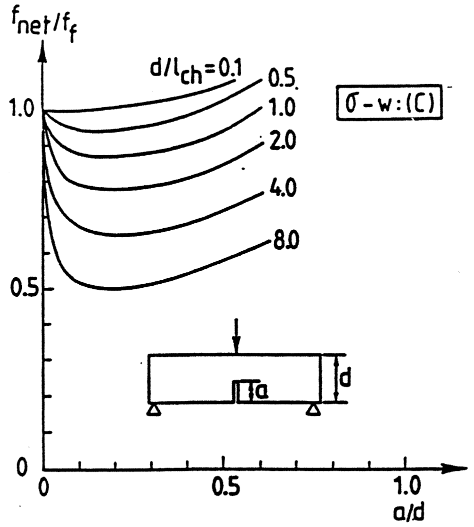

Fig. 14. Influence of the notch depth on the net bending strength.

Fig. 13 shows the variation of the strength of a notched beam with d/l_{ch}. In this case the strength is very sensitive to the depth for deep beams. As a matter of fact the strength for deep beams approaches values which are predicted by linear elastic fracture mechanics, which means that they are inversely proportional to the square root of the beam depth.

Fig. 14 shows how the depth of the notch influences the net bending strength of a notched beam. For a low value of d/l_{ch} the notch has practically no influence on the net bending strength f_{net}, which is nearly the same as the bending strength f_f of an unnotched beam. These beams are said to be notch insensitive. For high values of d/l_{ch} the value of f_{net} decreases as soon as there is a notch, which means that these beams are notch sensitive. It can be noted that the **notch sensitivity** is not a material property, but a property that depends on the beam depth d as well as on the material property l_{ch}.

In all the figures it can be seen that the strength depends on the size d of the beam. Thus there is a **size effect**, which is explained by means of the fracture mechanics approach. The size effect is greater for notched beams than for unnotched, particularly for deep notched beams. For unnotched beams this size effect increases when shrinkage or temperature stresses are acting.

In Figs. 11 and 13 it can be seen that the strength approaches the value predicted by the theory of plasticity for small beams, and that it approaches the value predicted by the theory of elasticity for large beams. The analysis covers all cases between these extremes for unnotched as well as notched beams. It thus has a general applicability. A small value of the "brittleness number" d/l_{ch} gives a more plastic-tough behaviour, whereas a high value gives a more elastic-brittle behaviour.

Sensitivity analysis.

The formal strength according to the above results depends on the value of d/l_{ch}, where l_{ch} in its turn depends on E, G_F snd f_t according to the relation $l_{ch} = EG_F/f_t^2$. The diagrams are given in logaritmic scales (except Fig. 12). For a small change in d/l_{ch} the relation can approximately be written

$$\ln(f_f/f_t) = A - B\ln(d/l_{ch}) = A - B\ln(df_t^2/EG_F)$$

$$\ln f_f = A + (1-2B)\ln f_t - B\ln d + B\ln E + B\ln G_F$$

where A and B are constants, with B showing the negative slope in the diagram at the studied part of the curve.

A differentiation gives

$$\frac{df_f}{f_f} = (1-2B)\frac{df_t}{f_t} - B\frac{dd}{d} + B\frac{dE}{E} + B\frac{dG_F}{G_F}$$

This expression shows the relative change in the formal strength f_f for a small relative change in one of the parameters. This can be called the **sensitivity**, and it is determinded from the slope $-B$ in the diagrams. It must be noted that the diagrams are given with the scale on the vertical axes 4 times as large as the scale on the horizontal axis. Therefore the slopes, which are measured in the figures, must be divided by 4. If for example the measured slope is -0.6, the value of B is 0.15, which means that the sensitivity with regard to G_F is 0.15 and with regard to f_t 0.7. In this case an increase in f_t with 10 percent increases f_f with 7 percent, whereas an increase in G_F with 10 percent increases f_f with 1.5 percent. In the same case an increase in the beam depth d with 10 percent decreases f_f with 1.5 percent.

Application to unreinforced concrete pipes.

An interesting practical application has been made to the strength of unreinforced concrete pipes. For these there are essentially two different types of failure, that are of interest, see Fig. 15. One is the bending failure (or beam failure), where the pipe is supported and loaded like a beam. The other is the crushing failure (or ring failure), where the pipe is loaded and supported along its length. This type of load results in bending failures in sections along the pipe, at the top and the bottom, and at the two sides. The structure is under these conditions statically indeterminate, which means that a moment redistribution can take place before the maximum load is reached. The amount of this moment redistribution depends on the toughness of the structure, and therefore increases with a decrease in size.

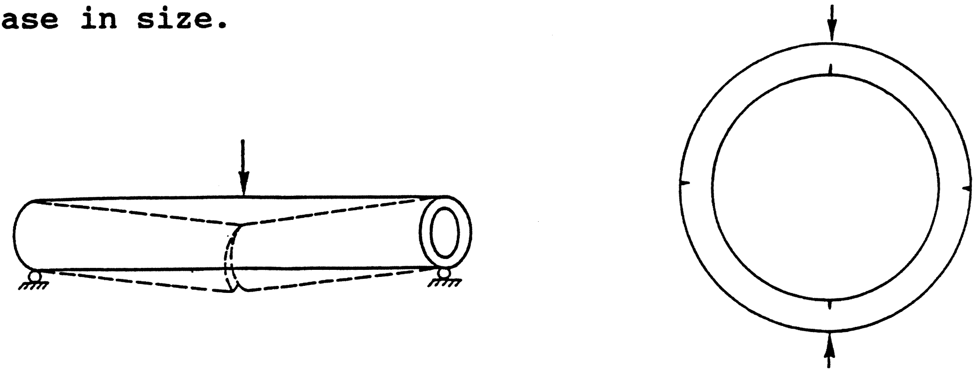

Fig. 15. Bending failure and crushing failure of a pipe.

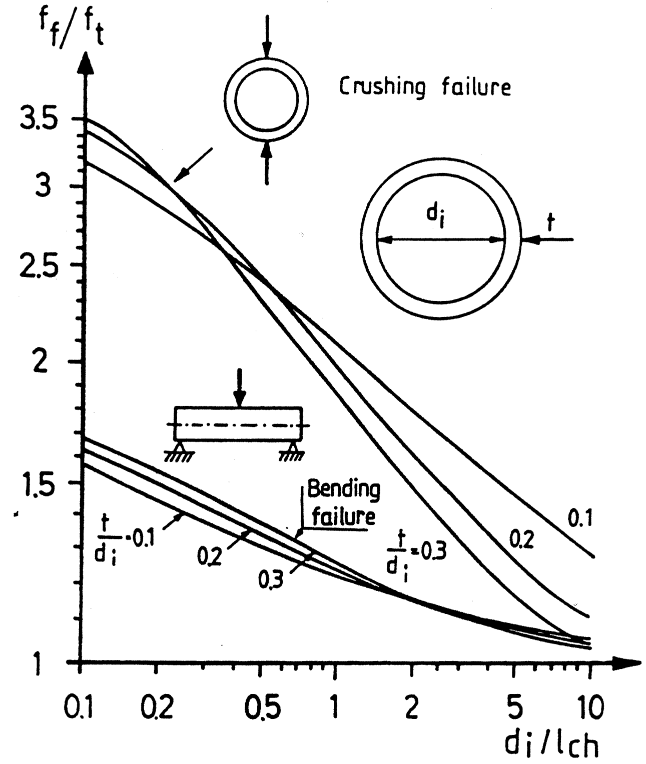

Fig. 16. Variation of formal bending strength of a pipe.

In Fig. 16 the variation in the formal bending strength with the size of the pipe is shown for these two loading situations. The formal strength f_f is the maximum stress at maximum load, calculated according to the theory of elasticity.

From the figure it is evident that the formal strength is much higher for the crushing failure than for the beam failure. The size dependence is also much higher for the crushing failure. The reason for the difference in strength is that the section depth for the acting moment is much lower for the crushing failure (the wall thickness) than for the beam failure (the diameter of the pipe). The reason for the higher size dependence for the crushing failure is that this structure is statically indeterminate.

The values according to Fig. 16 are in a good agreement with test results. They have found a practical application for redesign of certain pipes.

Application to shear failure of beams.

The shear strength of reinforced beams without shear reinforcement has also been analysed by means of the fictitious crack model. This is a very complicated case, as it depends not only on the concrete properties in tension, but also on concrete properties in compression and shear, on the steel properties, on the bond behaviour between concrete and steel, and on many other factors. The fracture zone and the resulting cracks are curved, and they can appear in many different positions.

Due to the complexity of the shear fracture the analysis which has been performed so far has had to be performed on the basis of many approximations and simplifications. Thus only one crack at a time has been studied, but this crack has been varied in order to find the most dangerous situation. The shape and position of the crack has been assumed in advance for each calculation, but afterwards it has been checked that the crack is nearly perpendicular to the principal tensile stress. Dowel action has not been taken into account, nor aggregate interlock. The properties of the reinforcement, bond properties, and failure in the concrete compression zone have been taken into account.

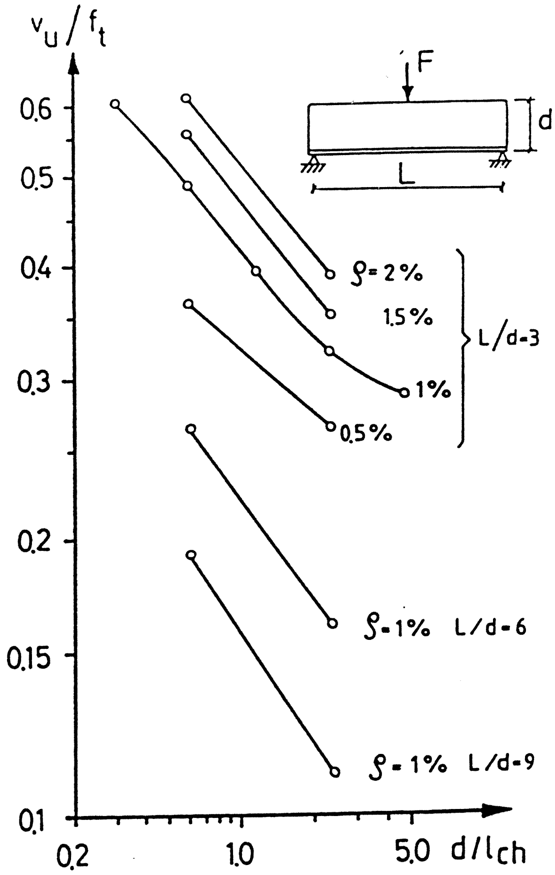

Fig. 17. Theoretical ratio between formal shear strength and tensile strength for a beam with longitudinal reinforcement.

The results of the analyses are shown in Fig. 17. The variables have been the depth (expressed as d/l_{ch}), the span to depth ratio, and the reinforcement ratio ρ. Of a special interest is the influence of the beam depth, which is wellknown from tests, but which has not earlier had any rational explanation.

A very large number of tests have been performed regarding the shear strength of beams, and as a matter of fact all our knowledge, as expressed in building codes and text books, is based on these tests. As we now for the first time have a pure theoretical analysis of the shear failure, it is interesting to compare this with test results and with the code formulas. Such comparisons are shown in Figs. 18 - 20. As all the material parameters in the tests are not known, particularly not the fracture enegy G_F, it has only been possible to make relative comparisons, which means that all curves in a diagram have been drawn through one common point.

From all the figures it is evident that the theoretical results are in a good agreement with the test results. Regarding the influence of beam depth and reinforcement ratio they are also in a good agreement with the CEB Model Code, which is mainly based on the same test results. The ACI code does not show any good agreement with the theoretical results or the test results.

In Japan (Iguro et al, 1984) a test series has been performed, where the beam depth has been varied between 0.1 m and 3 m, i e by a factor of 30. From these tests it was concluded that the shear strength is inversely proportional to the fourth root of the depth. This corresponds to a 45° slope in Fig. 17, and it is thus in a good agreement with the theoretical results.

Based on the theoretical analysis and the test results it can approximately be assumed that the following equation is valid for a beam with a constant span to depth ratio and a constant reinforcement ratio:

$$v_u/f_t = k(d/l_{ch})^{-1/4} = k(l_{ch}/d)^{1/4}$$

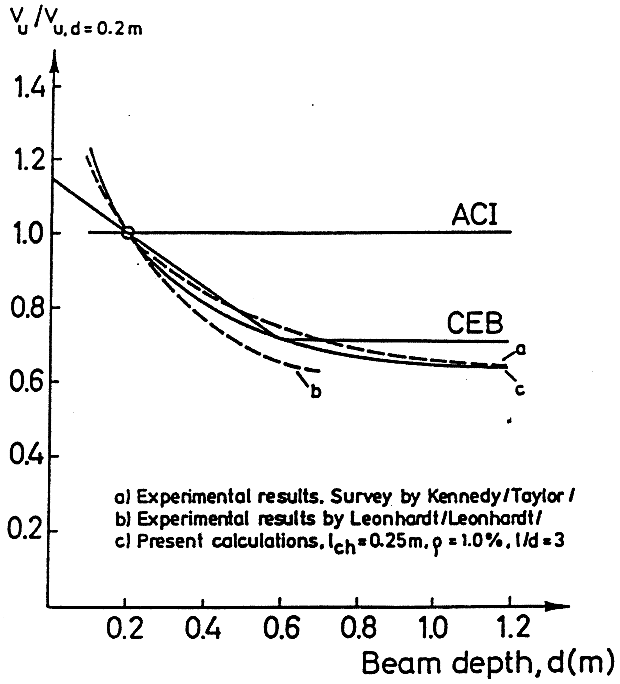

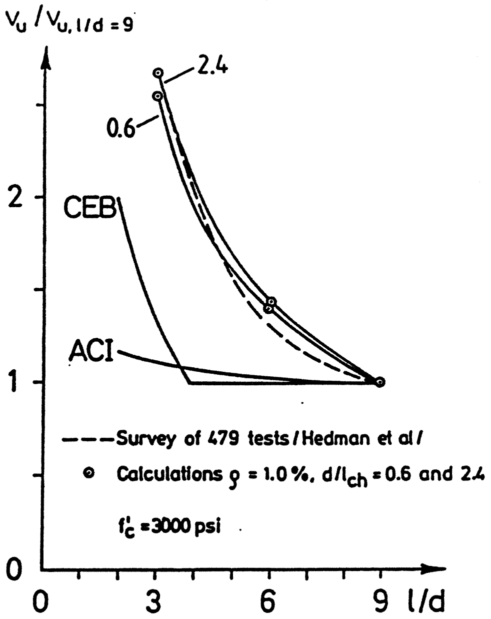

Fig. 18. Influence of beam depth.

Fig. 19. Influence of span to depth ratio.

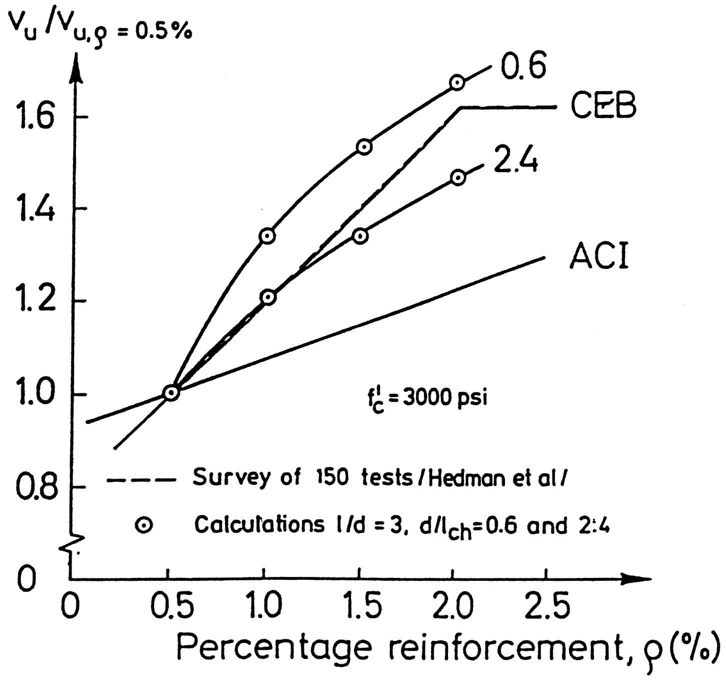

Figs. 18 - 20. Comparisons between theoretical values, test values and code values regarding the influence of different factors on the shear strength of reinforced beams.

Fig. 20. Influence of reinforcement ratio

where v_u is the formal shear strength (shear force divided by the cross section area) and k a constant. This expression can be rearranged by inserting the definition $l_{ch} = EG_F/f_t^2$:

$$v_u = kf_t(EG_F/df_t^2)^{1/4} = k(EG_Ff_t^2/d)^{1/4}$$

From this expression it can be seen that the shear strength depends as much on G_F as on f_t^2. It is generally accepted that the tensile strength f_t is approximately proportional to the square root of the compressive strength. Thus f_t^2 can be assumed to be proportional to the compressive strength. The conclusion from this is that the shear strength of a beam depends as much on the fracture energy of the concrete in the beam as on its compressive strength.

When a laboratory test is performed on a concrete structure, the compressive strength is traditionally always measured and reported. From the above it follows that the fracture energy should also be measured and reported where shear tests are performed, as this property is as important as the compressive strength. The same may hold also for many other types of structural tests.

Also in code formulas for shear strength the fracture energy ought to be taken into account in some way or other. How this should be done is too early to specify, but one possibility could be to give some type of correction factor, depending on the type of concrete, for example reduction factors for light weight concrete and for high strength concrete.

Direction of future research.

It has been demonstrated above that the application of fracture mechanics to concrete structures can give important contributions to the understanding of the behaviour of structures in cases where our knowledge earlier has been mainly based on empirical studies, like the ratio between flexural and tensile strength, the influence of shrinkage on the flexural strength and the shear strength of beams.

Still we are however only in the beginning of a development. If we for example look on the application to shear fracture, the results which were demonstrated are based on analyses where many rather rough approximations have been made. These were partly due to a lack of knowledge, e g regarding the aggregate interlock and the dowel action, and partly on the complexity of the problem, which made it too difficult to take all factor into account with the existing finite element program.

Thus one important type of research is to find more adequate material properties to be inserted into the finite element analyses. One example of such a research work is mentioned below.

An other important type of research is to develop finite element programs, which are better adopted to handle this type of fracture mechanics, with localization of fracture zones and strain softening.

It is also important to apply the model in a systematic way to real structures in order to achieve a better understanding of different types of behaviour, e g as a background for better design rules and codes. The results of such systematic analyses can preferrably be given in dimensionless general diagrams of the types shown above.

Present research in Lund (spring 1988).

A large test program is going on regarding the behaviour of a fracture zone in mixed mode, i e with shear deformations and stresses in a fracture zone after it has started in tension. Some results were presented in 1987. More systematic results will be presented at a conference in Vienna in July 1988, and the final complete report is expected to appear in 1989. One example of a test result is presented in Fig. 21.

A first attempt has also been made to apply the model with localization and strain hardening to the fracture in the compression zone of a reinforced beam. These first results indicate that the stress-strain relation to be used for the practical design should preferrably have an ultimate strain equal to k_1/x, instead of the normally assumed 3.5 permille, where k_1 is a material property and x is the depth of the compression zone. If this conclusion is correct, it will have a significant influence in many practical situations. Further research is needed before the result is sufficiently confirmed.

In a third project a number of tests are being performed on some simple unreinforced structures in order to check the general applicability of the fracture mechanics aproach. A wide range of different materials are tested, particularly with respect to different toughness. Very brittle materials are tested, like pure cement paste, as well as wery tough materials, like fibre reinforced concrete, and some materials in the intermediate range.

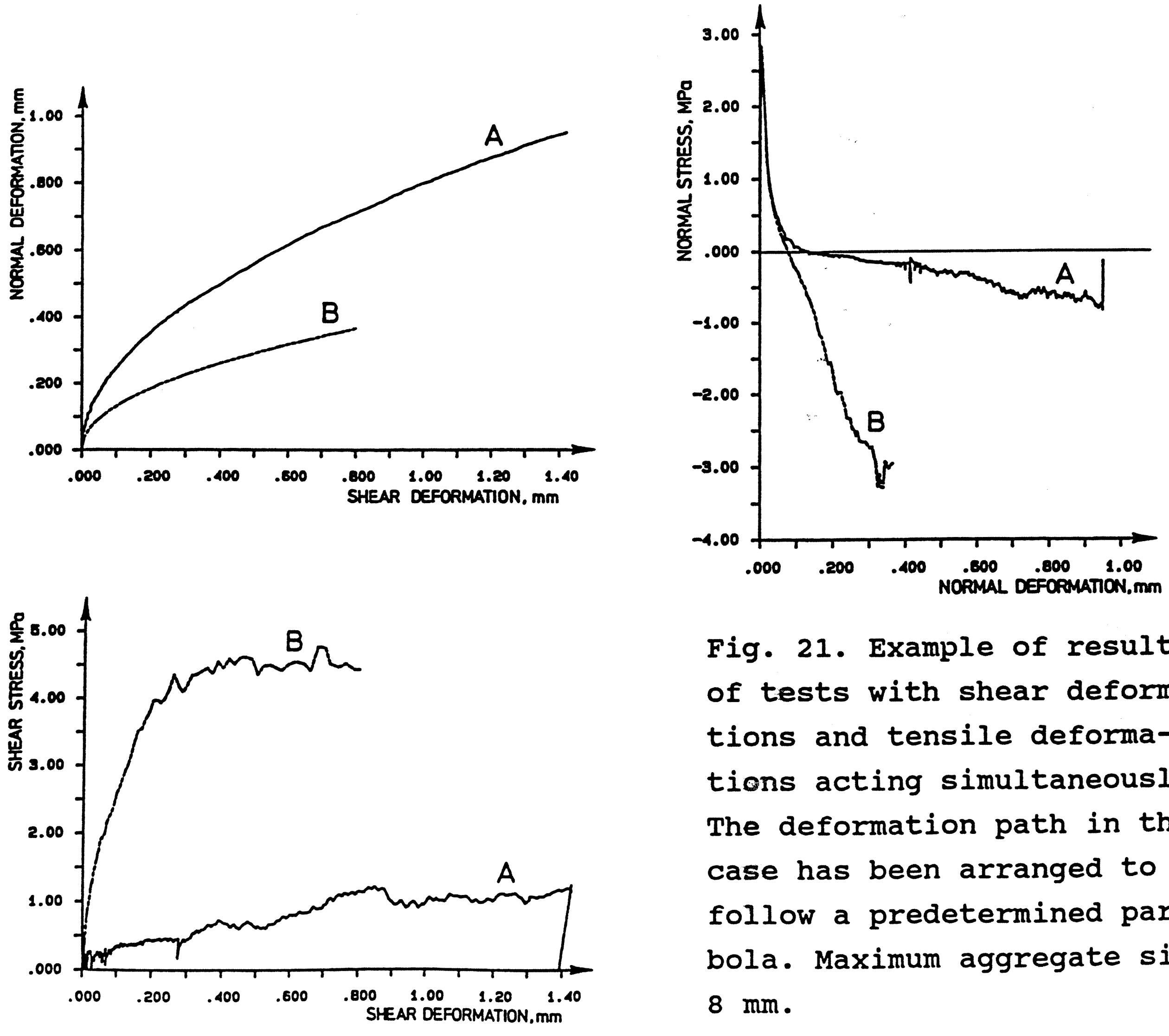

Fig. 21. Example of results of tests with shear deformations and tensile deformations acting simultaneously. The deformation path in this case has been arranged to follow a predetermined parabola. Maximum aggregate size 8 mm.

References

American Concrete Institute (1983) Building code requirements for reinforced concrete, ACI 318-83.

Bazant, Z.P. and Oh. B.H. (1983) Crack band theory for fracture of concrete. RILEM, Materials and Structures, Vol 16, No 93, 155-177.

CEB/FIP Model Code for Concrete Structures (1978). CEB Bulletin 124/125-E.

Hillerborg, A., Modéer, M. and Petersson, P.E. (1976) Analysis of crack formation and crack growth in concrete by means of fracture mechanics and finite elements. Cem. and Concre. Res., 6, 773-782.

Iguro, M., Shioya, T., Nojiri, Y. and Akiyama, H. (1984) Experimental studies on shear strength of large reinforced concrete beams under uniformly distributed load (in Japanese), Proceedings, Japan Society of Civil Engineers (Tokyo), No. 348/V-1, Aug. 1984, 175-184. Also Concrete Library International, JSCE, No. 5, Aug. 1985, 137-154 (in English).

Gustafsson, P.J. (1985) Fracture mechanics studies of non-yielding materials like concrete. Report TVBM-1007, Div. of Building Materials, Lund Inst. of Technology, Sweden.

Petersson, P.E. (1981) Crack growth and development of fracture zones in plain concrete and similar materials. Report TVBM-1006, Div. of Building Materials, Lund Inst. of Technology, Sweden.

RILEM (1985) Determination of the fracture energy of mortar and concrete by means of three-point bend tests on notched beams, RILEM, Materials and Structures, Vol 18, No 106, 185-290.

JOURNEES TUNISO-SUEDOISES
sur les "CIMENTS ET BETONS" 1 et 2 Juin 1988.

On a model based on thermodynamic concepts for reinforced concrete behaviour at degradation state .

By A.FRIAA * and K.BEN AMARA **.

Introduction .

The main aim of this work is to reach a constitutive law for reinforced concrete ; a constitutive law taking in acount particularities of this composite material ; besides we wish this law to manage in the best way the compromise : Simplicity - scientific rigour .

For doing , we apply thermodynamic laws [] to reinforced concrete constituants taking care of the following assumptions:

1- All evolutions are isotherm.

2- Plane cross sections still plane during deformations .

3- Tensiled concrete work is neglected .

---

* Prof. of Civ.Engrg ., ENIT ., Tunis Univ ., TUNIS

** Asst ., of Civ.Engrg ., ENIT., Tunis Univ., TUNIS

Thermodynamic formulation of evolution problem .

Let's consider a beam stump ,From the third hypothesis , we can call ρ the crack depth in the beam , we call ω the relative rotation of the two cross sections and λ the strain of moyen line of the beam . With ω , λ and ρ we are able to construct the thermodynamic potential ψ of this stump .

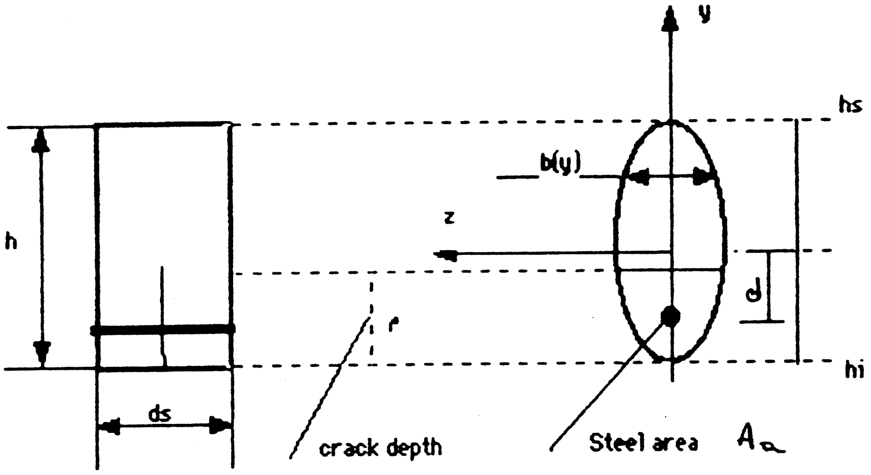
y
hs
b(y)
z
h
d
ρ
hi
ds
crack depth
Steel area A_a

Cross section of a beam

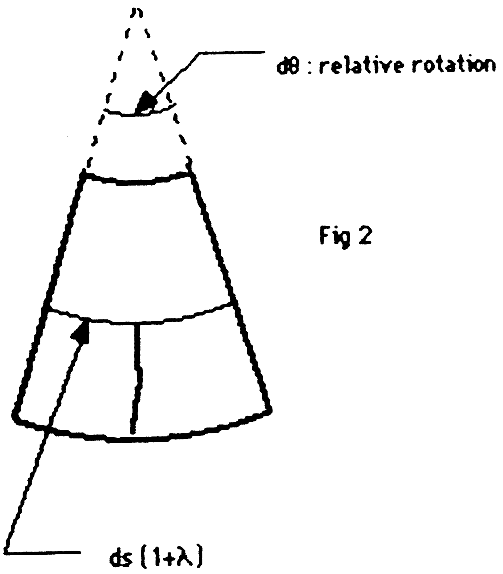
dθ : relative rotation
ds (1+λ)
y

Fig 2

To ω , λ and ρ are associated respectively the thermodynamic forces : M , N and د . Clausius-Duhem inequality can therefore be written :

$$F_\omega \dot{\omega} + F_\lambda \dot{\lambda} - \frac{\partial\psi}{\partial\chi_i} \dot{\chi}_i \geqslant 0$$

or

$$Di = (F_\omega - \frac{\partial\psi}{\partial\varepsilon})\,\dot{\omega} + (F_\lambda - \frac{\partial\psi}{\partial\lambda})\,\dot{\lambda} - \frac{\partial\psi}{\partial\varrho}\,\dot{\varrho} \geqslant 0 .$$

that give us :

$$M = \frac{\partial\psi}{\partial\omega} \quad (1)$$

$$N = \frac{\partial\psi}{\partial\lambda} \quad (2)$$

$$\text{ر} = -\frac{\partial\psi}{\partial\varrho} \geqslant 0 \text{ for } \dot{\varrho} \geqslant 0 \quad (3)$$

The first two equalities give the state laws , the last one express dissipation positivity .

Thermodynamic potential :

We choose thermodynamic potential as the elastic energy trapped into safe concrete and steel within beam stump during its deformation we can easily obtain :

$$\psi(\varepsilon,\varrho) = \frac{1}{2}\, {}^t\varepsilon\, \Lambda_\varrho\, \varepsilon \text{ with :}$$

$$\Lambda\varrho = \begin{bmatrix} \Lambda_{11} & \Lambda_{12} \\ \Lambda_{12} & \Lambda_{22} \end{bmatrix} \qquad \varepsilon = \begin{bmatrix} \omega \\ \lambda \end{bmatrix}$$

$$\Lambda_{11} = \int_{\rho}^{h_s} E_b\, y^2\, b(y)\, dy + E_s A_s d^2 \qquad \Lambda_{12} = \int_{\rho}^{h_s} E_b\, y\, b(y)\, dy + E_s A_s d$$

$$\text{et} \quad \Lambda_{22} = \int_{\rho}^{h_s} E_b\, b(y)\, dy + E_s A_s$$

taking in acount the quadratic form of ψ , constitutive law is written :

$\sigma \begin{bmatrix} M \\ N \end{bmatrix}$ we obtain : $\sigma = \dfrac{\partial \psi}{\partial \varepsilon} = \Lambda_{\rho}\, \varepsilon$

or
$$M = \Lambda_{11}\, \omega + \Lambda_{12}\, \lambda$$
$$N = \Lambda_{12}\, \omega + \Lambda_{12}\, \lambda$$

Evolution law

For a brittle material like concrete , we assume that dissipation is managed by a convex potential .

$\Phi(\rho) = < 2\gamma\rho >$ avec $< x > = x$ if $x > 0$ and 0 if $x \leqslant 0$ i.e

if we call Φ^* the dual fonction of Φ , we can easily show that Φ^* is nothing but the convex indicator χ_c , we have consequently :

$$\lrcorner \in \partial\Phi(\rho)$$

or $\quad \rho \in \chi_c(\lrcorner) \qquad C : [\,0\,,\,2\gamma\,]$

where ∂ denotes a generalisation of comon derivative concepts we note here analogy with plasticity ,and when the convex c still constant , we show that :

$$\dot{\text{ں}}\,\dot{\rho} = 0$$

so for positive $\dot{\rho}$ we have $\dot{\text{ں}} = 0$ and since

$$\text{ں} = -\frac{\partial \psi}{\partial \rho}$$ is fonction of ε and ρ so :

we obtain : $$\dot{\rho} = -\frac{\dfrac{\partial^2 \psi}{\partial \rho\, \partial \varepsilon}\dot{\varepsilon}}{\dfrac{\partial^2 \psi}{\partial \rho^2}}$$

For a rectangular cross section we have the incremental law :

$$d\rho = -\frac{1}{\omega}\left(\rho\, d\omega + d\lambda \right).$$

this law shows that strain in the crack head still constant since it reaches a limit value .

Numerical simulation of strain in steel bars in a cracked cross section under increasing load .

The idea is to consider a succession of evolution problems under constant loads, this hypothesis can hold because of the crack growth rapidity in concrete .

Some results and conclusion .

In fig we show Moment-strain curve in steel for near to crack and far from crack gages ; we note that our models is suitable to describe evolutions near the crack , same remarks can be hold for concrete strain , this goes obviously with safety considerations .

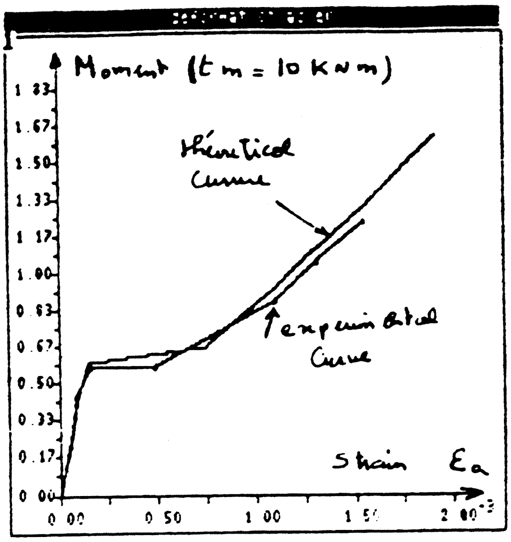

Fig . Experimental and theoritical curves for strain in steel bars for a gage near to crack .

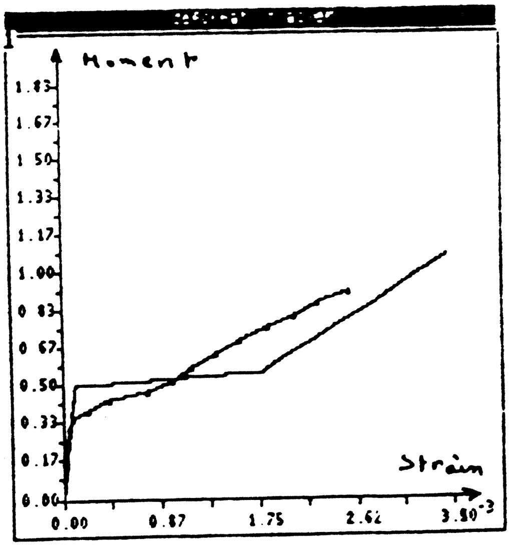

Fig : The same for a point far from the crack.

Application to displacement calculations .

The purpose of this paragraph is to caculate displacement on reinforced concrete beams by using our consitutive law and virtual work principle to a succession of equilibrium states .

Let's consider the beam of fig below .

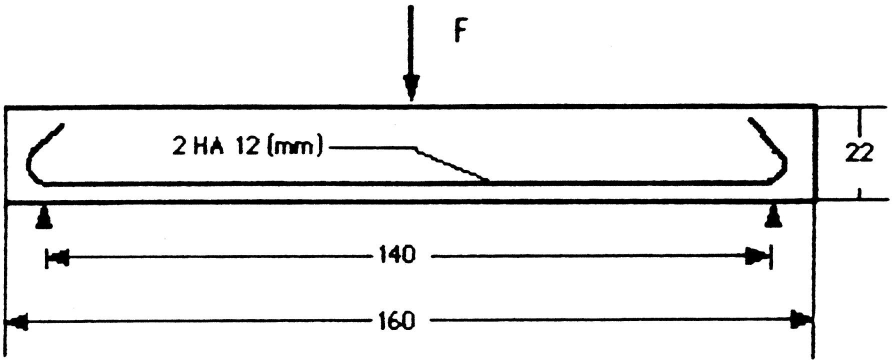

cross section width 15 cm concrete modulus Eb = 30 000 MPa
all dimensions are in cm .

we can associate to this beam a virtual one loaded by a single unit force . if we call $\sigma^*(M^*, N^*)$ internal forces in virtual beam and $\sigma(M, N)$ internal forces in real beam ; q is the displacement under the force F .

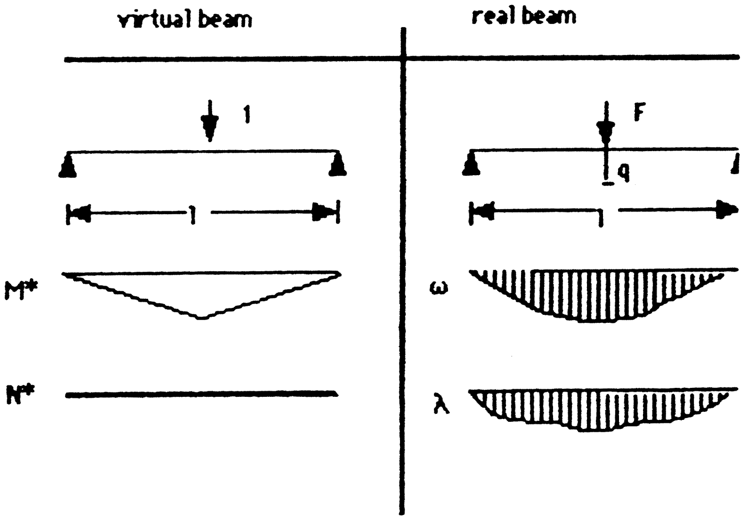

by Appling virtual work principle we obtain :

$$q = \int_0^l \sigma^*(x) \; [\Lambda^{-1}(x) \; \sigma(x)] \, dx \quad , \quad l \text{ is the beam length}$$

for numerical calculation we devide the beam on n stumps with the same length dx the former formula is then written .

$$q = \sum_{i=1}^{i=n} \sigma_i^* \; \Lambda_i^{-1} \; \sigma_i \, dx \qquad \sigma_i = \sigma(x_i)$$

in order to calculate the displacement q under increasing load F we apply gradually the load $F_i = \alpha_i F$ α_i varing from 0 to 1

On the figure below is shown experimental curve compared to model curve for n = 20 .

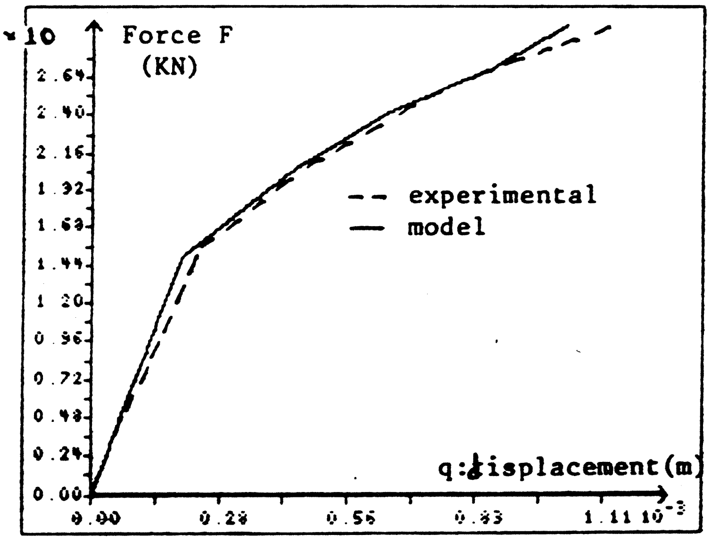

Application to limit analysis .

The aim of this paragraph is to construct the domain of rupture for a beam cross section , the idea is to apply the model for straight way of loading as shown on Fig 1 , for every value of angle α we obtain a point A_{α}, this point denotes the couple (M, N) where rupture happens by excess in steel stress or in concrete . By connecting points we obtain the domain :

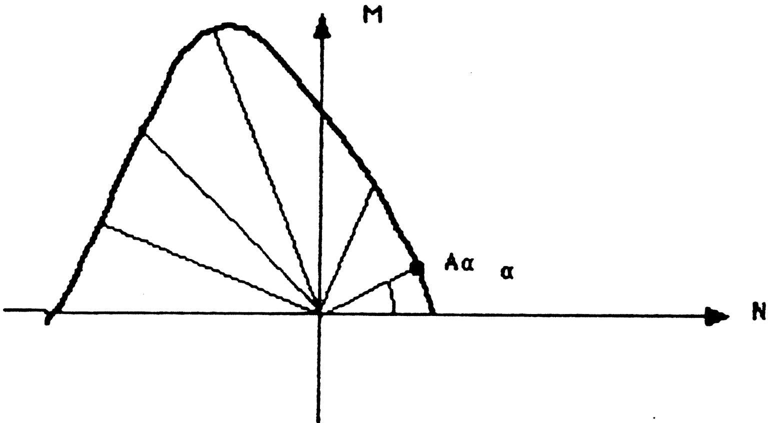

Fig -1 : Chemin de chargement linéaire .

a comparaison between the two domains fig.2 respectively obtained by our model and by virlogeux [ ] (who bases the calculations on stress-strain curves of steel and concrete) shows that brittle crack has influence on maximum moment but not on normal forces .

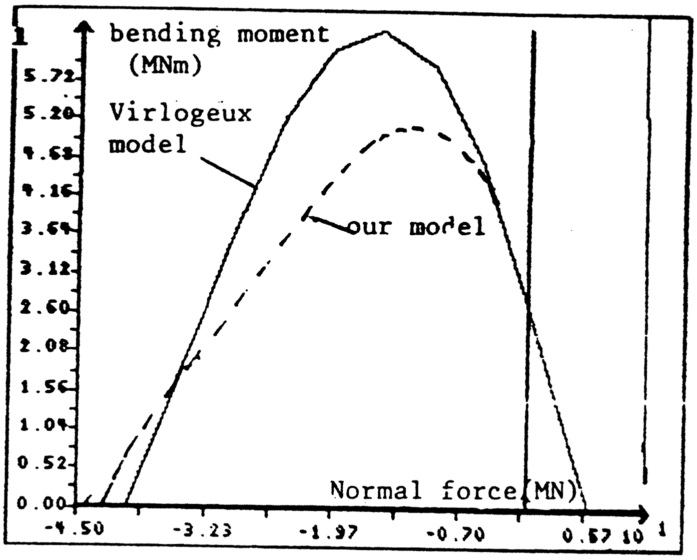

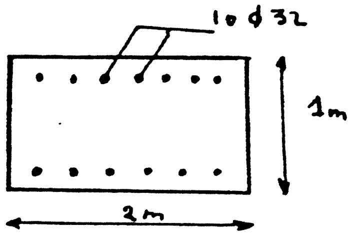

Cross section for calculations

Conclusion :

We can note that the model is able to take care of non linarity problems , where tridimensionnal formalism is heavy to deal with , besides , application to micro-computers is quite simple relatively to other methods

References

Baïkov.v ; Stronguine.s.

" *Calcul des structures* "Edition Mir , Moscou .

Ben Amara.k.

"*Sur un modele de comportement non linéaire au stade de dégradation mécanique des sections de poutres en béton armé* "

Actes du premier Colloque Maghrebin sur les Modeles Numériques de l'Ingenieur .USTHB. Alger .1987.

Ben Amara.k.

"*Un modéle de calcul à la fissuration des sections en béton armé* "

Diplome d'Etudes Approfondies mecanique appliquée . Université de Tunis 1986 .

Ben Amara.k.

"*Etude comparative des réglements BAEL et CCBA68* "

Projet de fin d'etude , Filiére longue ENIT , (1984) .

Bui.H.D.

" *Macanique de la rupture fragile*" Masson , Paris (1978).

Courbon.J .

"*Resistance des matériaux* " Dunod. Paris.

Friaa. A .

"*cours de mécanique des milieux continus* " polycope 1986 . ENIT

Germain P.

" *Cours de mécanique des milieux continus* " , Chapitre : Thérmodynamique des milieux continus " . Ecole polytechnique . Palaiseau. France.

Griffith A.A.

Phil.trans.Soc . London ,ser .A.221 (1920).

" *The theory of rupture* ".Proc,1st Int.Cong On applied machanics (1924).

Jaoua.M.

"*Analyse mathématique et numérique de quelques problémes en mécanique de la rupture* "

Thése . Université Pierre et Marie Curie . Paris 6 (1983)

Mazars .J.

"*Application de la mecanique de l'endommagement au comportement non linéaire et à la rupture du béton de structure*" Thése .Paris 6 .(1984) .

M'nasri farhat ; Kamel ben Amara :

" *Etude du comportement non linéaire des ossatures en béton armé* "

Rapport interne .Dpt Genie civil ,ENIT (à paraitre).

Moreau.J.J.

" *Fonctionelles convexes* "Seminaire sur les équations aux dérivées partielles , Collége de France ,Paris 1966.

Surendra.P Shah , A.M Asce , Fred J.Mc Gary .

"*Griffith fracture criterion and concrete* "

Journal of the Engeneering Mecanics Division . Proceeding of the American Society of Civil Engeneering.

M.Virlogeux ; A. M'Rad .

"*Etude d'une section de poutre en élasticité non linéaire . Application au béton armé ou précontraint , et aux sections mixtes* "

Annales de l'ITBTP N°444 Mai 1986 Serie béton 237 .

DEVELOPMENT 1944 - 1988 WITHIN THE SWEDISH CEMENT INDUSTRY

OLOF PETERSON
Division of Building Materials
Lund Institute of Technology

This paper contains some of my experience from my work at, and later contacts with, the Swedish cement company CEMENTA AB.

The paper is divided into four divisions:

1. Something to observe
   when the central laboratory has to cooperate with a cement factory or a cement user.
2. Development of the laboratory during the period.
3. Development in the production of cement.
4. Influence of changes in production:
   - the economy of the production
   - and the quality of the cement

1. Something to observe when the central laboratory has to cooperate with a cement factory or a cement user

When ready with my studies at the Royal Technical University of Stockholm, my first employment as a chemical engineer was in 1944, at the central laboratory of Cementa AB at Malmö, in SW of Sweden.

One of my two fields of responsibility was to assist the six factories, which were run by the company. Many times, an investigation could be performed within less time, and with less cost, if an examination, or at least a part of it, could be performed at the laboratory, rather than as a full scale work.

Two quite essential things are

how the laboratory is informed about the nature of the trouble

how the results of laboratory work are reported back to the factory.

Often the laboratory work is started as a contact from the Director of one of the factories to the Director of the laboratory.

The two directors do not necessarily understand the nature of the troubles, so there are several risks of misunderstanding, and the laboratory may happen to get upon the wrong track.

As time went on, we found that it might be preferable if I had to contact the Director of the factory and, at least the first time, also visit the factory where the troubles occured. Sometimes a trouble comes and goes, but even if everything happens to be in order at my visit, it is useful for me as a laboratory man to see the equipment and the process and, not less important, to meet the staff at the factory and perhaps take some samples. Then it may be time to agree with this staff about what to do next time something happens.

Another question, which is to look up for in the cooperation between the laboratory and the factory, is how to write the laboratory report. A naked table of figures does not necessarily tell the technicians at the factory anything at all. The laboratory man who visited the place of trouble in the factory should read the primary results from the laboratory work, and then write a report from the view of the factory. To this technical report, the primary laboratory results should be attached as an appendage.

The second field of responsibility of mine was problems for users of cement. The problems often were caused by something that happened within the concrete factory, but some times by something that happened in the cement factory.

Sometimes the concrete factory experienced that cement may be difficult to transport from one place in the factory to another, especially when compressed air was used for the transport. It could be sufficient that the temperature in the grinding process was somewhat too high, and the cement could get a tendency to stick to the transport ducts because of static electricity.

If the concrete manufacturer believed that the error came with the cement from the cement factory, he had to prove this with samples. If the change of the cement quality seemed to come slowly, a general sampling might very well be enough. If, on the other hand, his impression was that the cement quality could change suddenly, a great number of random samples might be necessary for tracing the troublesome cement.

Even with such a good sampling, it may be difficult to find out what has happened with the cement. As an example, one user claimed that the concrete sometimes stiffened rapidly. I was lucky enough that the cement factory was situated in the same town as the concrete factory, so I could pay a visit.

The clinker was stored in a hall on a concrete slab directly on the ground. At one place, the layer of clinker was very thin. I could observe that a part of the clinker was wet, and partially whitened.

A chemical analysis revealed that the whitened clinker contained some potassium carbonate. When such a clinker is ground to cement, just this cement will cause rapid stiffening, while cement ground from normal clinker gives normal set and normal hardening.

In this case, the concrete factory used a special type of cement, which was stored in a separate silo. This limited volume of the cement store increased the risk that the customer would notice when he received cement from whitened clinker.

Troubles of such a type may give concrete with irregular character, and it is difficult to unmask the cause. When the real cause, at last, is suspected, it is necessary to have access to many random samples, or it will be almost impossible to find the cement with alkali carbonate.

2. Development of the laboratory during the period

In 1944, when my employment started, the laboratory already had good equipment for **physical testing** of **cement, mortar, and concrete.** Cement was tested according to Swedish standards, and according to standards, which were demanded by countries, which Sweden exported cement to.

The **chemical analyses** were performed according to **wet methods.** The classical methods were modified so that **calcium, silica, alumina, and ferric oxide** could be analysed with reasonable accuracy within few hours. The analysis became much more complicated and time-consuming when it was necessary to determine sodium and potassium.

Already at this time, the laboratory could determine **sulphate in cement** with a rapid method, used also at the cement mills for controlling the gypsum addition. A sample of cement was dissolved, and finely ground barium sulphate was added. Then the sulphate ions formed a fine white suspension of barium sulphate. With **a simple photometer** we could, in short time, determine the sulphate content in the cement.

Later, more elaborate **spectro-photometers** were developed, which allowed rapid and accurate determination of coloured ions, such as **chromate.**

An important improvement came when the laboratory could start to use its first **flame emission photometer.** This simplified the determination of **sodium and potassium** very much, analyses which earlier were very time-consuming and laborious.

Another physical method for chemical analysis was the **X ray fluorescence analysis** for the main components magnesium, aluminium, silicium, potassium (we could not determine sodium), calcium, and iron. The development was first performed for one of the cement factories, but later this type of analysis grew the most common method at the laboratory, and also in factories.

Determination of loss on ignition was always important for checking the condition of cement. **Thermogravimetric analysis** was an improvement of such determinations, which meant that the mass of the specimen could be registered continously during the treatment in the furnace.

The method could be used for investigation of the influence of moisture in storing cement, and Figure 1 shows that thermogravimetric analysis also is good for checking the condition of the gypsum after the grinding of the cement. The text of the figure explains why the sample must be protected against dry air in the furnace.

In the **furnace microscope**, Figure 2, a small cube or cylinder, pressed from sample, which was finely ground with water (or some other liquid), is heated rapidly. The temperature is followed all the time.

The microscope shows the profile of the test specimen, illuminated from behind or, if the temperature is sufficient, luminous. The picture may be photographed.

As soon as the component with the lowest melting point becomes liquid, the profile may change. The specimen may shrink, or its corners may become rounded. At rising temperature, the content of liquid phase will increase, and the profile may approach a semi-circle. At last, the whole specimen may become almost flat.

The furnace microscope is suitable for study of reactions between the raw materials and the refractory brickwork in the cement kiln, in case of overheating.

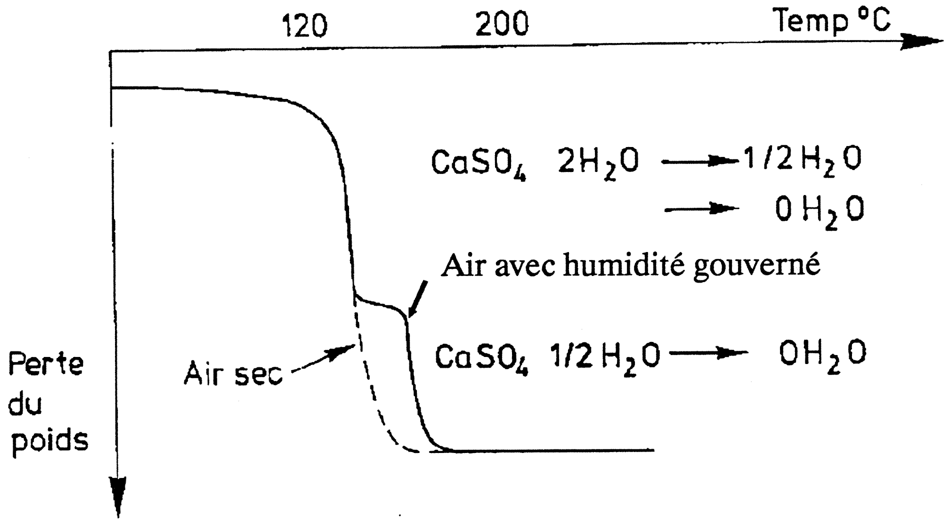

Figure 1. Analyse thermogravimetrique de gypse et plâtre.

The diagram shows how a sample of gypsum loses mass when heated in the furnace of the thermobalance.

If the sample is surrounded with dry air, all the water of the gypsum is lost, as shown by the broken graph.

If the sample is wrapped in a metal foil, the air around the sample becomes moist, and the loss of water will stop temporarily when all but half a molecule of water has left the gypsum.

The residual water, belonging to calcium sulphate semihydrate, will be given off at a somewhat higher temperature, in accordance to the solid graph.

Thus, the sample must be protected from dry air when the aim of the examination is to find out, to what degree the gypsum sample had already lost crystal water.

Figure 2.

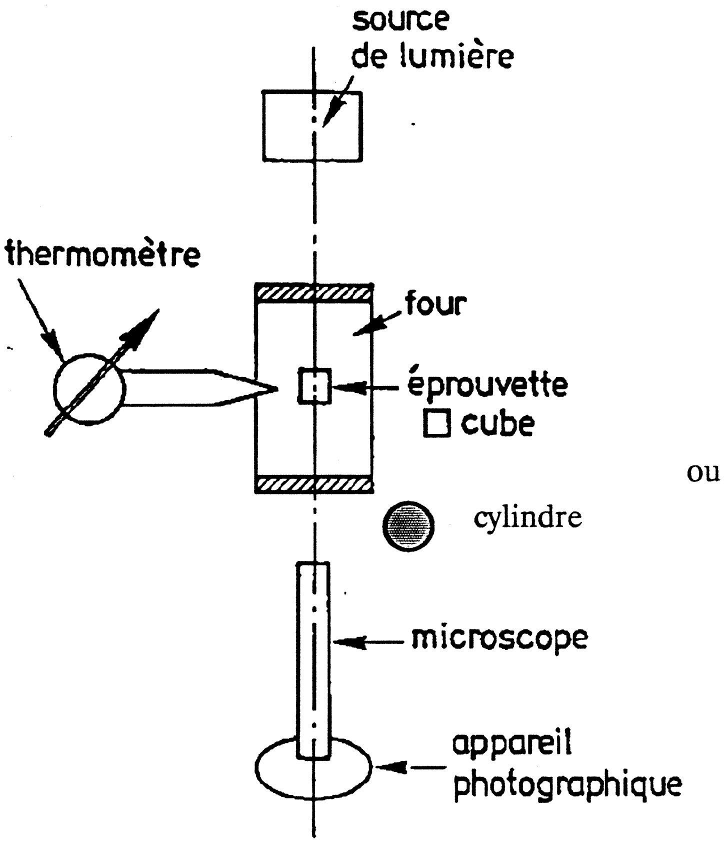
source de lumière
thermomètre
four
éprouvette
□ cube
ou
cylindre
microscope
appareil photographique

Microscope à four

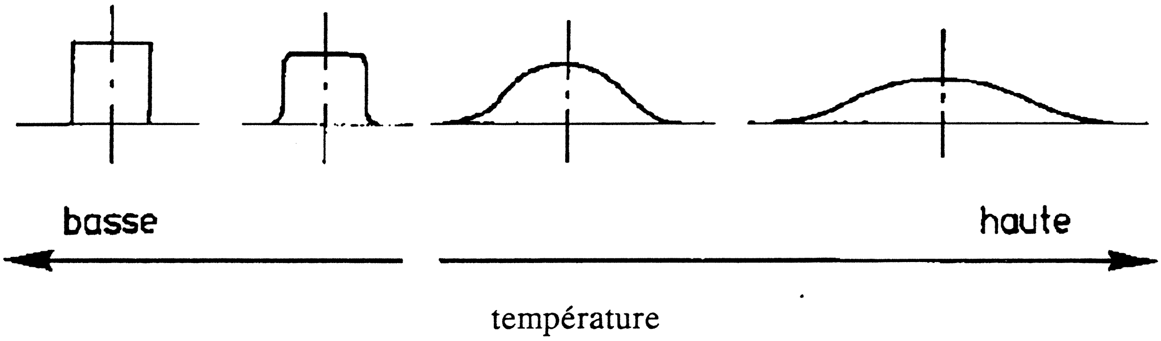
basse
haute
température

Profil de la éprouvette

Clinker can easily be examined with an **optical microscope**. First, some clinker balls are cut. If the material is porous, it may be supported by filling the pores with a suitable plastic. Then the surface is ground with several grades of grinding paper. At last, the clinker surface is polished to mirror glaze. Whit suitable techniques of etching, the different clinker minerals are given different degrees of reflectance.

By such microscopic study of clinker in reflected light, the thermical history of the clinker can be elucidated. For making cement, it is still more interesting to study whether the granulometry of the raw materials was suitable. In the Chapter 4, some examples, with pictures, are given.

Since 1979, the central laboratory of Cementa is situated at Slite, on the island of Gotland in the Baltic Sea. After my retirement, I have been in position to use the facilities of the new laboratory several times.

A very useful piece of equipment is a sweeping electron microscope, which allows chemical semiquantitative analysis (with X-rays) of an optionally large surface.

The Slite laboratory now has equipment also for X-ray diffraction analysis.

3. Development in the production of cement

During my active period in Cementa, the clinker was made in accordance to the dry process in some factories, but in most of the factories in accordance to the wet process.

The dry process is the oldest one, and it was used in shaft kilns and, earlier, in annular kilns. Cementa, for some years, had to operate two shaft kilns. Both types worked in countercurrent and they used the fuel in a reasonably efficient way. The shaft kilns are now not very common, and Figure 3 may serve as an aid for understanding the problems with such a stationary type of cement kiln, even if the figure shows a clinker that was made in a rotary kiln, and not in a shaft kiln.

In Figure 3, most of the large crystals of alite (light) and belite (dark) remain solid even at the high temperature in the clinkering zone of the kiln.

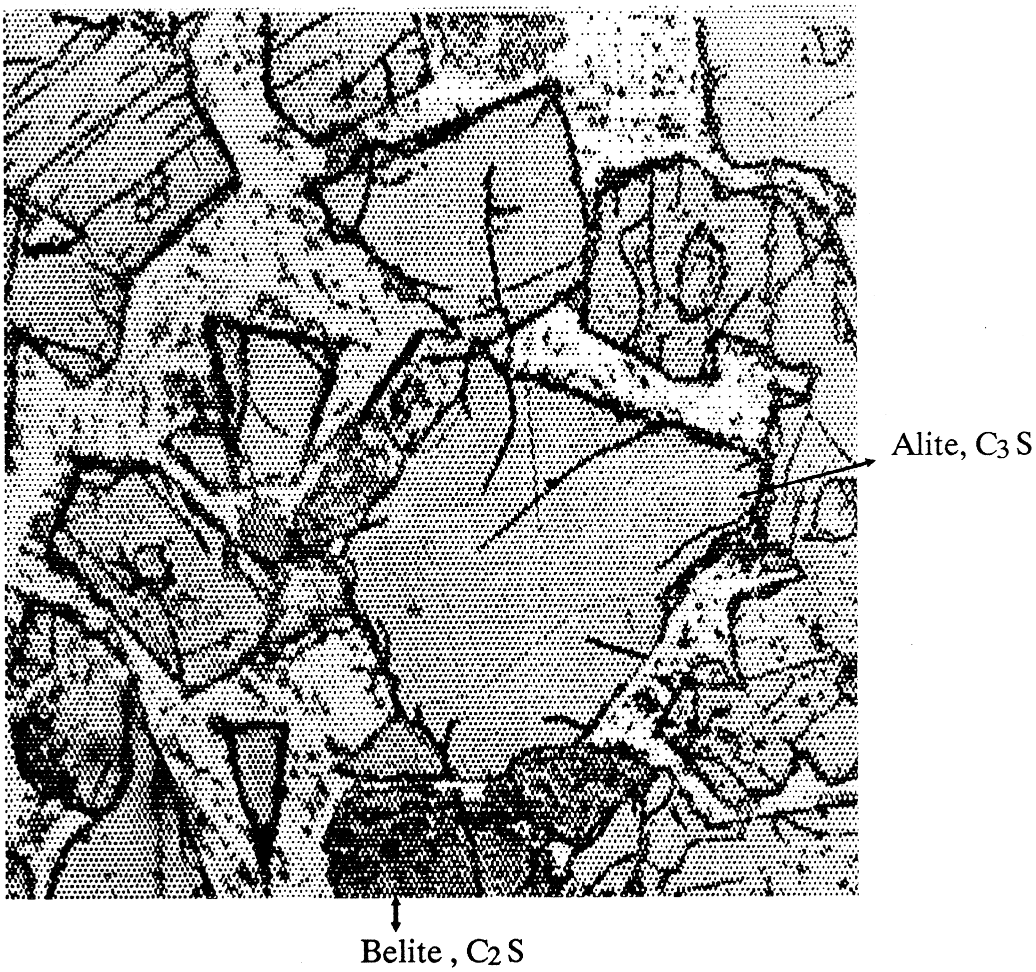

Figure 3.

A microphoto of a Portland clinker (Limhamn, Sweden), magnification 500 times.

The crystals of alite (mainly tricalcium silicate) remain solid, even at a high kiln temperature.

The belite (mainly dicalcium silicate) is somewhat more soluble in the molten material, but most of this phase remains as solid crystals. At rapid cooling of the hot clinker, the dissolved part of the belite

1. precipitates on solid belite crystals
2. precipitates on solid alite crystals which gives them thick contours
3. precipitates as very small independent crystals

Pieces of clinker, which are hot enough to contain molten material, freeze together to a solid mass, when the molten phase solidifies.

The interstitial material is liquid at the temperature in this zone, but it will freeze as soon as the temperature decreases below about 1250 degrees Celcius, and this may make it difficult to get the clinker out from a stationary type of kiln, such as the shaft kiln.

When the rotary kiln was introduced in the cement industry, the handling of the freezing clinker became much facilitated. The rotary kiln also opened the way for the wet process. The raw materials were ground with water to form a slurry with the least possible water content that still allows pumping of the slurry.

Figure 4 Figure 4 shows a rotary kiln for the wet process. Quite as the shaft kiln, the rotary kiln works in countercurrent.

If the materials are chosen with care, the freshly formed calcium oxide starts to react with some of the acid materials, containing silicon dioxide and aluminium oxide, already in the calcining process. In this case, there is no place in the kiln where calcium oxide can be found in a quantity corresponding to the calcium carbonate in the raw materials.

The clinker formation is very rapid where the residual mixture of basic and acid materials are in a semiliquid state, quite close to the flame.

Most of heat is consumed for drying of the slurry and for the calcination of the calcium carbonate. Though the temperature at the clinker formation is high, very often about 1450 degrees Celcius, the process does not consume much heat. Principally, the reaction between calcium oxide and silicon dioxide **releases** a good deal of heat, and this happens partially in the calcining process, partially in the clinkering process, dependent of the choise of raw materials.

The ready-burned clinker can not be handled before it is cooled, so that all molten materials are frozen to solid state. The cooling has double purposes:

1. The heat is saved back into the process in the form of hot air.

2. The clinker is cooled down to a temperature which allows easy handling, i. e. not very much above 100 degrees Celcius.

With a separate cooler with moving grids and a battery of fans, both steps can be combined in the same unit.

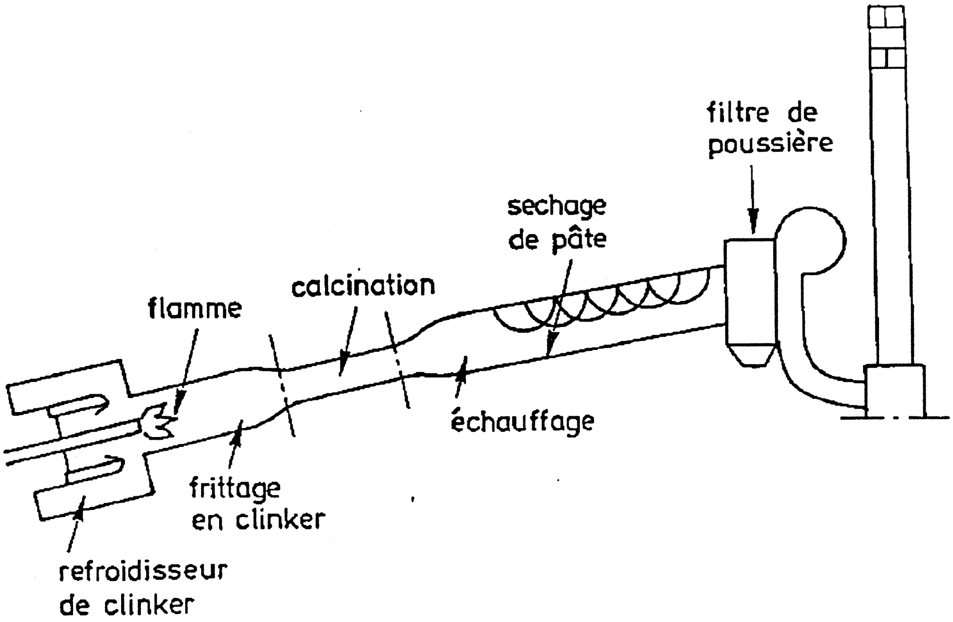

Figure 4. Four rotatif. La voie humide.

The rotary kiln is slightly inclined, and the slurry of ground raw materials and water is fed into the kiln in its right, upper part.

For improving the heat exchange to the slurry from the gases, the slurry first passes a part of the kiln, which is equipped with steel chains. These chains, in addition, contribute to a good transport of the drying and increasingly viscous slurry.

When the raw materials are dry, their temperature rise, and at a certain level, the calcium carbonate in the limestone loses its carbon dioxide. The rapid gas evolution makes the material strongly fluid in this "calcining zone", which is shown narrow in the picture. As this process consumes very much of heat, the material's temperature remains principally constant during the calcining process.

When the material has lost most of its carbon dioxide, the temperature can start to rise again and, with suitable composition, the clinker minerals will start to form. At still higher temperature, the clinker will sinter. The rotation of the kiln will prevent the sintering mass from forming a solid mass. Most commonly, the clinker forms nodules, mainly in the range 5 - 20 millimeters.

At last, the clinker leaves the kiln and enters the clinker coolers. Thus the clinker will be cooled down, and much of its heat will be returned to the combustion air.

The cooler can also be built as a part of the kiln, but in this way only the first purpose can be satisfied, not the second one. On the other hand, the installation is less complicated.

A drawback is that the "planetary cooler" is heavy and loads a sensitive part of the kiln shell so that there will be risks for cracking.

The rotary kiln introduced a revolution in the cement industry, but as a heat exchanger it is poor, except in the clinkering zone, where **radiation** of heat plays an important roll. This will limit the production rate of a wet process rotary kiln, even if the cost of evaporating the water from the slurry can be accepted.

The production rate will be improved when the kiln is fed with a dry mixture of materials. Above all, the consumption of fuel is reduced essentially. Still the production rate is limited by the fact that a step with such a high heat consumption as the calcining process has to be performed in the rotary kiln.

In modern forms of the dry process, rotary kilns are used essentially for the clinkering process. Other types of equipment is preferred for heat exchange at moderate temperature values, where the materials do not contain any liquid phase. To day in Sweden, cyclone exchangers is the choice in cement kilns. Some years ago two kilns were equipped with a chain grate according to LEPOL, with double passages of gas.

There is a limit for how large a diameter the refractory lining in a rotary kiln can have, and still remain stable.

This means that a good deal of the calcination process, about 90 per cent, should be performed already in the cyclones and not in the rotary kiln. If the kiln is combined with a system of cyclones, the gases from the rotary kiln do not contain enough heat for covering the much heat-consuming calcination.

According to Figure 5, the amount of the fuel for the flame in the rotary kiln is limited, so that the gases contain oxygen in excess.

Thus, a suitable amount of fuel may be burned in an auxiliary furnace in order to give the gases a heat content that is sufficient for heating the raw materials and for 90 percent of the calcination. The method is used at the Slite factory and is known to give a very long life to the refractory bricks of the rotary kiln.

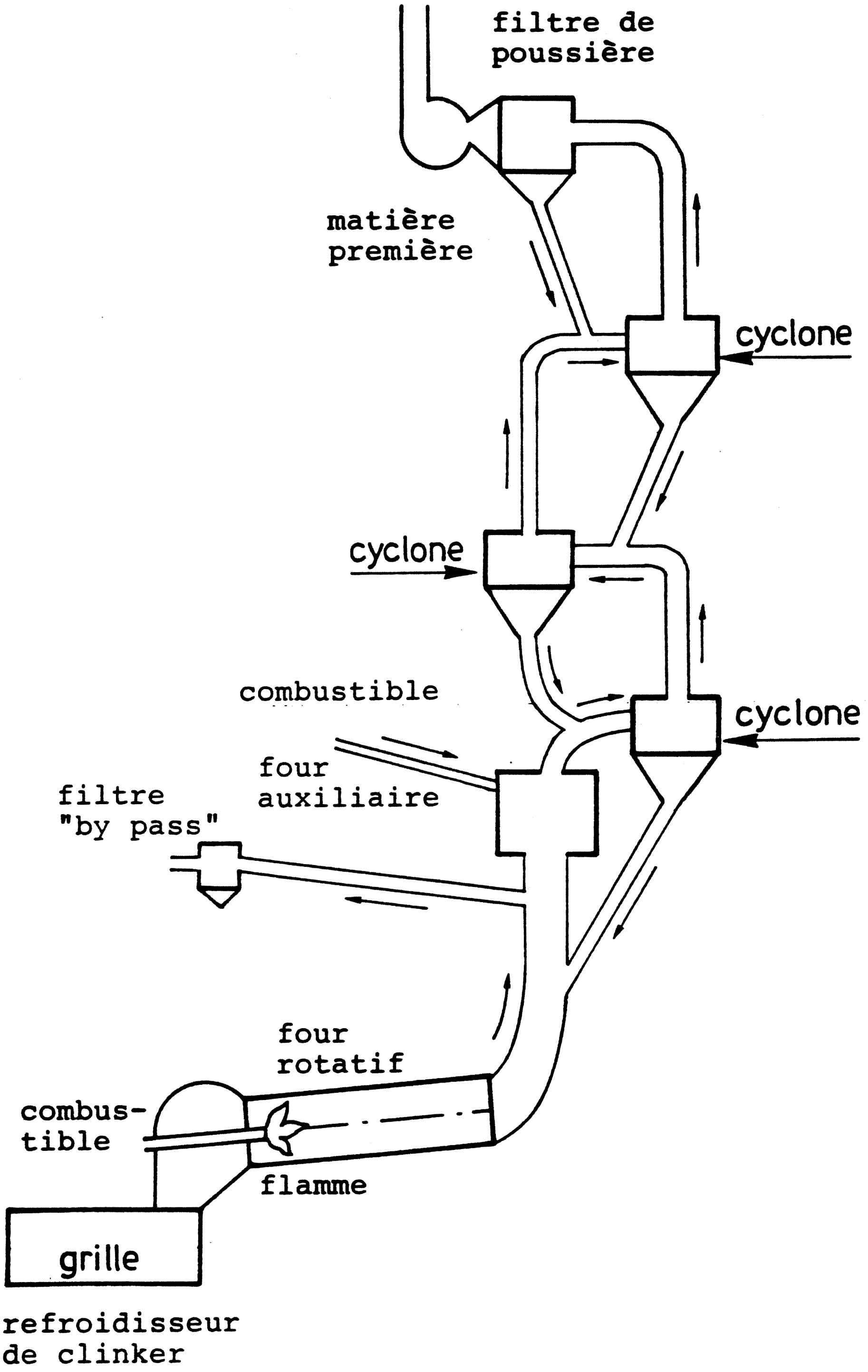
filtre de
poussière
matière
première
cyclone
cyclone
combustible
cyclone
four
auxiliaire
filtre
"by pass"
four
rotatif
combus-
tible
flamme
grille
refroidisseur
de clinker

Figure 5. Example d'un four suivant la voie sèche

Another way, which allows a still higher production rate, is to use more fuel in the rotary kiln, so that most of the oxygen will be consumed, and transfer hot air directly from the clinker cooler to the auxiliary furnace.

As told above, it is necessary to limit the amount of calcination that is allowed to take place in the cyclone system. Thus, the temperature of the material will be limited, and no material will melt. This is essential for use of stationary parts, like cyclones, in a kiln system. No part of the raw material is allowed to melt in the cyclone system, or the flow of raw material, and eventually also the flow of gas, will be blocked.

Such liquids may form in other ways than overheating the calcination process. Especially common are melts of volatile matter, such as potassium chloride, sodium chloride, and also potassium sulphate.

Limited amounts of volatile materials may be "by passed" from the gas duct between the rotary kiln and the auxiliary furnace. This will "steal" a small amount of the raw materials and a part of the heat from the process, but at the same time the operation will be more smooth, and the alkali content of the klinker will possibly be somewhat reduced.

When most of the calcination process was transferred from the rotary kiln to the auxiliary furnace and the cyclones, the object was to **increase the production rate** at a certain diameter of the rotary kiln. The change did **hardly** improve the **heat efficiency** of the total kiln machinery.

Normaly a dry process kiln takes about 750 kilocalories for each kilogram of clinker, and a wet system takes more, how much more is dependent of the water content of the slurry.

4. Influence of changes in production; the economy of the production and the quality of the cement

For many years, coal and oil was so cheap in Sweden that the wet process played an important role in the cement industry, because several types of lime raw materials, such as chalk, could be used in spite of their high water content.

To day, there exist only two large factories and one small, all for the dry process. Lime quarries with high water content are closed, or used for lime production only.

An economic factor that speaked for a change to the dry process was that the cement quantity that was necessary for Sweden could be produced in a few rather large factories, which could be operated by a rather small staff. This factor, on the other hand, makes the production more sensitive at a breakdown.

In Sweden, a tendency has been observed that the contents of potassium and sodium in the cement has increased when the wet process factories disappeared.

This is not mainly a result of the change from the wet process to the dry process. It is more a consequence of that the character of the raw materials turned different, as a average in all Sweden.

According to my opinion, much of the change in cement quality, which aluminium was given the credit for, is due to potassium and sodium. That the aluminium has got the role, is the statistical result of the fact that potassium very often follows aluminium in the raw materials.

During a period, a slag cement was produced at one of the wet process factories in Sweden. This production gave the important experience that the potassium and sodium content of the cement has to be kept constant, and not too low, if the contribution of the slag to the strength of the cement shall be appreciable and even.

The following is true for all production of portland cement, whether the dry or the wet process is used:

1. The chemical composition of the raw materials mix is important. Thus, a lower lime saturation factor is used in one of the Tunisian factories than in the Swedish factories for standard cement. The difference corresponds to a higher average temperature at concrete work in Tunisia.

   However, the total chemical composition is not enough for governing the burning process. In the old Limhamn factory, the raw materials were built upon components which all were very difficult to melt. The process demanded very much fuel, and each time as I had the opportunity to measure the temperature of just formed clinker, I read 1620 degrees Celcius just below the flame. This is a very high temperature, and the thermal charge upon the refractory bricks in the clinkering zone was high.

2. At least one of the minerals in the raw mix should melt at a temperature, not too much above 1000 degrees Celcius. Usually such a mineral is composed of silica, alumina, potassium and sodium oxides and, compared with calcium oxide, the molten mineral has a strongly acidic reaction.

   During the calcination, the calcium carbonate loses carbon dioxide, and calcium oxide remains, which is a very strong base.

   The calcium oxide is usually not soluble in the small drops of molten minerals, but because of their different acid-base reaction, a very rapid chemical reaction starts, and much heat is liberated. In this way the clinker minerals start to form.

   When the clinker minerals tricalcium aluminate and brownmillerite have formed, which contain alumina and iron, they will enter the melt already at a rather low temperature. With the aid of this melt, the other clinker minerals form, at a temperature, which not necessarily must exceed 1350 - 1450 degrees Celcius. A rather beautiful example of a ready clinker is found in Figure 3.

3. Often the mineral quartz is used as a carrier of silica. Quartz is very difficult to dissolve in the primary melt, and consequently it must be ground very finely, if the clinker shall become uniform. If there are too coarse quartz grains in the material mix, the silica rich clinker mineral belite collects as big "islands".

   Figure 6 shows such an island with a diameter of 0.44 mm. If the distribution of the clinker minerals becomes too uneven, the quality of the cement may be reduced.

4. It may be a temptation to believe that the clinkering process would be improved if more fuel is used. However, a fuel excess will increase the cost of the clinker. Moreover, the clinker formation will start further from the flame, and this will reduce the clinkering temperature.

   At this lower temperature, the clinker will contain less of molten materials, which will hamper the nodule formation. Thus the clinker remains as a dust or as a fine sand. Particles with too high or too low lime content cannot equalize, which would be very well possible within a nodule.

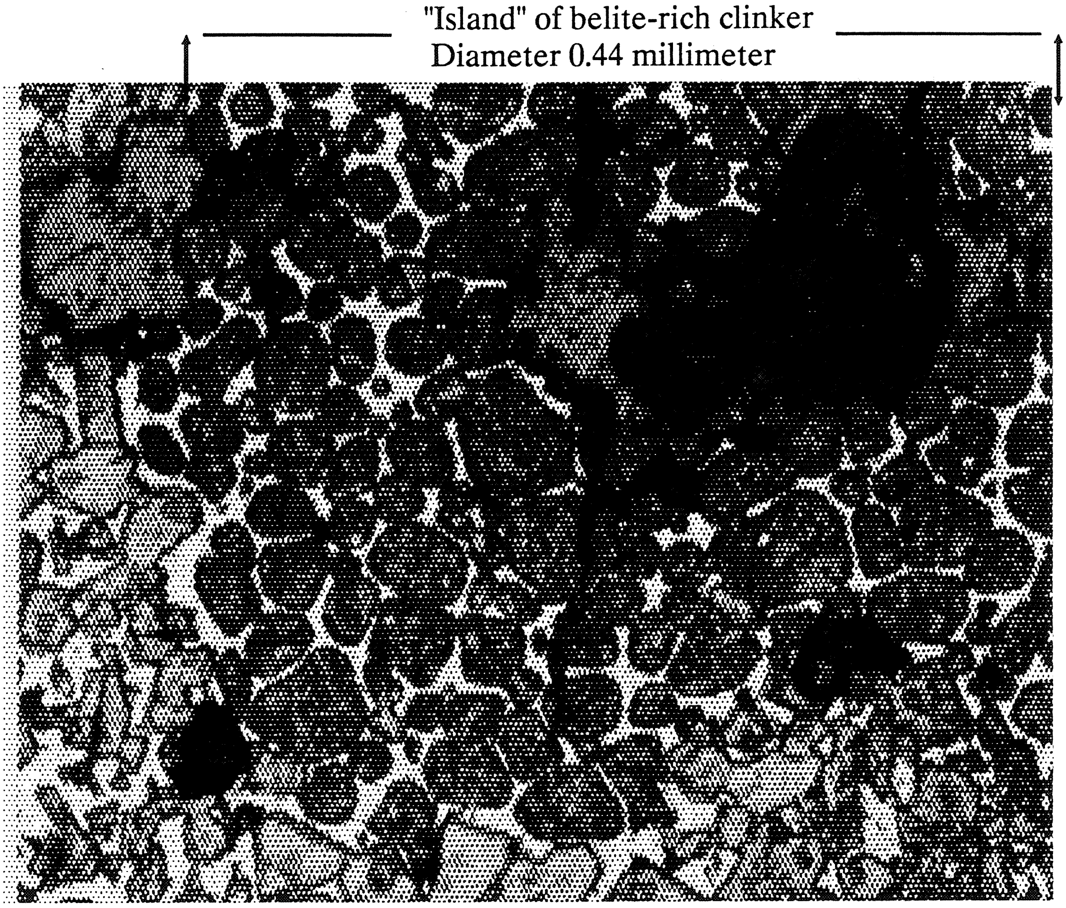

Figure 6.

A microphoto of a Portland clinker (Skoevde, Sweden), magnification 260 times.

The dark, rounded crystals in the upper, right part of the picture, are belite (mainly dicalcium silicate). The diameter of the belite island in the figure is about 0.44 millimeter.

The light crystals in the lower and left part of the picture are alite (mainly tricalcium silicate).

Normally, the belite crystals are evenly distributed in the clinker. When the belite crystals are concentrated in large fields, as in this picture, one of the minerals which contribute the silica, for example quartz, occurs in the raw meal as too large grains.

Figure 7 shows a very porous clinker, which contains parts with free lime, and other parts with the clinker mineral belite, which indicates a local excess of silica. The two parts are separated with a number of pores, which indicate that they have formed as separate, small clinker grains, without any subsequent equilizing of the compositions of the grains.

Figure 6 and Figure 7 show that the optical microscope may be a good help in recognizing unfavourable conditions at the clinker formation.

Especially in installations, where a great part of the calcining is performed in the rotary kiln, the operator feels so much fear of the conditions with too scarce a fuel supply, that he has a tendency to oversupply the fuel. As shown, this also may impair the quality of the clinker.

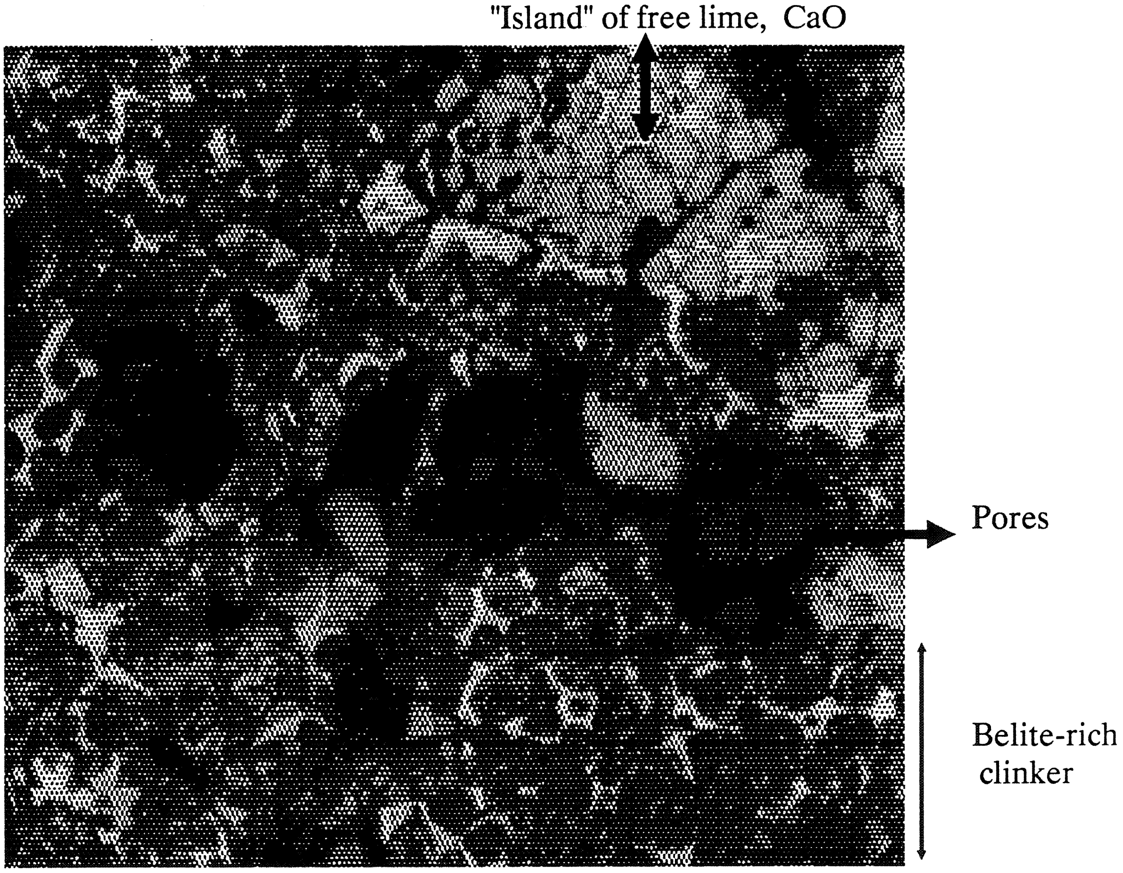

Figure 7.

A microphoto of a Portland clinker (Skoevde, Sweden), magnification about 200 times.

In the top right part of the picture there is an "island" of rounded light crystals of free calcium oxide.

In the lower right part of the picture there is one of several islands of belite (mainly dicalcium silicate).

It does not seem reasonable that two components with so different lime saturation can exist in a distance of only 100 micrometer from each other.

The system of large pores between the free lime and the belite indicates the possibility that the clinker is built from small particles, sintered together at a moderate temperature.

This may be the consequence of burning the clinker with too much fuel, shaping a clinkering zone too far from the flame.